

Alma Mater Studiorum – Università di Bologna

DOTTORATO DI RICERCA IN
SCIENZE E TECNOLOGIE AGRARIE, AMBIENTALI E ALIMENTARI

Ciclo XXXV

Settore Concorsuale: 07/E1

Settore Scientifico Disciplinare: AGR/13

**SEWAGE SLUDGE AS ORGANIC FERTILIZER IN AGRICULTURE. A STUDY OF
PHYSICO-CHEMICAL PROPERTIES, AGRONOMIC EFFICIENCY AND
ENVIRONMENTAL SAFETY, WITH A SPECIFIC FOCUS ON TANNERY SLUDGE**

Presentata da: Salvatore Rapisarda

Coordinatore Dottorato
Prof. Massimiliano Petracci

Supervisore
Prof. Luciano Cavani

Co-supervisore
Prof. Claudio Ciavatta

Esame finale anno 2023

TABLE OF CONTENTS

ABSTRACT	7
GENERAL INTRODUCTION	8
OVERVIEW AND AIMS OF THE RESEARCH	11
CHAPTER 1	14
PHYSICO-CHEMICAL CHARACTERIZATION OF SEWAGE SLUDGE: A COMPARISON BETWEEN TANNERY AND MUNICIPAL SLUDGE	14
1.1 INTRODUCTION	15
1.2 MATERIAL AND METHODS	16
1.2.1 Sewage sludge	16
1.2.2 Carbon and nitrogen elemental analysis, $\delta^{13}\text{C}$ and $\delta^{15}\text{N}$	18
1.2.3 ATR FT-IR analysis	18
1.2.4 TG-DTA.....	19
1.2.5 Statistical analysis.....	19
1.3 RESULTS	19
1.3.1 Carbon and nitrogen elemental analysis, $\delta^{13}\text{C}$ and $\delta^{15}\text{N}$	19
1.3.2 ATR FT-IR analysis	22
1.3.3 TG-DTA analysis	23
1.4 DISCUSSION	26
1.4.1 Evaluation of C and N analysis.....	26
1.4.2 Evaluation of ATR FT-IR and TG-DTA analysis.....	28
1.5 CONCLUSIONS	30
CHAPTER 2	32
NITROGEN AVAILABILITY IN ORGANIC FERTILIZERS FROM TANNERY AND SLAUGHTERHOUSE BY-PRODUCTS	32
2.1 INTRODUCTION	33
2.2 MATERIALS AND METHODS.....	35
2.2.1 General description of the organic fertilizers.....	35
2.2.2 Characterization of the organic fertilizers	36
2.2.3 Soil description and characterization	37
2.2.4 Incubation of organic fertilizers into soil.....	38
2.2.5 Hot-water extractable nitrogen.....	39
2.2.6 Data handling and statistical analysis.....	40

2.3 RESULTS	40
2.3.1 Characterization of organic fertilizers	40
2.3.2 Incubation of organic fertilizers in the soil	42
2.3.3 Hot-water extractable nitrogen.....	45
2.3.4 Correlation and linear regression between indicators of available nitrogen.....	46
2.4 DISCUSSION	49
2.4.1 Characterization and soil incubation of the organic fertilizers	49
2.4.2 Relation between indicators of available nitrogen	50
2.5 CONCLUSIONS	52
CHAPTER 3.....	53
STUDY AND CHARACTERIZATION OF THE INTERACTION OF OXYBENZONE WITH SOIL	53
3.1 INTRODUCTION	54
3.2 MATERIALS AND METHODS.....	55
3.2.1 Oxybenzone	55
3.2.2 Soils.....	55
3.2.2.1 Analysis	55
3.2.2.2 Main characteristics	56
3.2.3 Adsorption and desorption study.....	58
3.2.3.1 HPLC-UV analysis	58
3.2.3.2 Adsorption kinetics.....	58
3.2.3.3 Adsorption isotherms	59
3.2.3.4 Desorption isotherms	60
3.2.4 Humic acids.....	60
3.2.4.1 Extraction from soil	60
3.2.4.2 Purification	61
3.2.5 ATR-FTIR analysis of humic acids.....	63
3.2.6 Raman analysis of oxybenzone.....	63
3.2.7 SERS analysis.....	63
3.2.7.1 Preparation of silver nanoparticles	63
3.2.7.2 Instrumentation and technical setting	64
3.2.7.3 Analysis of oxybenzone	64
3.2.7.4 Analysis of humic acids.....	65
3.2.7.5 Analysis of the complex oxybenzone – humic acids.....	65
3.3 RESULTS	65

3.3.1 Adsorption and desorption study.....	65
3.3.1.1 Adsorption kinetics.....	65
3.3.1.2 Adsorption isotherms.....	66
3.3.1.3 Desorption isotherms.....	68
3.3.2 Raman and SERS analysis of oxybenzone.....	69
3.3.3 Analysis of humic acids.....	73
3.3.3.1 ATR-FTIR analysis.....	73
3.3.3.2 SERS analysis.....	75
3.3.4 SERS analysis of the complex oxybenzone-humic acid.....	76
3.4 DISCUSSION.....	78
3.4.1 Adsorption and desorption study.....	78
3.4.2 Investigation of humic acids quality.....	80
3.4.3 Study of oxybenzone-humic acids interactions.....	82
3.4.4 Relations between SERS results and adsorption/desorption study.....	85
3.5 CONCLUSIONS.....	86
GENERAL CONCLUSIONS.....	87
REFERENCES.....	89

ABSTRACT

In recent decades, the use of organic fertilizers has gained increasing interest mainly for two reasons: their ability to improve soil fertility and the need to find a sustainable alternative to mineral and synthetic fertilizers. In this context, sewage sludge is a useful organic matrix that can be successfully used in agriculture, due to its chemical composition rich in organic matter, nitrogen, phosphorus and other micronutrients necessary for plant growth.

This work investigated three indispensable aspects (i.e., physico-chemical properties, agronomic efficiency and environmental safety) of sewage sludge application as organic fertilizer, emphasizing the role of tannery sludge. In a comparison study with municipal sewage sludge, results showed that the targeted analyses applied (total carbon and nitrogen content, isotope ratio of carbon and nitrogen, infrared spectroscopy and thermal analysis) were able to discriminate tannery sludge from municipal ones, highlighting differences in composition due to the origin of the wastewater and the treatment processes used in the plants. Regarding agronomic efficiency, N bioavailability was tested in a selection of organic fertilizers, including tannery sludge and tannery sludge-based fertilizers. Specifically, the hot-water extractable N has proven to be a good chemical indicator, providing a rapid and reliable indication of N bioavailability in soil. Finally, the behavior of oxybenzone (an emerging organic contaminant detected in sewage sludge) in soils with different physico-chemical properties was studied. Through adsorption and desorption experiments, it was found that the mobility of oxybenzone is reduced in soils rich in organic matter. Furthermore, through spectroscopic methods (e.g., infrared spectroscopy and surface-enhanced Raman spectroscopy) the mechanisms of oxybenzone-humic acids interaction were studied, finding that H-bonds and π - π stacking were predominantly present.

KEYWORDS: sewage sludge, tannery sludge, nutrients recycling, physico-chemical analysis, nitrogen bioavailability, oxybenzone.

GENERAL INTRODUCTION

Wastewater treatment plants are key infrastructures that purify the contaminated effluents produced by domestic, urban and industrial activities, ensuring the discharge of cleaner water in rivers, lakes and seas. At the same time, this process creates large amounts of sewage sludge (SS), a semisolid residual material resulting from the sedimentation of the suspended solids contained in the effluents (Lamastra et al., 2018).

Obtaining information on global production is a challenge, as only scarce or outdated data are available in the scientific literature and institutional documents. For instance, it was estimated that in the EU approximately 10 million tons of SS are produced annually (Gil et al., 2018; Kominko et al., 2018), 4.5 million tons were produced in US in 2021 (EPA, 2021), while 6.25 million tons were produced in China in 2013 (Yang et al., 2015). The certain fact on which several authors agree is that SS production is set to increase significantly in the coming years (Di Giacomo & Romano, 2022; Durdevic et al., 2022; Sharma et al., 2017). Factors supporting this hypothesis are related to the rising world population, increased migration to large cities and the new “ecological awareness” that should lead to the construction of more wastewater treatment plants (Drechsel et al., 2015).

Based on this statement, it seems clear that special attention should be paid to the management of this class of organic waste in order to minimize the environmental impact. In this context, the use of SS in agriculture as organic fertilizer is the most sustainable option according to the waste management hierarchy proposed by Sharma et al. (2017), ensuring complete nutrients recovery in line with the circular economy principle advocated by the EC (2020). Indeed, beside this application, the most common alternatives are landfilling and incineration. It is well known that landfill disposal of SS creates several concerns, leading to potential leaching of inorganic and/or organic contaminants and the direct emission of CO₂ to the atmosphere (Barberio et al., 2013). Incineration represents an attractive disposal method, allowing a large reduction of SS volume and the recovery of renewable energy; on the other hand, it requires the management of ashes produced as waste and the possible harmful emissions (Ciešlik et al., 2015; Samolada & Zabaniotou, 2014).

The application of SS in agriculture is also sustained by its intrinsic properties, being a recognized source of organic matter, nitrogen (N), phosphorus (P) and other plant nutrients (Singh & Agrawal, 2008, 2010b, 2010a)

Organic matter is perhaps the most valuable constituent that we cannot afford to waste, as the soil degradation and desertification risk (soils with less than 1% organic carbon content) represents a crucial problem in the Mediterranean basin (Salvati, 2014; Zdruli, 2014). In fact, it is well demonstrated that supplying SS to soils deficient in organic matter, such as soils of semi-arid Mediterranean croplands, has positive effects on fertility (Diacono & Montemurro, 2010; Mattana et al., 2014; Zdruli et al., 2004). Several other authors reported improvement of soil physico-chemical properties, in terms of water-holding capacity, formation of stable aggregates, cation exchange capacity and soil porosity (Koutroubas et al., 2014; Kumpiene et al., 2008; Lal, 2004; Lloret et al., 2016; Pascual et al., 2009).

Concerning soil biological properties, instead, it was demonstrated that SS amendment leads to an increase in soil microbial and enzymatic activities and soil basal respiration (Banerjee et al., 1997; Bettiol & Ghini, 2011; Kizilkaya & Bayrakli, 2005; Roig et al., 2012). However, the potential presence of heavy metals in the sludge can adversely affect the soil microbiota, causing, for example, the inhibition of some enzymatic activities (Fernández et al., 2009; Kandeler et al., 2000; Tejada et al., 2011).

As mentioned above, this class of organic waste is a source of macro- and micronutrients required for plant nutrition. As a result, many studies have been carried out with the aim to monitor plant growth after the application of SS to the soil, testing a wide variety of crops both in field and pot experiments (Antolín et al., 2005; Kołodziej et al., 2015; Riaz et al., 2018; Singh & Agrawal, 2008; Wang et al., 2008). Generally, outcomes recorded an increment in total biomass and yield responses, demonstrating the potentiality to use SS as sustainable alternative to mineral fertilizers. This aspect represents an additional benefit to the environment, as mineral and synthetic fertilizers create concerns both for their improper use and production. In recent decades, intensive agricultural practices related to their use have caused damage not only to the soil itself, accelerating erosion and acidification processes, but also to other environmental compartments, leading to coastal eutrophication, air pollution and loss of biodiversity (Billen et al., 2013; Galloway et al., 2003; Lassaletta et al., 2014). In terms of production, the synthetic processes from which they derive are environmentally impactful, as they consume a lot of energy and rely on fossil fuels and fossil mineral deposits (Sigurnjak et al., 2017; Svanbäck et al., 2019). For instance, one kilogram of N fertilizer requires almost 60 MJ of energy (Huo et al., 2012), while P fertilizers are produced exploiting phosphate rocks, a non-renewable

source which is estimated to be exhausted within 50-400 years (van Dijk et al., 2016). In this context, recycling N and P from SS must be a priority, in order to reduce the exploitation of non-renewable sources and to contain the dissipation of such nutrients in the environment.

OVERVIEW AND AIMS OF THE RESEARCH

The concept of circular economy is closely related to territoriality and industrial ecology, as explained by Veyssi re et al. (2022), who wrote that “...*industrial ecology aims at shifting the current industrial system into an industrial ecosystem in which the consumption of materials and energy is optimized and the by-products of one process serve another process. Industrial symbiosis is about building this ecosystem on a territory, with mutualisation among stakeholders in close proximity*”.

This statement well explains the reason for which, in addition to SS deriving from municipal wastewater treatment plants (WWTPs) (hereinafter referred to as MS), tannery sludge (hereinafter referred to as TS) was also considered in this PhD thesis. In fact, Italy is a world leader in leather production (16 % of global turnover), with industries mainly located in Veneto, Tuscany, Campania and Lombardy (Alibardi & Cossu, 2016). Tanning is the process of converting animal skin to leather, which requires high volumes of water and chemicals, resulting in TS as waste. Several authors have already reported on the possibility of successfully using TS in agriculture as organic fertilizer (Araujo et al., 2020; Ciavatta et al., 2012; Giacometti et al., 2012). For the same reasons discussed in the previous paragraph, this choice would be the best solution for sustainable management, in addition to allowing nutrients recovery from industry-derived waste. However, knowing the physico-chemical properties of TS is essential to apply them rationally and safely in agriculture; furthermore, a comparison with MS would allow to highlight the differences between the two matrices and obtain information on the traceability of sludge. The first chapter of this thesis attempts to achieve this goal through the application of several analytical techniques. Specifically, elemental and isotopic analysis of carbon and nitrogen, infrared spectroscopy (FT-IR) and thermal analysis (TG-DTA) were applied to several TS and MS samples with the aim to characterize the different SS and discriminate their origin.

Nowadays, the approach taken to optimize agronomic efficiency involves SS formulations in combination with other biomass or mineral fertilizers in order to add value to the final product (Deeks et al., 2013; Głodniok et al., 2022; Jastrz bska et al., 2022; Kominko et al., 2019). In the specific context of organic fertilizers, SS can be mixed with organic matrices (e.g., meat and bone meals, leather meals, blood meals) to obtain a final product generally rich in organic matter and increased N (and P) content due to such matrices. Compared with the application of the sole SS, this class of organic fertilizers

certainly brings more benefits to the soil and plant growth; on the other hand, both the amounts of inorganic and potentially mineralizable organic nitrogen may vary depending on the type of raw materials used and the transformation processes they undergo during the production (Cassity-Duffey et al., 2020).

Therefore, the second chapter (recently published, Rapisarda et al., 2022) investigates this aspect by describing a laboratory trial involving a selection of organic fertilizers obtained from tannery and slaughterhouse by-products. In particular, the hot-water extractable nitrogen was tested as chemical indicator to predict N bioavailability (i.e., the sum of inorganic and potentially mineralizable N), as an alternative to the time- and reagent-intensive incubation essay.

In addition to the benefits described above, there is also a “dark side of the sludge” related to public concern about the possible presence of toxic organic compounds (Aparicio et al., 2009; Suciú et al., 2015) and Potentially Toxic Elements (PTE). (Duan et al., 2015; Hei et al., 2016). However, legislation imposes limiting concentrations for soil application with the aim of preventing environmental pollution and ensuring safety for human health. For instance, in the EU, the Sludge Directive (EC, 1986) regulates the limit values for PTE concentrations in SS, while the presence of organic contaminants is regulated by national legislations in individual countries. Occurrence, toxicity and dangerousness of PTE is widely reported by scientific literature (Fuentes et al., 2004; Malara & Oleszczuk, 2013; McBride, 2003). Conversely, the context of organic contaminants is more complex, as it includes many molecules that can be (macro)classified into “classic” and “emerging contaminants” (R. M. Clarke & Cummins, 2015). The term “classic” usually refers to persistent organic pollutants (POPs), a particularly well-studied class that includes chlorinated dioxins and furans, polycyclic aromatic hydrocarbons, organochlorine pesticides, polychlorinated biphenyls and alkanes (Alcock et al., 1996; B. O. Clarke et al., 2010; Gomes et al., 2009; Stevens et al., 2001; Wild et al., 1991). Emerging contaminants are probably less known than POPs and include pharmaceuticals, antibiotics, steroids, oestrogens, brominated flame retardants, perfluorinated compounds and UV filters (B. O. Clarke & Smith, 2011; Díaz-Cruz et al., 2009; Martín-Pozo et al., 2019; Vicent et al., 2013). The third chapter focused on oxybenzone, an emerging contaminant largely employed (and consequently detected in SS) as UV filter, whose fate in soil has been poorly addressed so far (Camino-Sánchez et al., 2016; Jeon et al., 2006; Sánchez-Brunete et al., 2011). In particular, oxybenzone

adsorption and desorption capacities in different types of soils with contrasting physico-chemical properties were determined through the Freundlich model. Furthermore, humic acids were extracted from the mentioned soils and analysed by means of infrared spectroscopy (FT-IR) and surface enhanced raman spectroscopy (SERS). This approach allowed to obtain information on the functional groups of humic acids, and to predict the interaction mechanisms occurring between oxybenzone and humic acids by taking advantage of the possibility of one-pot solution analysis given by the SERS.

CHAPTER 1

PHYSICO-CHEMICAL CHARACTERIZATION OF SEWAGE SLUDGE: A COMPARISON BETWEEN TANNERY AND MUNICIPAL SLUDGE

1.1 INTRODUCTION

Based on its origin, sewage sludge (SS) can be classified as municipal and industrial sludge. Municipal sludge is generated in treatment plants that primarily collect wastewater from domestic activities, while industrial sludge is produced in treatment plants where wastewater from manufacturing industries (e.g., paper, petrochemical, tannery) converges (Devi & Saroha, 2017).

In Italy, the production of municipal sludge (MS) was estimated at over 3 million tons in 2015 (Mininni et al., 2019). Among the industrial sludge, tannery sludge (TS) plays an important role, since the Italian leather industry holds a leading position worldwide. Unfortunately, no data are available about the TS production, but it is reasonable to think that the amount is not negligible as the tanning process consumes more than 100 L of water and 2 kg of chemicals per square meter of the final product (Alibardi & Cossu, 2016).

According to several authors, SS production is expected to increase in the coming years, supported by expected population growth (Di Giacomo & Romano, 2022; Durdevic et al., 2022).

Based on this finding, it becomes increasingly important to find sustainable management for these types of matrices. Application in agriculture would lead to a dual beneficial effect, enabling nutrients recovery according to circular economy concepts (EC, 2020) and representing a valid alternative to an impacting disposal, such as incineration and landfill (Folgueras et al., 2003; Kacprzak et al., 2017). In fact, SS is commonly rich in nutrients useful to maintain or increase soil fertility and plant nutrition (e.g., nitrogen and phosphorus) and organic matter, which contributes to improve soil characteristics in terms of biological activity, porosity and water retention (*BS ISO 19698 : 2020*).

Several authors investigated the quality and the chemical composition of MS, obtaining satisfying results using the stable isotope analysis (Onodera et al., 2021; Sáez et al., 2020), infrared spectroscopy (De Oliveira Silva et al., 2012; Kowalski et al., 2018) and thermal analysis (De Oliveira Silva et al., 2012; Francioso et al., 2010). In particular, stable isotope analysis provided information on the water entering the WWTPs and treatment processes undergone. Infrared spectroscopy and thermal analysis were able to provide evidence on the presence of specific classes of molecules. Chemical characterization of TS is scarcely reported in the literature and generally involves routine analysis, such as the measurement of pH, organic carbon, total nitrogen and PTE content (Haroun et al.,

2007; Juel et al., 2016; Zhai et al., 2020). In the perspective of its reuse in agriculture, either alone or mixed with other fertilizers, it is necessary not only to ensure the safety of the product in terms of concentration of potential contaminants, but also to acquire detailed information on its composition and traceability.

This study aims (i) to gain a more comprehensive understanding of the physico-chemical properties of TS through the use of specific analytical techniques (elemental and stable isotope analysis of carbon and nitrogen, infrared spectroscopy, thermal analysis) and (ii) to compare the results with those obtained from MS, highlighting differences that allow the origin to be traced.

1.2 MATERIAL AND METHODS

1.2.1 Sewage sludge

The sewage sludge object of this study were collected from January 2019 to April 2021, as specified in Table 1.1.

TS samples were provided by the wastewater treatment plant (WWTP) “Consorzio Cuoidepur SpA”, located in the Tuscan tannery industrial area in the Pisa province.

MS samples were collected from WWTPs located in different Italian regions.

Once received in our laboratory, samples were placed in an oven (FD 23 model, Binder GmbH, Tuttlingen, Germany) at 105°C until they reached the constant weight, ground by means of a ball mill (Mixer Mill MM400, Retsch GmbH, Haan, Germany) and sieved at 0.5 mm.

Table 1.1 - Table of sewage sludge samples indicating code, type and sampling time

Code	Type	Sampling time
TS01	Tannery sludge	25-01-19
TS02	Tannery sludge	11-04-19
TS03	Tannery sludge	26-05-19
TS04	Tannery sludge	05-07-19
TS05	Tannery sludge	17-12-19
TS06	Tannery sludge	30-01-20
TS07	Tannery sludge	29-06-20
MS01	Municipal sludge	15-02-19
MS02	Municipal sludge	15-02-19
MS03	Municipal sludge	15-02-19
MS04	Municipal sludge	03-12-19
MS05	Municipal sludge	03-12-19
MS06	Municipal sludge	03-12-19
MS07	Municipal sludge	03-12-19
MS08	Municipal sludge	07-12-20
MS09	Municipal sludge	07-12-20
MS10	Municipal sludge	07-12-20
MS11	Municipal sludge	09-04-21
MS12	Municipal sludge	09-04-21
MS13	Municipal sludge	09-04-21
MS14	Municipal sludge	09-04-21
MS15	Municipal sludge	09-04-21
MS16	Municipal sludge	09-04-21
MS17	Municipal sludge	09-04-21

1.2.2 Carbon and nitrogen elemental analysis, $\delta^{13}\text{C}$ and $\delta^{15}\text{N}$

Aliquots of about 5 mg of samples were weighed into tin capsules and analysed with an elemental analyser (Flash 2000 CHNS-O Elemental Analyzer, Thermo Scientific GmbH, Dreieich, Germany) to determine the carbon (C) and nitrogen (N) total content. The isotopic analysis was conducted with the Isotope Ratio Mass Spectrometer (Delta V Plus IRMS, Thermo Scientific GmbH, Dreieich, Germany), directly coupled to the elemental analyser. Regarding C, the isotopic ratio is expressed as units of $\delta^{13}\text{C}$ and was calculated according to the following equation:

$$\delta^{13}\text{C} \text{ ‰} = \frac{R_{\text{sample}} - R_{\text{standard}}}{R_{\text{standard}}} \cdot 1000$$

where R_{sample} is the isotope ratio $^{13}\text{C}/^{12}\text{C}$ of the sample, while R_{standard} is the isotope ratio $^{13}\text{C}/^{12}\text{C}$ of the Pee Dee Belemnite (PDB) standard.

In the same way, N isotopic signature is expressed as units of $\delta^{15}\text{N}$ and was calculated according to the following equation:

$$\delta^{15}\text{N} \text{ ‰} = \frac{R_{\text{sample}} - R_{\text{standard}}}{R_{\text{standard}}} \cdot 1000$$

where R_{sample} is the isotope ratio $^{15}\text{N}/^{14}\text{N}$ of the sample, while R_{standard} is the isotope ratio $^{15}\text{N}/^{14}\text{N}$ of the air.

Analyses were performed in triplicate.

1.2.3 ATR FT-IR analysis

A small aliquot of sample was deposited on the diamond Attenuated Total Reflection (ATR) device (Quest Single Reflection ATR Accessory, Specac Ltd., Orpington, England) connected to an infrared spectrophotometer (Tensor 27, Bruker Corporation, Billerica, USA). Background spectra of air were acquired before sample analysis. Once the sample had been analysed, the diamond surface was cleaned with a dampened ethanol cloth. Spectra were recorded from 4000 to 400 cm^{-1} , setting a spectral acquisition of 4 cm^{-1} and 64 scans.

1.2.4 TG-DTA

Thermogravimetric analysis (TG) and differential thermal analysis (DTA) were carried out using a TG-DTA instrument (TG-DTA92, Setaram, Caluire-et-Cuire, France). About 10 mg of sample were weighed in alumina crucible and heated from 30 °C to 700 °C in a dynamic air atmosphere (flow rate 8 L h⁻¹) with a rate of 10 °C min⁻¹. An empty crucible was used as reference material.

1.2.5 Statistical analysis

Data of C and N total content, $\delta^{13}\text{C}$ and $\delta^{15}\text{N}$ were statistically analysed through Hierarchical Cluster Analysis (HCA), performed by means of OriginPro 2022b (OriginLab Corporation, 2022).

Similarly, FT-IR spectra and thermograms were also statistically processed through HCA, using the package “ChemoSpec” of the R environment (R Core Team, 2022).

The result of HCA consists of a dendrogram, showing the objects and clusters on the horizontal axis and the Euclidean distance between clusters on the vertical axis. Data were preliminarily normalized in the range 0-1 and processed through the “Group Average” clustering algorithm.

Regarding FT-IR spectra and thermograms, the median and its interquartile range were obtained through the package “ChemoSpec” of the R environment (R Core Team, 2022).

1.3 RESULTS

1.3.1 Carbon and nitrogen elemental analysis, $\delta^{13}\text{C}$ and $\delta^{15}\text{N}$

On average, total C (C_{tot}) showed values ranging from 22 to 44 % for MS and between 23 and 27 % for TS (Figure 1.1), in agreement with those reported by previous studies (Gherghel et al., 2019; Kavouras et al., 2015; Mininni et al., 2019). The higher distribution of data observed for MS is due to the different sites where they were collected and, consequently, to the different treatment processes to which they were subjected. The same trend was observed in the total N (N_{tot}) results. In particular, TS presented values between 2 and 2.8 %, while MS ranged from 3.1 to 6.6 % (Figure 1.1).

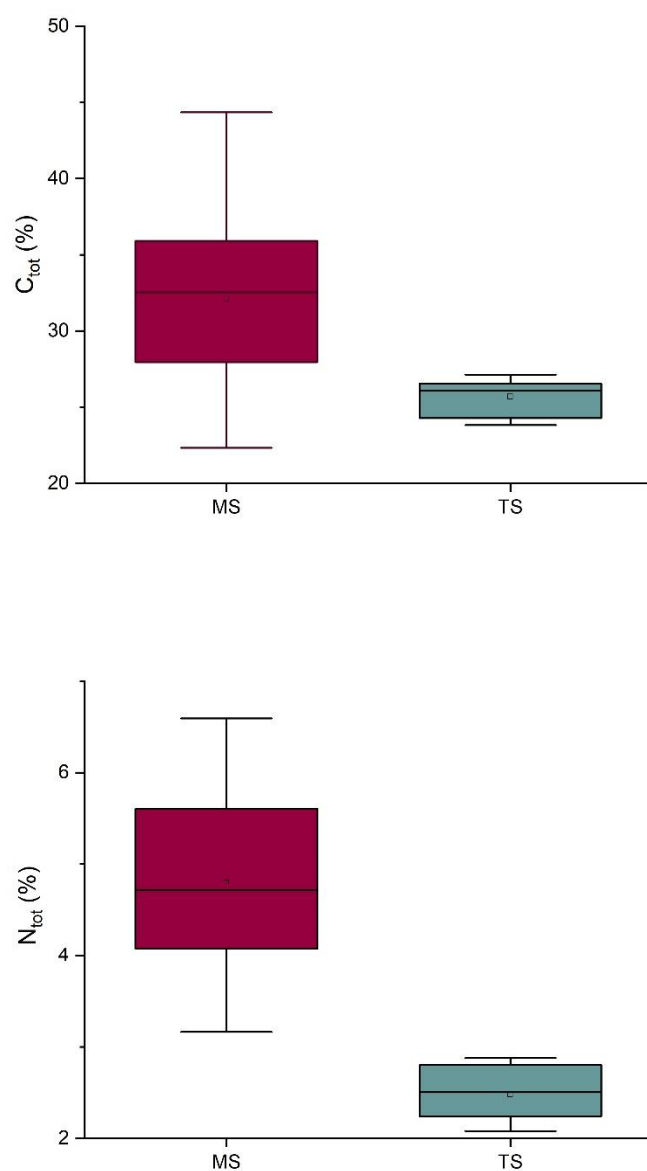


Figure 1.1 - Total C (top panel) and N (bottom panel) content. (MS = municipal sludge; TS = tannery sludge).

The different origin of SS also emerged in the isotopic signature results (Figure 1.2). In fact, MS showed a lower $\delta^{13}\text{C}$ than TS, ranging from -24.3 to -27.6 ‰, while values > -25 ‰ were found for the industrial derived sludge. Conversely, MS exhibited, on average, a higher $\delta^{15}\text{N}$ (2 – 11.6 ‰) than TS (5.3 – 6 ‰). The data related to MS agree with those

obtained by Onodera et al. (2021), while no previous data have been found in the scientific literature for TS.

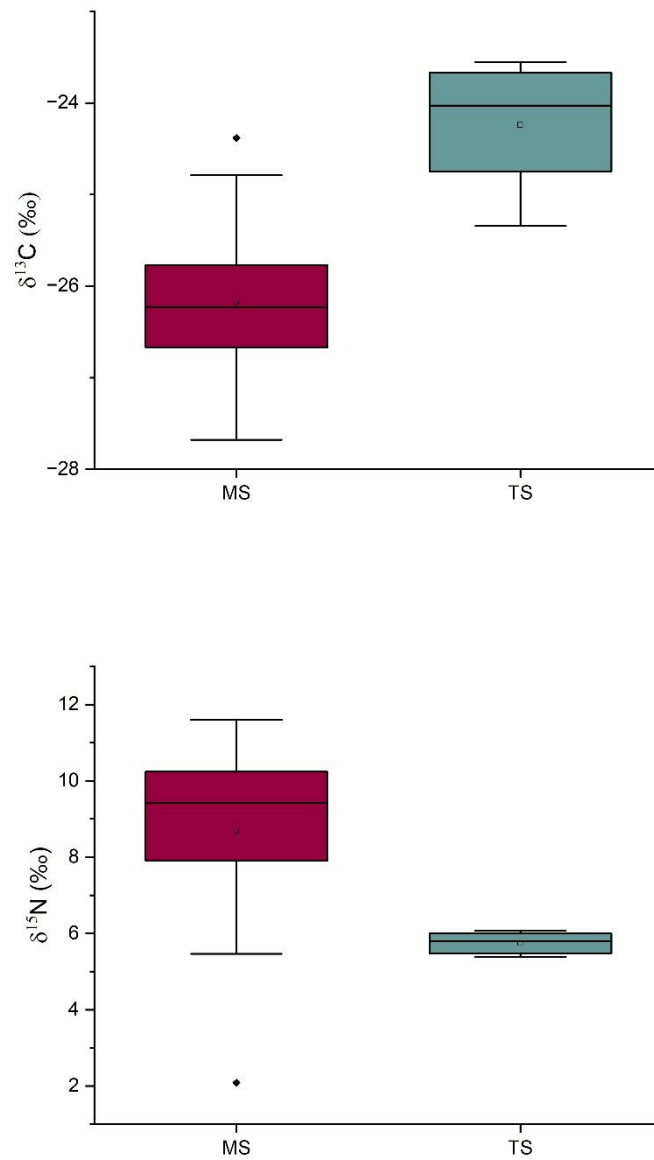


Figure 1.2 - $\delta^{13}\text{C}$ (top panel) and $\delta^{15}\text{N}$ (bottom panel). (MS = municipal sludge; TS = tannery sludge).

In agreement with the data description above, the dendrogram from HCA (Figure 1.3) showed an efficient separation of the two types of sludge. Only MS05 was excluded from

the rest of MS group. Furthermore, the short Euclidean distance observed in the TS group confirmed their similarity.

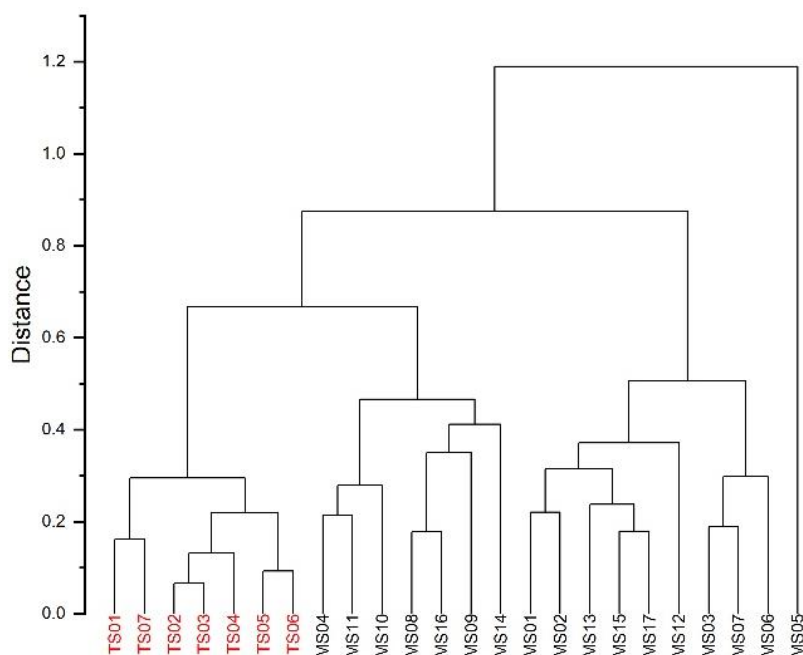


Figure 1.3 - Dendrogram from HCA related to the C and N analysis. Y-axis refers to the Euclidean distance.

1.3.2 ATR FT-IR analysis

Figure 1.4 shows the median (black line) and its interquartile range (the area between the red lines) of all the spectra acquired for both TS and MS samples. Spectra were characterized by distinct patterns, particularly in the 800 – 1800 cm^{-1} spectral region. Specifically, a sharp peak at 870 cm^{-1} appeared in the TS spectra; furthermore, a dominant and well-defined band at 1410 cm^{-1} distinguished these spectra from the municipal ones. Conversely, an intense band at 1030 cm^{-1} appeared only in the MS spectra.

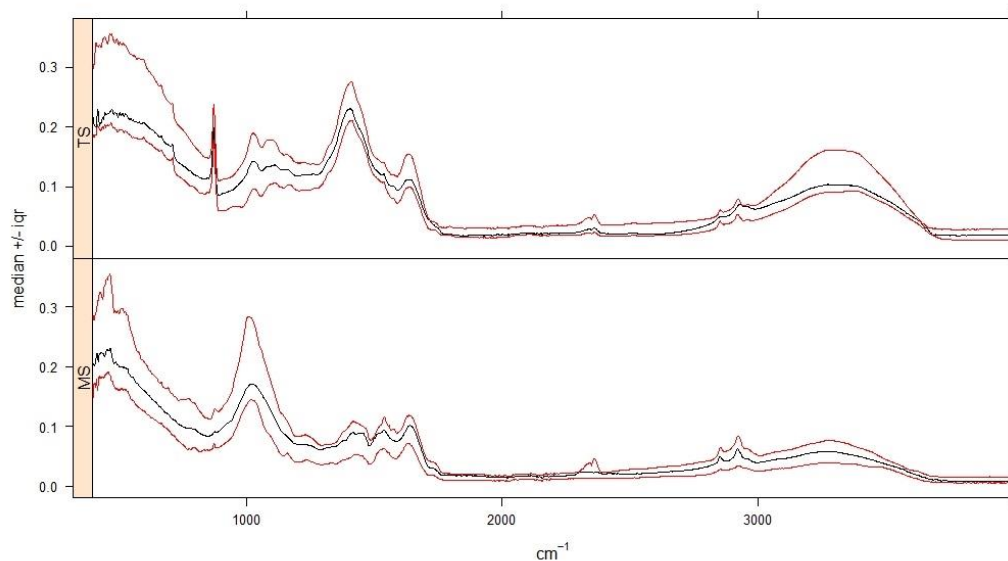


Figure 1.4 - FT-IR spectra of tannery sludge (TS; top panel) and municipal sludge (MS; bottom panel). Median (in black) and its interquartile range (in red)

The HCA performed considering FT-IR data in the specific range $800 - 1800 \text{ cm}^{-1}$ (the range with greater differences between the two types of sludge according to Figure 1.4) resulted in a dendrogram with no cluster based on sludge origin (Figure 1.5).

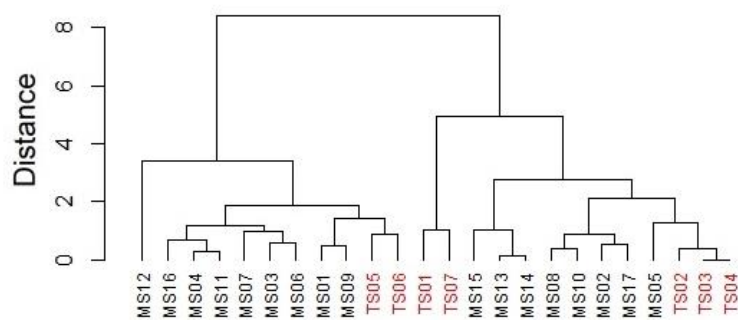


Figure 1.5 - Dendrogram from HCA related to FT-IR spectra. Y-axis refers to the Euclidean distance.

1.3.3 TG-DTA analysis

Figure 1.6 shows the median (black line) and its interquartile range (the area between the red lines) of all the DTA thermograms acquired. Three different regions can be identified.

The first, in the range 30 – 180 °C, was not discriminant of the two types of SS. Conversely, the region from 180 to 500 °C showed significant differences, with an intense exothermic peak approximately at 300 °C for TS, while MS presented a much less intense reaction at this temperature. In addition, the region 500 - 700 °C appeared different for the two types of SS; in fact, a broad band up to 700 °C appeared in TS, while a defined peak centred approximately at 500 °C characterized the profiles of MS.

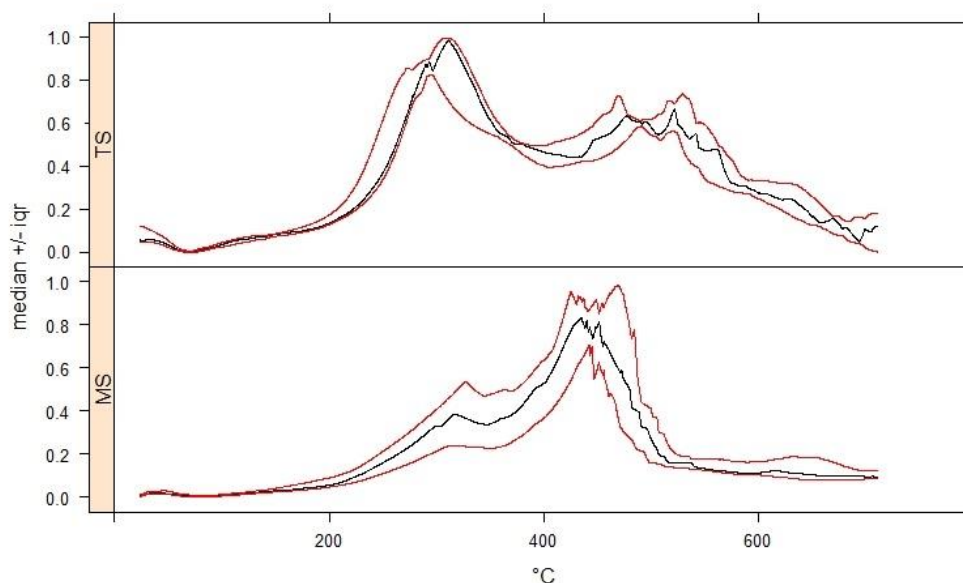


Figure 1.6 – Differential thermal analysis (DTA) of tannery sludge (TS; top panel) and municipal sludge (MS; bottom panel). Median (in black) and its interquartile range (in red).

The TG curves (Figure 1.7) showed the mass loss as a function of the temperature and in agreement with DTA results, the differences between the two types of SS were observed starting from 300 °C. A greater mass loss was evidenced by the MS at the intermediate temperatures; conversely, in the hottest region (above 500 °C), TS showed a decreasing trend, while the curve related to MS was clearly flat.

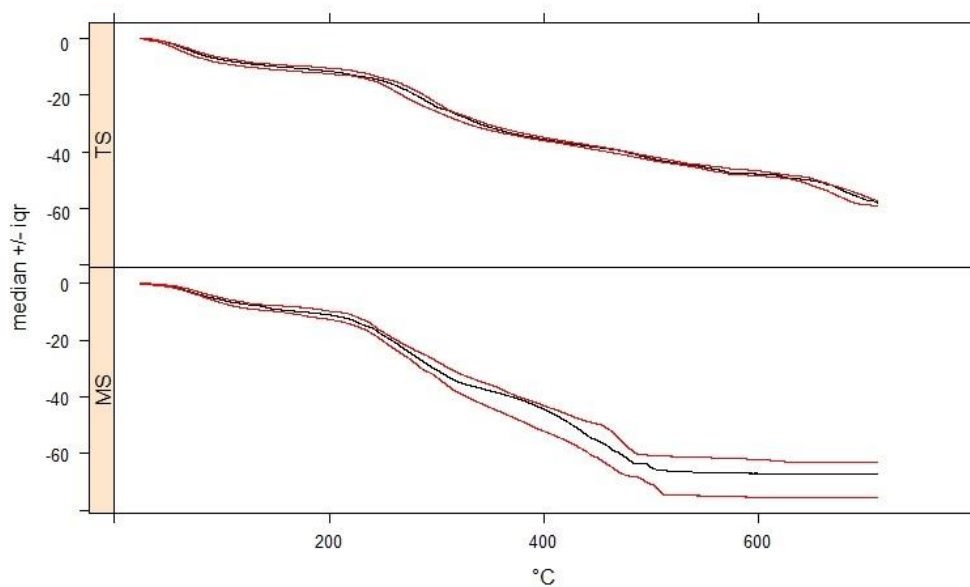


Figure 1.7 – Thermogravimetric analysis (TG) of tannery sludge (TS; top panel) and municipal sludge (MS; bottom panel). Median (in black) and its interquartile range (in red).

The HCA was applied for both DTA (Figure 1.8) and TG (Figure 1.9) data. Compared to the dendrogram obtained with the FT-IR spectral data, in this case the results showed a significant clustering of the sludge types. Concerning the DTA, TS samples clustered in a different group from MS samples, which were instead found to be divided into two clusters, the smallest of which, constituted by MS16, MS04 and MS14, was more similar to TS samples than the remaining MS ones; in the case of TG, only MS14, MS08 and MS16 samples were in the same group of TS. This is probably because these four MS had similar characteristics to TS.

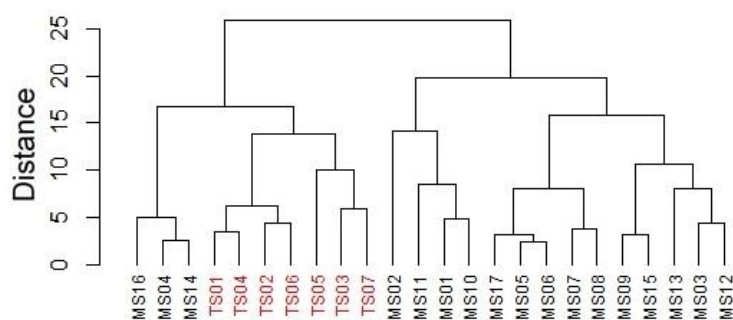


Figure 1.8 - Dendrogram from HCA related to differential thermal analysis (DTA). Y-axis refers to the Euclidean distance.

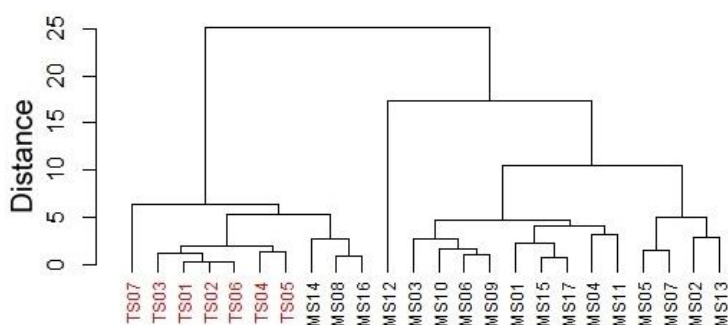


Figure 1.9 - Dendrogram from HCA related to thermogravimetric analysis (TG). Y-axis refers to the Euclidean distance.

1.4 DISCUSSION

1.4.1 Evaluation of C and N analysis

Elemental analysis of total C and N allowed getting preliminary information on SS quality. The high data distribution showed by the MS surely reflects the different site of origin of the samples and probably a different treatment process. Indeed, the organic matter in SS is commonly subjected to degradation with the aim to stabilize the final

products, and as explained by Anjum et al. (2016), many pre-treatment and treatment technologies have been developed, and can be applied as single or combined procedures (e.g., thermal, Fenton, microwave, ultrasonic, photocatalysis). Moreover, the SS intrinsic characteristics play a key role in determining the efficiency of these processes, since the presence of toxic heavy metals, complex structural components and/or other inhibitory compounds could affect the organic matter degradation mechanisms (Anjum et al., 2016; Manara & Zabaniotou, 2012). As a result, these factors might lead to SS characterized by very different C and N amounts, probably due to the different degree of volatilization that occurs in the processes discussed above. For instance, anaerobic digestion represents one of the most common methods for sludge stabilization, as it allows for reducing odours, pathogens and volatile solids transforming the organic matter C in methane and carbon dioxide (Nazari et al., 2017). Regarding the N fate, it mainly depends on the wastewater treatment, in which the conventional nitrification/denitrification process is the most applied method (McCarty, 2018). In particular, N is removed as N_2 through a first oxidation step conducted by autotrophic bacteria in aerobic conditions (NH_4^+ is oxidized first to NO_2^- and then to NO_3^-), followed by a reduction step operated by heterotrophic bacteria in anoxic environment (NO_3^- is reduced to N_2) (Capodaglio et al., 2016). Conversely, the small distribution data observed for the TS is clearly related to the fact that samples were provided by the same WWTP. It is noteworthy that the average total content of C and N in TS samples was lower than in MS ones; this outcome is probably (unfortunately, operators of WWTPs do not release precise information on the types of treatments adopted) due to supplementary or more-targeted treatments applied on TS necessary to reduce the high load of inorganic compounds (sulphides, ammonia, etc...). Indeed, Kavouras et al. (2015) reported that tannery wastewaters are pre-treated with lime and inorganic coagulants to achieve the precipitation of the dissolved chromium. In addition, the research paper by Zhao et al. (2022) listed other specific treatment processes for the tannery wastewater, such as adsorption, electrochemical, biological, membrane filtration and advanced oxidation methods, which could significantly impact on C and N content.

The results of isotopic ratio, as well as the analysis of total C and N, yielded promising outcomes. In fact, quite different values distinguished the two types of SS, showing a higher $\delta^{13}C$ but a lower $\delta^{15}N$ for TS. As reported by several authors (Boecklen, 2011; Hoeninghaus & Zeug, 2008; Post, 2002), the study of stable isotope can be exploited to

investigate the trophic relationship. In our case, it could be assumed that the feeding of the cattle involved in the tanning of hides plays an incisive role in determining such differences. In fact, one of the main feed in their diet is corn, a C_4 plants characterized by a $\delta^{13}C$ ranging from -12 to -14 ‰ (Bontempo et al., 2012; Ohkouchi et al., 2015), thus potentially leading to an increase of the $\delta^{13}C$ of TS. In addition, the lower $\delta^{15}N$ values found for TS can be related to the food chain, indeed Behkami et al. (2017) reported low $\delta^{15}N$ values ranging from -1 to 6 ‰ for C_4 plants.

This hypothesis is closely related to the statement by Onodera et al. (2021) that SS isotopic signature might be influenced by food consumed locally. Furthermore, this consideration contributes to explain the wider distribution data observed for MS, probably linked to the different WWTPs in which MS were sampled.

Another interpretation may be related to the different treatment processes the SS undergoes. In fact, the methane fermentation is responsible of isotopic fluctuation of $\delta^{13}C$ (Onodera et al., 2015, 2021), leading to higher values in sludge generated in plants where anaerobic treatment is not foreseen. This observation might suggest that the TS considered in this study were not subjected to anaerobic digestion, but other steps mentioned above might have been preferred. Moreover, the scientific literature reports that also the biochemical and chemical reactions related to N, such as ammonia stripping, nitrification and denitrification, have a distinct isotopic enrichment in ^{15}N (Onodera et al., 2015, 2021). Consequently, the lower $\delta^{15}N$ measured in the TS samples could suggest that these processes are partially or totally not applied in wastewater treatment at that WWTP.

The two hypotheses proposed (food chain and treatment processes) might be alternatives or concomitants. In any case, the HCA grouped MS and TS well, which means that both the total content and the isotopic signature of C and N discriminated the origin of these of SS.

1.4.2 Evaluation of ATR FT-IR and TG-DTA analysis

FT-IR and TG-DTA were chosen as analytical techniques to characterize the samples with the aim to highlight the differences between the two types of SS considered. Indeed, several authors have applied these methods to obtain a qualitative evaluation of a wide spectrum of organic matrices, such as organic fertilizers, amendments, anaerobic

digestate and SS (Cuetos et al., 2010; De Oliveira Silva et al., 2012; Eskicioglu et al., 2006; Francioso et al., 2010; Kowalski et al., 2018; Smidt & Schwanninger, 2005).

Regarding the FT-IR, the spectral area ranging from 800 to 1800 cm^{-1} was of greatest interest in this study. In fact, no relevant differences were found for the peaks at 2920 and 2850 cm^{-1} , which means that the two types of SS did not significantly differ in the amount of aliphatic compounds (Cuetos et al., 2010; Smidt & Schwanninger, 2005). Conversely, a sharp peak at 870 cm^{-1} and a large and intense band at 1405 cm^{-1} were present only in the TS spectra. The first peak is typically associated to the presence of carbonate (Smidt & Schwanninger, 2005); this result may be the evidence of the use of propylene carbonate, which is commonly employed as green solvent in the chrome tanning process (Sathish et al., 2016; Zhang et al., 2019). Even the band at 1405 cm^{-1} can be ascribed to the C-O stretching of the carbonate (Smidt & Schwanninger, 2005), but Cuetos et al. (2010) reported that it can be attributable also to the C=O stretching of phenols. The latter attribution is supported by the findings of many authors, which reported a high presence of phenolic compounds in the tannery wastewater (Liknaw et al., 2017; Yuan et al., 2021). On the other hand, a band at 1030 cm^{-1} prevailed in the MS spectra, while in the TS it appeared much less intense. Smidt & Schwanninger (2005) associated this band to the presence of silicates, which represent a class of minerals widely used in the wastewater treatment plants due to their capability to act as sorbents for both biogenic compounds and PTE (Wiśniowska & Włodarczyk-Makuła, 2016). This band showed a wider distribution around the median of MS spectra (Figure 1.4), a factor probably due to the different amount of silicates used in the WWTPs.

Despite the qualitative differences described above, the HCA was unable to differentiate the SS on the basis of their origin (Figure 1.5); however, this result is not surprising since it is quite difficult to identify, with a single analysis, complex matrices such SS, which can widely differ in their composition and in the treatment undergone.

Thermal analysis (TG-DTA) gave more promising results in terms of ability to differentiate the two types of sludge. The DTA curves showed for both the types of SS an exothermic peak in the region 250 - 350 °C, attributable to the combustion of organic thermolabile components, such as polysaccharides, proteins and peptides (Francioso et al., 2010; Montecchio et al., 2006). TS samples developed a greater heat flow with respect to MS samples in this temperature range, thus meaning that they are richer of these classes of organic compounds. This outcome was expectable, as TS contains a significant amount

of proteins and peptides deriving from leather tanning process (Basegio et al., 2002). The second exothermic peak found in the region 400 – 500 °C is commonly associated to the thermal decomposition of aromatic rings, long chain N-alkyl structures and saturated aliphatic chains (De Oliveira Silva et al., 2012; Montecchio et al., 2006). In this case, the amount of heat flow produced was greater in MS than in TS, reflecting the greater presence of these more refractory compounds. This result agrees with the outcomes of De Oliveira Silva et al. (2012), which found a similar DTA profile in the thermal analysis of MS collected in Brazil. The temperature region > 550 °C could be considered equally interesting, as it appeared different for the two types of SS. Indeed, while the curve of MS is substantially flat, the TS curve is characterized by a significant exothermic band, which is extended up to 700°C. The reason for this difference could be related to the combustion of inorganic salts present in TS, probably used as coagulants in the tannery wastewater to remove the dissolved chromium (Kavouras et al., 2015).

The TG curves confirmed the DTA dynamics in the temperature range 550 – 700 °C, in fact, while there was no mass loss for MS, a steady lowering was observed for TS.

The differences discussed above reflected the results of HCA, which efficiently separated the two types of SS. Only MS14, MS08 and MS16 clustered close to the TS group and more distant from the remaining MS samples, probably because they were characterized by a higher percentage of recalcitrant C, which degrades at temperature above 550 °C.

1.5 CONCLUSIONS

The results showed that the analyses applied in this study are potentially useful in discriminating a SS from a tannery or municipal WWTP. Both elemental and isotopic analysis of C and N delivered interesting outcomes, leading to assume that the different wastewater treatments strongly affect their final concentration in SS. In addition, the intrinsic properties of the materials entering the WWTPs could play a relevant role; for instance, livestock feeding could characterize the isotopic ratio of the final TS.

The cluster analysis applied to the FT-IR spectra did not yield a satisfying grouping of the two types of SS; however, a comparison between the spectra showed characteristic peaks for each of the two groups, highlighting differences probably related to the different chemical reagents used in the treatment processes.

The thermal analysis turned out to be a targeted analysis to reach the aim of this study, as confirmed also by the cluster analysis. TG and DTA showed different profiles for each type of SS, corroborating the hypothesis that they are characterized by a different chemical composition. In fact, a greater presence of proteins and inorganic salts are attributed to TS, while aromatic rings and/or saturated aliphatic chains prevail in MS. The analytical methods outlined in this study, accompanied by a complete physico-chemical characterization of the products, could provide useful information for the rational application of SS in agriculture.

CHAPTER 2

**NITROGEN AVAILABILITY IN ORGANIC FERTILIZERS
FROM TANNERY AND SLAUGHTERHOUSE BY-
PRODUCTS**

2.1 INTRODUCTION

The use of organic fertilizers (OFs) represents a common agricultural practice to increase both nutrients and organic matter (OM) content in the soil (Luo et al., 2018). This class of fertilizers contributes to alleviation of problems related to desertification and soil erosion, improving physical, chemical and biological properties of depleted soils by supplying OM (Carbonell et al., 2011; Spångberg et al., 2011; Svanbäck et al., 2019; Zhang et al., 2019). They also play an important role in the reduction of environmental impact, minimizing the use of chemical fertilizers, which create concerns both in their (mis)use and in their production (Ott & Rechberger, 2012; Spångberg et al., 2011; Svanbäck et al., 2019; Zhang et al., 2019). Furthermore, using OFs partially permits solving problems related to the disposal of biomasses, usually destined to landfill or incineration creating potential risks for the environment (Sharma et al., 2019).

Despite their “green attitude”, OFs, as well as the chemical ones, must be managed with awareness, since excessive and misleading use could lead to environmental contamination or pollution due to the dispersion of nutrients in other parts of the ecosystem (Song et al., 2017). In particular, nitrogen (N) represents the most crucial macronutrient for plant nutrition. Still, at the same time, the amount that is not absorbed by plants impacts not only on the soil itself, leading to acidification process, but also on the other environmental compartments in terms of coastal eutrophication, air pollution, increase of greenhouse gas emissions, and loss of biodiversity (Billen et al., 2013; Galloway et al., 2003; Lassaletta et al., 2014; Sutton & Bleeker, 2013).

The OFs are typically divided, by source, into: (i) animal-based, such as blood meal, fish meal, leather meal, horn and hoofs meal, slaughterhouse by-products, and manure and (ii) plant-based, such as crop residues and seaweed extracts. Unfortunately, we have only partial data about the amount of global animal by-products available for OFs production; for example, in the European Union and UK about 1.4 billion tons of manure are generated annually (Köninger et al., 2021), and the global slaughterhouse by-products are estimated at about 150 million tons per year (Limeneh et al., 2022). Therefore, considering that the global production of meat is projected to progressively grow until 2050 (Bustillo-Lecompte & Mehrvar, 2015), we expect that the amount of animal by-products available for OFs productions will increase. The recycling of this huge amount of materials containing N in agriculture as fertilizers is an opportunity, but also a matter

of concern considering the lack of knowledge about the availability of N to plants (Cassity-Duffey et al., 2020; Lazicki et al., 2020; Sigurnjak et al., 2017).

Organic N fertilizers are generally constituted by two different pools of N consisting in inorganic (N_{in}) and organic (N_{org}) forms (Figure 2.1). While the N_{in} compounds, ammonium (NH_4^+) and nitrate (NO_3^-), are readily available to plants, the N_{org} component is characterized by a wide spectrum of organic substances (Whalen et al., 2019), which, according to their chemical characteristics, have a different behavior in soil and can be readily as well as scarcely bioavailable. In fact, the N_{org} fraction can be immediately available or speedily mineralizable by microorganisms (i.e., amino acids and small peptides), or recalcitrant and slowly mineralizable (i.e., polypeptides and heterocyclic N compounds). For these reasons, OFs management is still a challenge for agronomists, as knowing the potentially mineralizable organic N (N_0) and its mineralization rate is critical to achieve appreciable N use efficiency of OFs. Since these pools are strictly related to the raw materials and the transformation process from which OFs derive, the amount of N_0 as well as the rate at which it becomes bioavailable in soils (Figure 2.1) is highly affected by OFs' origin (Cassity-Duffey et al., 2020).

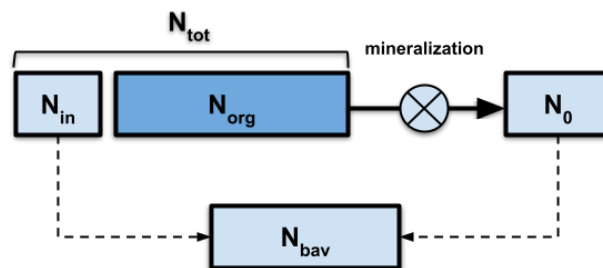


Figure 2.1 - Schematic representation of the bioavailable fraction of nitrogen in organic fertilizers (N_{tot} = total N; N_{in} = inorganic N; N_{org} = organic N; N_0 = potentially mineralizable organic N; N_{bav} = bioavailable N).

In order to optimize N efficiency, it is therefore important to know the amount of N_{in} , as well as of N_0 , since these pools are potentially available for crops and their sum can be defined as bioavailable N (N_{bav}). While N_{in} is obtainable by straightforward chemical analysis (i.e., extraction with 1 M KCl and determination of ammonium and nitrate in the extract), the determination of N_0 requires a long-time incubation essay, resulting in a time- and reagents-consuming experiment (Honeycutt et al., 1988; Stanford & Smith, 1972).

Therefore, developing a rapid method capable of giving a reliable indication of the N_0 content in both soils and fertilizers has always aroused great interest. For instance, several authors (Bremner & Keeney, 1965; Curtin et al., 2006; Hussain et al., 1984) found satisfying methods to estimate the organic N mineralization capacity (i.e., N_0) of the soil through a single chemical extraction using hot water, potassium permanganate and warm water, respectively. Dell'Abate et al. (2003) conducted a study on leather meal-based fertilizers, determining the faster and slower soluble N pools using phosphate buffer extractions and correlating them with the fertilizers' particle sizes. Cassity-Duffey et al. (2020) stated that the total N (N_{tot}) content of the fertilizers could be used as an estimate of the N_0 , while according to other authors (Delin et al., 2012; Lazicki et al., 2020) the C:N ratio is the most indicative parameter.

The aims of this study were (i) to determine the bioavailable N in organic fertilizers from animal by-products subjected to different treatment such as anaerobic digestion, thermobaric hydrolysis, chemical and biological stabilization, (ii) to determine the hot-water extractable N in the organic fertilizers, and (iii) to study the relation between bioavailable N and chemical indicators of N availability, thus assessing the possibility to predict the bioavailable N starting from these indicators.

2.2 MATERIALS AND METHODS

2.2.1 General description of the organic fertilizers

Nine organic fertilizers (OFs) obtained from the manufacturer or from the market were codified by an increasing numbering from OF01 to OF09 (Table 2.1). OF01 and OF07 were anaerobic digestates obtained from slaughterhouse by-products, and were classified as nitrogen-phosphorus (NP) OFs. Similarly, OF02 was a NP OF derived from chemical stabilized tannery sludge mixed with meat and bone meals. OF03 and OF05 were N OFs resulting from mixing chemical stabilized tannery sludge and leather meal. OF04, OF08 and OF09 were N OFs obtained from leather by-products after thermobaric hydrolysis. OF06 was a bio-solid derived from the biological stabilization of tannery sludge.

Table 2.1 - Codes, raw materials and transformation processes of the organic fertilizers collected.

Code	Raw Materials	Transformation Process
OF01	Slaughterhouse by-products	Anaerobic digestion
OF02	Tannery sludge + meat and bone meals	Chemical stabilization
OF03	Tannery sludge + leather meal	Chemical stabilization
OF04	Leather meal	Thermobaric hydrolysis
OF05	Tannery sludge + leather meal	Chemical stabilization
OF06	Tannery sludge	Biological stabilization
OF07	Slaughterhouse by-products	Anaerobic digestion
OF08	Leather meal	Thermobaric hydrolysis
OF09	Leather meal	Thermobaric hydrolysis

2.2.2 Characterization of the organic fertilizers

All the OFs were ground in a ball mill (Mixer mill MM400, Retsch GmbH, Haan, Germany) and sieved at 0.5 mm before analysis. The chemical reaction (pH) was measured in 1.5:25 mass-to-water ratio using a platinum electrode (5261 electrode, Crison Instruments SA, Alella, Spain) connected to a pH-meter (Compact titrator, Crison Instruments SA, Alella, Spain). The electrical conductivity (EC) was measured in 1:5 mass-to-water ratio using an electrical conductivity meter (Radiometer Analytical CDM 210, Hach Company, Loveland, CO, USA) equipped with a conductivity cell (Radiometer Analytical CDC 749, Hach Company, Loveland, CO, USA). Total solids (TS) and ashes were determined reaching the constant weight at 105 and 650 °C, respectively, using an oven (FD 23 model, Binder GmbH, Tuttlingen, Germany). Volatile solids (VS) were calculated by the difference between 100 and the ashes value. Total organic carbon (TOC) was determined according to the dichromate method (Springer and Klee, 1954). Total Kjeldahl nitrogen (TKN) was determined after acid digestion with sulfuric acid and selenium-potassium persulfate as catalyzer, using a Kjeldahl automatic instrument (KjelFlex K360, BUCHI Labortechnik AG, Flawil, Switzerland). The ammonium N ($\text{NH}_4^+\text{-N}$) was determined according to the 920.03 A.O.A.C. method (A.O.A.C. *Official*

Methods of Analysis, 1990). Briefly, OFs were extracted with 1 M potassium chloride (KCl) at 1:50 mass-to-volume ratio for 2 h, then an aliquot of filtrate (20 mL) was dispensed into a digestion tube and analyzed in the Kjeldahl automatic instrument after adding 1 g of magnesium oxide (MgO). The nitrate N (NO_3^- -N) was determined with the same method, after reduction with 0.5 g of Devarda alloy (Carlo Erba, Italy). The total organic nitrogen (N_{org}) was calculated by the difference between TKN and NH_4^+ -N. The total N was considered equal to TKN because the NO_3^- -N was under the detection limit of the method for all the OFs. Total phosphorus (P) was determined by an inductively coupled plasma optical emission spectrometer (Spectro Arcos ICP-OES Analyzer, Spectro Analytical Instrument GmbH, Kleve, Germany) after flame digestion with 96% nitric acid.

2.2.3 Soil description and characterization

The soil used in the incubation test was sampled from the surface layer (0–0.2 m) of a cultivated field from the University of Bologna experimental farm located in the southern part of Po Valley, Italy (45.53° N, 11.38° E, 28 m a.s.l.). Once arrived in the laboratory, the soil was air dried, sieved at 2 mm and cleaned from plant debris. The main soil physical and chemical properties were determined according to the Soil Science Society of America methods (Sparks et al., 1996) and the results are shown in Table 2.2. The soil was classified as a fine silty, mixed mesic Udic Ustochrept (*Soil Survey Staff Soil Taxonomy: A Basic System of Soil Classification for Making and Interpreting Soil Surveys*, 1999), and it was a sandy-loam soil characterized by a sub-alkaline pH with an average content of TOC and TN.

Table 2.2 - Main characteristics of the soil used in the trial.

Parameters	Unit	Value
Texture (U.S.D.A.)		sandy-loam
Sand	g kg ⁻¹	700
Silt	g kg ⁻¹	260
Clay	g kg ⁻¹	140
pH (in water)		7.8
Electrical conductivity	dS m ⁻¹	0.17
Cation exchange capacity	cmol _c kg ⁻¹	23.4
Total carbonates	g CaCO ₃ kg ⁻¹	65
Total organic carbon	g C kg ⁻¹	21.6
Total nitrogen	g N kg ⁻¹	2.15
C:N ratio		10.1
Available phosphorous	mg P kg ⁻¹	64
Exchangeable calcium	mg Ca kg ⁻¹	5150
Exchangeable potassium	mg K kg ⁻¹	430
Exchangeable magnesium	mg Mg kg ⁻¹	280
Exchangeable sodium	mg Na kg ⁻¹	32

2.2.4 Incubation of organic fertilizers into soil

Aliquots of 200 g of dry soil were placed into cylindrical plastic pots and pre-incubated for 15 days in controlled conditions of temperature (20 °C) and moisture (30% of full water holding capacity) in a growth chamber in the dark. During this period, moisture was checked and restored when needed. OFs were added to the pots in a weight equivalent to 100 mg N kg⁻¹ of dry soil (ds), corresponding approximately to 250–300 kg N ha⁻¹. The test was carried out in triplicate, according to a complete randomized design. In addition to the nine OFs, a negative control (CK) with no fertilizer added was included in the trial. The experiment, conducted under the same temperature and moisture conditions as the pre-incubation, lasted 7 weeks. A weekly soil sampling was carried out to

determine the inorganic N (N_{in}) according to the ISO 14256-2 protocol (ISO 14256-2:2005): aliquots of 5 g of soil were extracted in 50 mL of 1 M KCl for one hour, then the filtrate solution was analyzed by means of an automated flow analyzer (AutoAnalyzer 3, Bran Luebbe GmbH, Norderstedt, Germany).

The data obtained from the analysis of N_{in} were used to calculate the mineralized organic N (N_{min}) using the following equation:

$$N_{min(OF,t)} = [(N_{in})_{t=n} - (N_{in})_{t=0}]_{OF} - [(N_{in})_{t=n}]_{CK}, \quad (1)$$

where t is the sampling time, OF is the organic fertilizers added, CK is the control treatment.

The N_{min} values calculated for each product and for each sampling time were processed through a first order kinetic model:

$$N_{min} = N_0 \cdot (1 - e^{-kt}), \quad (2)$$

where N_0 is the potentially mineralizable organic N, k is the first order kinetic constant and t is the time. This equation provided qualitative and quantitative information on N mineralization, both in quantity and kinetic terms and it widely used in similar cases (Honeycutt et al., 1988).

Finally, using the data obtained from Equations (1) and (2), it was possible to calculate the N fraction made bioavailable by the OFs added to the soil (N_{bav}). It corresponds to the sum of the N_{in} at time zero and the N_0 :

$$N_{bav(OF)} = [(N_{in})_{t=0}]_{OF} - [(N_{in})_{t=0}]_{CK} + [N_0]_{OF}, \quad (3)$$

2.2.5 Hot-water extractable nitrogen

The determination of hot-water extractable nitrogen in OFs was performed following the procedure adopted by Curtin et al. (2006) to evaluate the soil nitrogen availability. Briefly, 5 g of product was added to 100 mL of deionized water and incubated in a water bath at 80 °C under agitation for 16 h. The sample was subjected to centrifugation (6000 rpm, 15 min, 20 °C) and filtration using Whatman No. 42 paper filters. The filtered extract was analyzed for N_{tot} , NH_4^+ -N and NO_3^- -N as described in Section 2.2.2.

The hot-water extractable N was then calculated by discriminating the hot-water total nitrogen (HWTN) and the hot-water organic nitrogen (HWON), according to the following equations:

$$\text{HWTN (\% } N_{\text{tot}}) = (\text{TN}_{\text{HW}}/N_{\text{tot}}) \times 100, \quad (4)$$

$$\text{HWON (\% } N_{\text{org}}) = (\text{TON}_{\text{HW}}/N_{\text{org}}) \times 100, \quad (5)$$

where TN_{HW} (hot-water total N) = $(\text{TN}_{\text{HW}} + \text{NO}_3^- - \text{N}_{\text{HW}})$ and TON_{HW} (hot-water total organic N) = $(\text{TN}_{\text{HW}} - \text{NH}_4^+ - \text{N}_{\text{HW}})$; TN_{HW} , $\text{NO}_3^- - \text{N}_{\text{HW}}$ and $\text{NH}_4^+ - \text{N}_{\text{HW}}$ are the total N, the nitrate N and the ammonium N extracted in hot-water; N_{tot} and N_{org} are the total N and the organic N of OFs.

2.2.6 Data handling and statistical analysis

The data obtained were handled and analyzed using the environment for statistical computing R (R Core Team, 2022). The first order kinetic model (equation 2) has two unknown parameters (N_0 and k), which are estimated using nonlinear regression procedure with the Marquardt–Levenberg algorithm and iterative method to find the parameters to minimize the residual sum of squares (Benbi & Richter, 2002). In some cases, manual adjustment of initial values was needed to obtain sensible results. The good-of-fitness of nonlinear models was estimated by the Pseudo- R^2 ($P\text{-}R^2$), calculated using the follow equation: $P\text{-}R^2 = 1 - (\text{RSS}/\text{TSS})$, where RSS is residual sum of squares and TSS is the total sum of squares (Schabenberger & Pierce, 2001). The half-time of organic N mineralization ($t_{1/2}$) was determined using the following equation: $t_{1/2} = \text{Ln}(2)/k$. The relationships between N mineralization (N_0 and N_{bav}) vs. hot-water extractable N (HWON and HWTN) and C:N ratio were assessed using simple linear regression analysis. The coefficient of determination ($R^2 = \text{SSreg}/\text{TSS}$, where SSreg is the sum of squares explained by regression and TSS is the total sum of squares) was calculated as an indicator of goodness of fit.

2.3 RESULTS

2.3.1 Characterization of organic fertilizers

The main characteristics of the OFs used are reported in Table 2.3. In general, the physico-chemical characteristics of OFs strictly reflected the raw materials and the production processes undergone. The OFs obtained from leather by-products (OF04, OF08, OF09) have acidic pH (4.3–4.7), probably due to the use of acids (i.e., sulfuric

acid) in the tanning treatment and in the leather by-products thermobaric hydrolysis (Ciavatta et al., 2012). The remaining OFs showed a sub-alkaline pH, ranging from 7.3 to 8.5, in agreement with previous research with similar materials (Kataki et al., 2017; Moukakis et al., 2018; Prado et al., 2022). The EC ranged between 0.9 to 5.3 dS m⁻¹, which represent typical values for this type of organic fertilizers (Kataki et al., 2017). Clearly, the EC depends on total soluble salts present in OFs, and the fact that OF04 showed the highest value is probably linked to the use of huge quantities of salts (i.e., NaCl) during the tanning process. However, high EC values were recorded in OFs subjected to chemical stabilization (OF02, OF03 and OF05).

Table 2.3 - Main physico-chemical characteristics of the organic fertilizers (*fw* = fresh weight, *dw* = dry weight).

Parameters	OF01	OF02	OF03	OF04	OF05	OF06	OF07	OF08	OF09
pH	7.7	7.9	7.6	4.3	7.5	8.5	7.3	4.7	4.3
Electrical cond. (dS m ⁻¹)	0.9	5.1	4.4	5.3	3.53	2.75	2.5	2.4	3.8
Total solids (% fw)	90.7	91.5	93.4	96.6	93.3	90.3	88.5	84.6	91.7
Volatile solids (% dw)	83	43	57.6	90.7	55.1	44.7	81.4	91.1	89.4
Ash (% dw)	17	57	42.4	9.3	44.9	55.3	18.6	8.9	10.6
Total organic C (% dw)	44.2	14.3	31.6	46.2	34.9	32.4	40.2	47.6	47.1
Total Kjeldahl N (%)	4.47	4.11	5.74	14.8	4.27	2.78	5.03	15.7	13.5
C:N ratio	9	5.2	5.5	3.1	8.4	12	8	3	3.5
Ammonium N (% dw)	0.17	0.51	0.14	0.25	0.1	0.07	0.60	0.05	0.03
Nitrate N (% dw)	<0.01	<0.01	<0.01	<0.01	<0.01	<0.01	<0.01	<0.01	<0.01
Organic N (% dw)	4.3	3.6	5.6	14.6	4.17	2.71	4.43	15.7	13.5

All samples were in dried form and contained approximately 90% of total solids (TS). Differently, the volatile solids (VS) were found in a wide range, from 43 to 91%. OFs derived from leather (OF04, OF08, OF09) and slaughterhouse by-products (OF01, OF07) showed higher VS, up to 70%, clearly due to the high content of OM of the raw materials. The percentage of ashes was inversely proportional to the content of VS, and was higher in OFs derived from tannery sludge (OF02, OF03, OF05 and OF06), probably due to inorganic compounds (i.e., inorganic salts) present in these materials.

Total organic carbon (TOC) of OFs ranged from 14 to 47% (Table 2.3). This large range of TOC is due to the different chemical characteristics of raw materials used for OFs production (Kataki et al., 2017; Moukazis et al., 2018; Prado et al., 2022) and represents an important indicator for OFs quality. Total Kjeldahl nitrogen (TKN), as well as total organic nitrogen (N_{org}), was significantly higher in OFs made from leather by-products (OF04, OF08 and OF09), presenting values ranging from 13 to 15%, clearly due to the large amounts of animal proteins (or polypeptides) in the raw material. The lowest value of TKN was found in OF06 (2.78%), the only sample obtained from tannery sludge that does not include the addition of other raw materials, such as for OF02, OF03, and OF05. As expected, the higher the TKN the lower the C:N ratio, which showed values approximately of 3 for OF04, OF08 and OF09, and of 12 for the OF06.

While the nitrate N (NO_3^- -N) content was below the detection limit of the method (<100 ppm), the ammonium N concentration (NH_4^+ -N) ranged from 0.03 to 0.60%. In this case, there was no discrimination based on raw materials; the differences probably depend on the specific productive processes used. In any case, the amount of inorganic (or ammonium) N was a small fraction of TKN, and the organic N was always higher than 95% of TKN.

2.3.2 Incubation of organic fertilizers in the soil

The dynamics of NH_4^+ -N showed significant differences only at the beginning of incubation (t_0) since this form of N is immediately released in soil by the input of OFs (Figure 2-top and Table 2.4). In fact, OF02 and OF07 presented the highest values of NH_4^+ -N released, being the two characterized by the highest percentage of NH_4^+ -N content (Table 2.3). In the subsequent samplings, all OFs showed values close to zero and equal to the untreated soil (CK) suggesting that NH_4^+ -N was subjected to soil nitrification process.

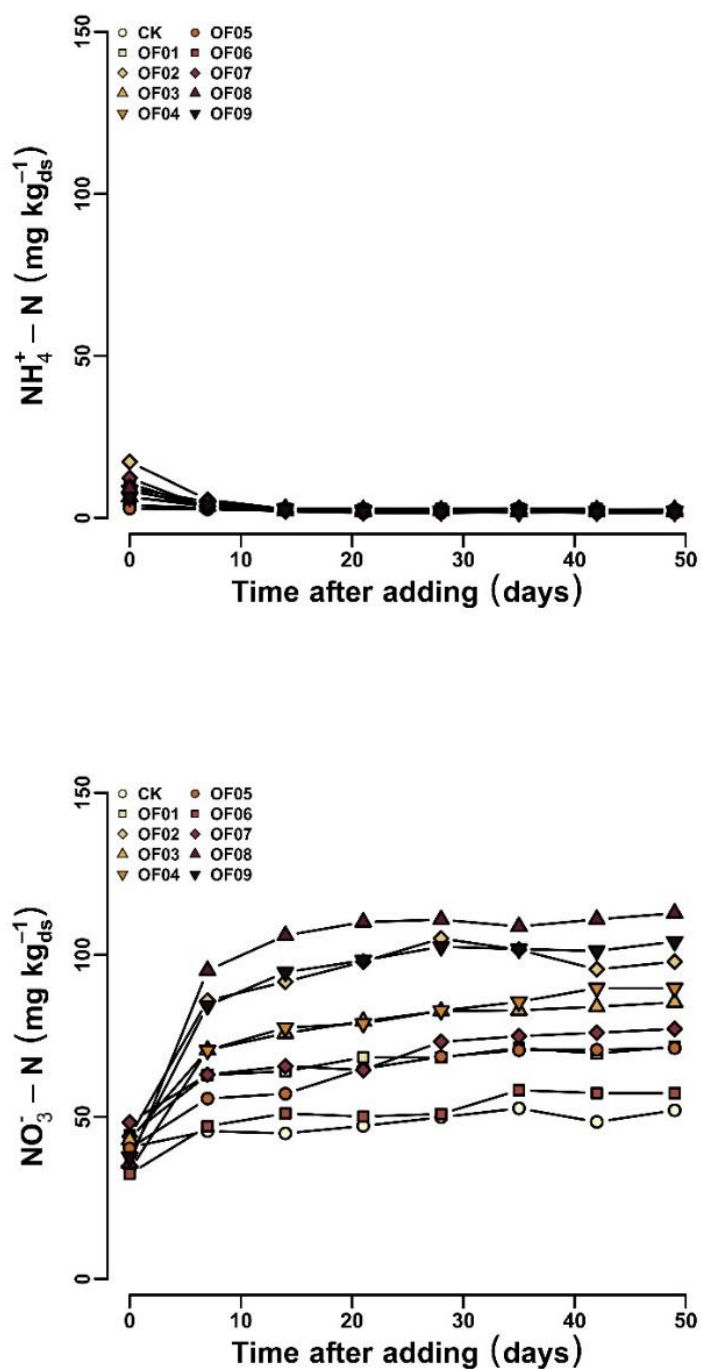


Figure 2.2 - Inorganic N release during the incubation of organic fertilizers in the soil: ammonium N (top), and nitrate N (bottom)

This view was supported by the analysis of nitrate which manifested an opposite trend to that of ammonium (Figure 2.2-bottom). In fact, an increase was observed in the first

period, from the beginning to the 14th day, followed by a general stabilization phase until the end of the incubation. In particular, OF08 was the sample that released the most nitrate N, showing values above 100 mg N kg⁻¹ d.s. starting from the fourteenth day. OF09 and OF02 showed approximately the same trend, achieving values around 90 mg N kg⁻¹ d.s. in the same period, followed by a slight decrease of OF02 in the last two samplings. A value of 75 mg N kg⁻¹ d.s. was reached and exceeded by both OF04 and OF03 during the incubation. In particular, the fertilizer deriving from leather meal (OF04) showed slightly higher values than OF03 in the last three sampling dates (t₃₅, t₄₂, t₄₉). OF07 displayed an increase between the 3rd and the 4th week of incubation (respectively t₂₁ and t₂₈), reaching values above 60 mg N kg⁻¹ d.s., as well as OF05 and OF01. OF06 was the sample that presented the lowest values (50 mg N kg⁻¹ d.s.), but showed a positive trend compared to the unfertilized control.

Table 2.4 - Fitting of inorganic N release in the soil after incubation with organic fertilizers (N_{in} is the inorganic N at the beginning of incubation, N_0 is the potentially mineralizable organic N, N_{bav} is the sum of N_{in} and N_0 , k is the first order kinetic constant, $t_{1/2}$ is the half-time of organic N mineralization and $P-R^2$ is the Pseudo R-squared coefficient of the first order kinetic model).

Data are reported as mean ± standard error of the mean.

Fertilizers	N_{in} (%N _{tot})	N_0 (%N _{tot})	N_{bav} (%N _{tot})	k (days ⁻¹)	$t_{1/2}$ (days)	$P-R^2$
OF01	7.9 ± 4.1	16.1 ± 1.0	24.0	0.177 ± 0.066	3.9	0.887
OF02	16.7 ± 5.5	36.1 ± 1.4	52.8	0.165 ± 0.035	4.2	0.959
OF03	4.8 ± 2.7	29.6 ± 1.9	34.4	0.162 ± 0.056	4.3	0.895
OF04	4.3 ± 2.9	36.0 ± 2.2	40.3	0.110 ± 0.023	5.8	0.951
OF05	2.8 ± 1.5	32.0 ± 1.0	34.8	0.173 ± 0.035	9.8	0.962
OF06	7.3 ± 3.2	6.8 ± 0.6	14.1	0.294 ± 0.252	28	0.766
OF07	12.0 ± 0.3	13.1 ± 1.4	25.1	0.037 ± 0.020	8.8	0.865
OF08	1.5 ± 0.5	63.1 ± 0.3	64.6	0.211 ± 0.016	3.6	0.996
OF09	0.5 ± 0.2	54.1 ± 0.6	54.6	0.260 ± 0.010	3.9	0.999

Figure 2.3 shows the curves of mineralization of the organic N during the incubation period. The asymptote of these first kinetic order curves is equal to N_0 , the potentially mineralizable organic N, results for which are reported in Table 2.4.

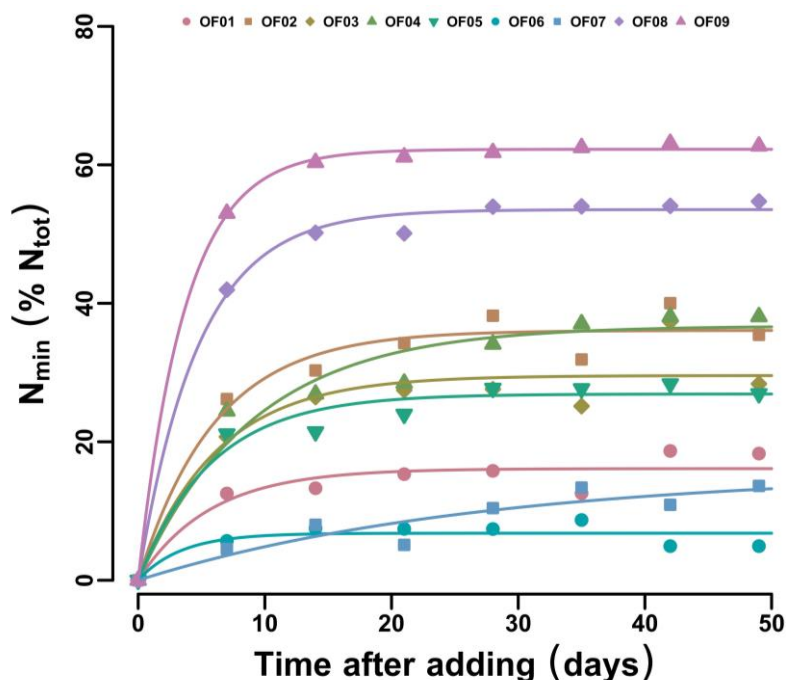


Figure 2.3 - First order kinetic model fitting of organic N mineralized in the soil incubated with the organic fertilizers.

As expected, the kinetic curves are very similar to those obtained with the NO_3^- -N analysis, since the NH_4^+ -N release showed no differences between the fertilized mixtures and the unfertilized control, except for t_0 . OF08 and OF09 showed the greater ability to mineralize, reaching values of mineralization of 63 and 54% of the total N added, respectively (Table 2.4). The mineralization percentage ranged from 29.6 to 36% for OF04, OF02, OF05 and OF03, while OFs deriving from anaerobic digestion, OF01 and OF07, attained 16 and 13%, respectively (Table 2.4). As confirmed by the NO_3^- -N analysis, OF06 is the one that manifested the lowest ability to mineralize the organic N (6.8%). These results were quite expected, as OF01, OF07 and OF06 probably suffered a consistent loss of organic matter during the digestion and the biological treatment.

2.3.3 Hot-water extractable nitrogen

The results of HWON and HWTN are reported in Table 2.5. The values of HWON ranged between 10.5 (OF06) and 46.3% (OF02) of N_{org} , a wide range which, however, agrees

with the results of N_0 previously reported (Table 2.4). The higher HWON was observed for OF02, OF03, OF04, OF08 and OF09 with values ranging between 35 to 45% of N_{org} . These OFs were characterized by leather and bone meals as raw materials and chemical or thermobaric hydrolysis as transformation process (Table 2.1). Otherwise, OF01 and OF06 showed the lowest HWON, ranging between 10 to 20% of N_{org} . These fertilizers were made from slaughterhouse by-products and tannery sludge, respectively. The other OFs, from the same by-products, showed an intermediate HWON, with values ranging from 25 to 30% of N_{org} . The values of HWTN were slightly higher than HWON (Table 2.5), but closely related. Only OF02 and OF07 showed a difference between HWTN and HWON higher than 5%, due to their greater N_{in} content (Table 2.4).

Table 2.5 - Results of hot-water organic N (HWON) and hot-water total N (HWTN) analyses of the organic fertilizers.

Fertilizers	HWON (% N_{org})	HWTN (% N_{tot})
OF01	16.9	19.2
OF02	46.3	53.9
OF03	39.7	41.5
OF04	43.1	44.1
OF05	31.1	32.4
OF06	10.5	10.9
OF07	28.6	35.7
OF08	39.6	40.8
OF09	34.8	36.0

2.3.4 Correlation and linear regression between indicators of available nitrogen

The data concerning indicators of N availability in OFs were analyzed for correlation using the Pearson coefficient. The results obtained are shown in Table 2.6. The N_0 , N_{bav} , HWON and HWTN were significantly and positively correlated (p -value < 0.001). On

the other hand, N_0 and N_{bav} were significantly but negatively correlated with C:N ratio (p -value < 0.05).

Table 2.6 - Correlation between indicators of bioavailable nitrogen in organic fertilizers.

Correlation	Pearson Coefficient	Degree of Freedom	p -Value
N_0 vs. N_{bav}	0.962	7	<0.001
HWON vs. HWTN	0.980	7	<0.001
N_{bav} vs. HWTN	0.728	7	0.027
N_0 vs. HWON	0.691	7	0.039
N_{bav} vs. C:N ratio	-0.873	7	0.002
N_0 vs. C:N ratio	-0.863	7	0.003

The capacity of HWON, HWTN and C:N ratio to estimate N_0 and N_{bav} was assessed using the linear regression approach. The results are shown in Figures 2.4 and 2.5. The HWON showed a significant (p -value = 0.039) linear regression with the N_0 (Figure 2.4-left) and a $R^2 = 0.478$. Even if the slope of the straight line was 1.065 ± 0.420 (p -value = 0.039), with a quite perfect linearity between the two indicators, the samples OF08 and OF09 deviated from linearity and fell outside the 95% confidence limit. HWTN and N_{bav} showed similar results (Figure 2.4-right), with a significant linearity ($R^2 = 0.53$, p -value = 0.027), a slope of 0.921 ± 0.328 (p -value = 0.027) and the same samples outside of the 95% confidence limits. In both cases the estimated intercept was not significantly different from zero (respectively: -2.5 ± 14.4 (p -value = 0.87) and 6.1 ± 12.1 (p -value = 0.63)).

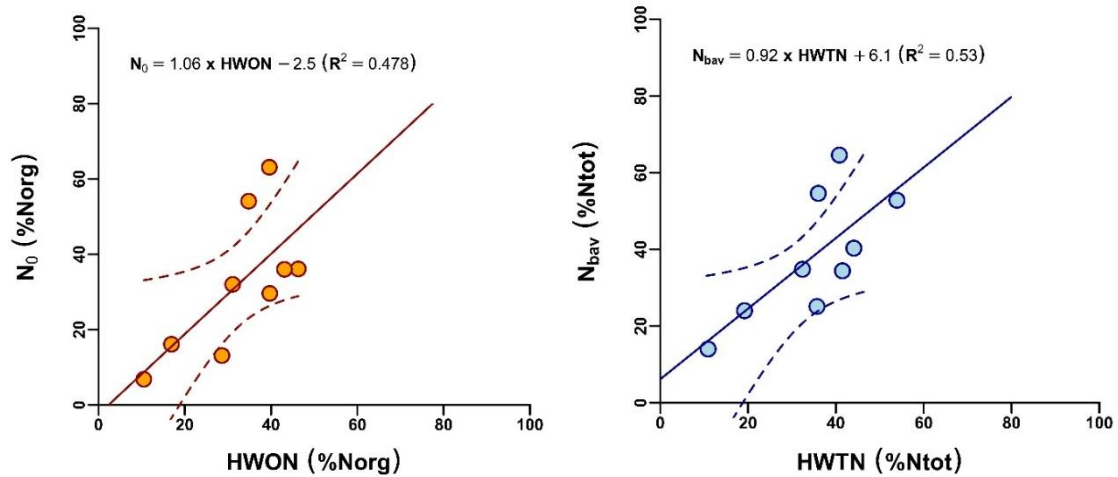


Figure 2.4 - Linear regression between: potentially mineralizable organic N (N_0) with hot-water organic N (HWON) (on the left), and bioavailable N (N_{bav}) with hot-water total N (HWTN) (on the right). The straight lines indicate the linear regression model and the dotted lines the 95% confidence limits.

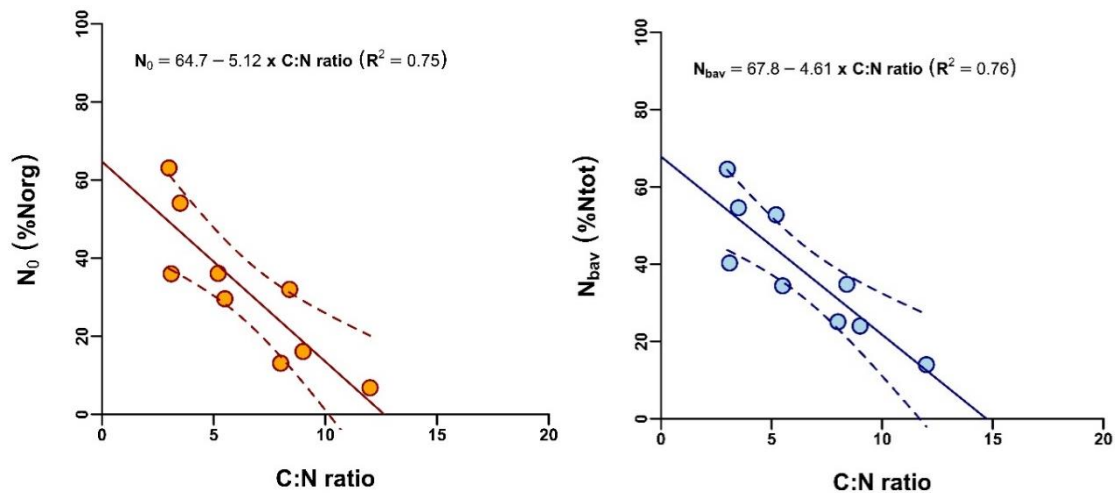


Figure 2.5 - Linear regression between: potentially mineralizable organic N (N_0) with C:N ratio (on the left), and bioavailable N (N_{bav}) with C:N ratio (on the right). The straight lines indicate the linear regression model and the dotted lines the 95% confidence limits.

The C:N ratio showed a significant linearity with N_0 ($R^2 = 0.75$, p -value = 0.003) (Figure 2.5-left) and N_{bav} ($R^2 = 0.76$, p -value = 0.002) (Figure 2.5-right). The slope was negative in both cases and significantly different from zero: -5.12 ± 1.13 (p -value = 0.003) and -4.61 ± 0.97 (p -value = 0.002), respectively, for N_0 and N_{bav} . The intercepts were higher than zero and corresponded to 64.7 ± 8.0 (p -value <0.001) and 67.8 ± 6.9 (p -value <0.001) for N_0 and N_{bav} , respectively.

2.4 DISCUSSION

2.4.1 Characterization and soil incubation of the organic fertilizers

After the physico-chemical characterization and incubation in soil, it is possible to classify the studied animal-based OFs in four groups: (i) leather meal from thermobaric hydrolysis, (ii) slaughterhouse by-products from anaerobic digestion, (iii) tannery sludge + animal based by-products from chemical stabilization, and (iv) tannery sludge from biological stabilization. In fact, this confirms that the source materials and treatment processes largely affected OFs characteristics and the N release in soil.

The OFs obtained from leather meals (OF04, OF08 and OF09) showed higher N_{tot} (12–14%) than other OFs, in agreement with the greater protein content of leather (Ciavatta et al., 2012; Corte et al., 2014; Dell'Abate et al., 2003). These OFs are characterized also by lower C:N ratio (3–3.5:1), higher volatile solids (77–88%) and lower ash contents (7.5–10%) than other OFs. Soil incubation indicated that this class of OFs mineralized more organic N, with a N_0 ranging from 36 to 63% of N_{tot} , resulting in 40–64% of bioavailable N (N_{bav}). The rate of mineralization was also higher than in other OFs studied, with a half-life time of 3.6–5.8 days at the experimental conditions applied in this study. Practically, the release of the bioavailable N in soil from these OFs proceeded intensely and quickly, similar to inorganic N fertilizers (Cayuela et al., 2010; Dell'Abate et al., 2003), due to the thermobaric hydrolysis that guaranteed a high availability of N_{org} for soil microorganisms, and to the lower C:N ratio that results in a lower N use efficiency by soil microorganisms and consequently a net N release into the soil (Mooshammer et al., 2014).

Slaughterhouse by-products after anaerobic digestion (OF01 and OF07) have been poorly studied as fertilizers (Bhunias et al., 2019; Limeneh et al., 2022), and they are characterized by a relatively high N_{tot} (4–5%) and low C:N ratio (8–9:1). Therefore, it is not surprising that these OFs released as N_{bav} only a quarter of the N_{tot} added to the soil. As previously discussed, the net mineralization of N_{org} in soil depends on the C:N ratio and on the quality or availability of OM for soil microorganisms. Regarding this class of OFs, a large part of the N_{bav} was directly released as N_{in} probably due to anaerobic digestion, which is well known to generate digestates that often contain important amounts of ammonium N (Albuquerque et al., 2012; Moukakis et al., 2018; Sigurnjak et al., 2017).

The tannery sludge-based OFs (OF02, OF03 and OF05) showed a N_{tot} content similar to the slaughterhouse by-products (3.5–5%), but with a lower C:N ratio (5–8:1). These OFs were obtained by mixing tannery sludge with other animal-based fertilizers (bone, meat and leather meals), thus increasing the N_{tot} . This reduced the C:N ratio compared to a pure tannery sludge from biological stabilization (OF06), which instead showed the lowest N_{tot} (2.5%) and the highest C:N ratio (16:1). The tannery sludge has been proposed as organic N fertilizer considering its interesting N content (Araujo et al., 2020; Giacometti et al., 2012; Guo-Tao et al., 2013), but it is often mixed with other OFs to meet commercial and agronomical requirements. Indeed, mixing tannery sludge with meat, bone and leather meal makes it possible to modulate N_{tot} and the C:N ratio of the final OF. This induces a distinct behavior of the OFs in soil and a different release of bioavailable N: for example, OF02 characterized by lower C:N ratio (5.2:1), showed higher N_{org} mineralization (36% of N_{tot}). The N_{bav} released by this group of OFs showed a wide range of values (34–52%) which is largely due to the different N_{in} content. Indeed, the high N_{in} (16%) in OF02 corresponded to the high N_{bav} (52%), and this probably derived from the raw materials (i.e., meat meal) or from the hydrolysis during the transformation process.

The characteristics of pure tannery sludge (OF06) were less interesting from the agronomical point of view, with the lower N_{tot} (2.5%), the higher C:N ratio (16:1) and the lower volatile solids (40%), compared to the other OFs. OF06 released only the 16% of N_{tot} in available form, a value much lower compared to those obtained testing sewage sludge deriving from different raw materials (Antil et al., 2011; Grigatti et al., 2019; Sciubba et al., 2014). This outcome is probably related to the more intensive biological treatment to which the tannery wastewater was subjected (Zhao et al., 2022) due to the high load of OM and stabilizing compounds, such as chromium, aluminum and glutaraldehyde (Guo-Tao et al., 2013; Sundar et al., 2011). Practically, this product is more like an amendment than a OF; indeed, the mineralization of organic N in soil was lower than for the other OFs (7%). For these reasons, the tannery sludge is generally mixed with other OFs to make it a marketable OF (Tahiri & De la Guardia, 2009).

2.4.2 Relation between indicators of available nitrogen

Three indicators were used to estimate the available N in animal-based OFs: HWON, HWTN and C:N ratio. All the indicators are relatively easy to determine and standardized

methods are available, making them a valid alternative to estimate the bioavailable N in OFs.

However, in some cases these indicators under- or overestimate the bioavailable N. In particular, OF08 and OF09, based on leather meal, mineralized the highest amount of organic N, but these results do not agree with those found in the analysis of HWON and HWTN that underestimate N_0 and N_{bav} . Conversely, in the case of OF02 and OF03, based on tannery sludge mixed with other materials, the hot-water indicators slightly underestimate only the N_{bav} . The reason for these discrepancies seems to be connected to the quality of N_{org} , which appears, in some cases, to be more hot-water extractable than mineralizable, and in other cases less so. In the case of OFs based on leather meal, the hot water may not be a strong enough extractant to guarantee the optimal solubility of collagen, the main component of leather meal (Dell'Abate et al., 2003), whereas it is well hydrolyzed by collagenase and protease in soil (Harper, 1980). In the case of tannery sludge, the hot water seems to extract the organic N fraction that is less accessible to or less degradable by the soil microbiota.

The C:N ratio of OFs was, as expected (Cassity-Duffey et al., 2020; Lazicki et al., 2020; Sigurnjak et al., 2017), a good indicator of organic N mineralization in soil. The C:N ratio was negatively correlated with bioavailable N; in fact, fertilizers with a low ratio induce high bioavailable N in soil (Mooshammer et al., 2014). The linear regression analysis between bioavailable N and C:N ratio was more significant ($R^2 = 0.75$) than that of hot-water indicators. Interestingly, the linear models estimate a maximum available N for the animal-based OFs near to 65–68% of N_{tot} (Figure 2.5, calculate for C:N = 0), and a C:N ratio limit between mineralization-immobilization of N near to 12–15:1 (Figure 5, calculate for N_0 and $N_{bav} = 0$), in agreement with findings of other authors (Cassity-Duffey et al., 2020; Lazicki et al., 2020). Indeed, a C:N ratio less than 15–25:1 generally results in net N mineralization, whereas a C:N ratio greater than 15–25:1 can lead to net N immobilization (Calderón et al., 2005; Gale et al., 2006; Lazicki et al., 2020), and all OFs studied fall in the first case. The C:N ratio is, unlike HWON and HWTN, an eco-stoichiometric indicator or an indicator that predicts the N availability on the basis of N and C use efficiency by soil microorganisms. When the C:N ratio is less than 15–25:1, the soil microorganisms face a substrate with an excess of N with respect to their needs, and this N is released in soil as inorganic (available for plant) form. Nevertheless, this is valid only theoretically, as in real cases the quality of the OM added with the OF and the

presence of other elements or compounds able to inhibit or stimulate the microbial metabolism can modulate the N mineralization. For example, the OFs based on leather meal (OF04, OF08 and OF09) have a similar C:N ratio, 3–3.5:1, but show three different N_{bav} , 40.3% (OF04), 64.5% (OF08) and 54.6% (OF09), that probably are due to differences in the treatment process (i.e., more or less hydrolysis conditions) or to a residual presence of stabilizing agents used for tanning the leather.

2.5 CONCLUSIONS

The results of this research can inform farmers and fertilizer producers about the N availability in organic fertilizers from animal by-products and the relationship with chemical indicators of N availability. It was demonstrated that it is difficult to predict N mineralization solely on the basis of their total N content; in fact, raw materials and treatment processes influence the ability of OFs to release N in inorganic forms. The hot-water extractable N proved to be a good indicator of N_{bav} , but underestimated it in the case of OFs based on leather meal. The C:N ratio provided the best linear fitting with N_{bav} , but also showed some limitations in estimating the N_{bav} .

This study has demonstrated that OFs from animal by-products are potentially useful as organic N fertilizers. However, to use them consciously and efficiently, the evaluation of C:N ratio and the hot-water extractable N analyses should be considered, as they are rapid and inexpensive methods that can provide a reliable indication of N availability in soil.

CHAPTER 3

STUDY AND CHARACTERIZATION OF THE INTERACTION OF OXYBENZONE WITH SOIL

3.1 INTRODUCTION

Oxybenzone (OXB) is an organic compound belonging to the class of aromatic ketones known as benzophenones. It is one of the most employed organic UV filters (Campos et al., 2017; Kim & Choi, 2014; Ramos et al., 2015), due to its high UV absorbing properties in both UV-A (320 – 400 nm) and UV-B (290 – 320 nm) ranges (Tarazona et al., 2010; Vela-Soria et al., 2011). OXB is mainly used in cosmetic products, such as sunscreen lotions, skin care and lip care products (Liao & Kannan, 2014; Ramos et al., 2015), in which it can be added up to 10% of the concentration of the final product according to the European legislation (EC, 2009). Moreover, it finds application also in objects of common use, such as textiles, rubbers and paints (Xue et al., 2017; Z. Zhang et al., 2011), to prevent induced UV degradation of such materials. In this case, no regulatory limit is imposed on the maximum usable quantity (Brooke et al., 2008).

However, displaying endocrine-disrupting properties (Kim & Choi, 2014; Paredes et al., 2014) and toxicity towards the marine environment (Brausch & Rand, 2011; Kim & Choi, 2014; Sánchez Rodríguez et al., 2015), OXB is considered an emerging contaminant. For these reasons, it was recently banned as active compound in sunscreen products in USA, being responsible for coral bleaching. (Ouchene et al., 2019; Vesper, 2020).

Wastewater treatment plants effluents and sewage sludge (SS) represent the main contamination sources of OXB (Mao et al., 2019). In particular, it is one of the most detected and abundant UV filters in SS, having been found it up to 2 mg kg⁻¹ of dry weight (Gago-Ferrero et al., 2011; Langford et al., 2015; Ramos et al., 2016); in fact, its lipophilic nature may favour the retention onto sludge during wastewater treatment and, considering that SS is widely used as fertilizer in agriculture OXB could enter the soil.

The occurrence of OXB in soils is scarcely documented; however, Jeon et al. (2006) detected this contaminant in Korean soils, while other authors found OXB in soils after fertilization with sewage sludge (Camino-Sánchez et al., 2016; Sánchez-Brunete et al., 2011).

In order to better understand the dynamic of OXB in soil, a lab-scale experiment was carried out considering four different soils (two agricultural and two forests soils) with contrasting physico-chemical properties. The objectives of this work were: (i) to study the adsorption and desorption phenomena through the Freundlich isotherms and the related parameters, (ii) to reveal the features of soil organic matter by characterizing humic acids (HA) using Fourier Transformed Infrared Spectroscopy (FT-IR) and Surface

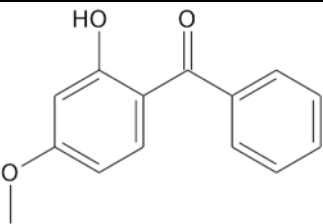
Enhanced Raman Spectroscopy (SERS) and (iii) to analyse the mechanisms of interaction between OXB and HA, exploiting the possibility of solution analysis given by the SERS.

3.2 MATERIALS AND METHODS

3.2.1 Oxybenzone

Oxybenzone (OXB) (IUPAC name: (2-Hydroxy-4-methoxyphenyl)-phenylmethanone) was a certified reference material purchased by Sigma-Aldrich (Merck KGaA, Darmstadt, Germany). Table 3.1 summarizes its main physico-chemical properties.

Table 3.1- Physico-chemical properties of oxybenzone

Chemical structure	Molecular weight g mol ⁻¹	Water solubility mg L ⁻¹	log k _{ow}	pK _a
	228.24	6	3.45	7.1

3.2.2 Soils

3.2.2.1 Analysis

Soil pH was measured using a glass electrode (5261 electrode, Crison Instruments SA, Alella, Spain) connected to a titrator (Compact titrator, Crison Instruments SA, Alella, Spain) in a 1:5 mass to Milli-Q ultrapure water ratio (*ISO 10390:2005*). The same soil-water ratio was applied in measuring the electrical conductivity (EC), using an electrical conductivity meter (Radiometer Analytical CDM 210, Hach Company, Colorado, USA) equipped with a conductivity cell (Radiometer Analytical CDC 749, Hach Company, Colorado, USA) (*ISO 11265:1994*).

Soil texture was evaluated according to the pipette method suggested by Gee & Bauder, 1986.

Organic carbon (OC) and total nitrogen (TN) content were determined by means of an elemental analyser (CHNS-O Elemental Analyzer 1110, Thermo Scientific GmbH, Dreieich, Germany). In particular, 10 mg of soil was weighted into tin caps and pre-treated adding 1 mL of 0.1 M HCl, in order to eliminate the possible presence of carbonates.

Cation exchange capacity (CEC) was measured according to a modified protocol of the *Norme AFNOR NFX 31-130*, 1993. Briefly, a soil sample of 2.5 g was previously extracted in 25 mL of 1 M ammonium acetate for 30 minutes. After a centrifugation step (Avanti J-26S Series XP, Beckman Coulter Inc., Brea, USA) (6.000 rpm, 15 minutes, 20°C), the precipitated soil was rinsed twice with 10 mL of ethanol and re-suspended in 25 mL of 2 M KCl for one hour. The mixture was filtered by means of Whatman N°42 filters and the exchanged ammonium was measured by spectrophotometry.

3.2.2.2 *Main characteristics*

Figure 3.1 shows the sites from which the soils object of this study were collected. Two agricultural soils (hereinafter named AGR1 and AGR2) and two forest soils (hereinafter named FOR1 and FOR2) were chosen.

All four soils were sampled from the top 30 cm soil profile, transported to the laboratory where they were left to air dry for fifteen days. Once dried, they were carefully cleaned from roots and plants debris and they were grinded by means of a ball mill (Mixer Mill MM400, Retsch GmbH, Haan, Germany).

AGR1 was collected at the experimental farm of the University of Bologna located in Cadriano (Northern Italy, 44°33'N, 11°24'E; 27 m a.s.l.). According to the World Reference Base for Soil Resource (WRB), it is classified as Eutric-Siltic Fluvic Cambisols. It is characterized by a sub-alkaline pH and by a quite high content of organic carbon and total nitrogen. In 2021, total annual rainfall and mean air temperature registered were 543 mm and 14.8 °C, respectively.

AGR2 was collected at an agricultural site in Pisa, in the Tuscany region (Central-Northern Italy, 43°40'N, 10°51'E; 52 m a.s.l.). It is classified as Calcaric Fluvic Cambisols (WRB). Compared to AGR1, it has a similar pH value, but lower values of organic carbon, total nitrogen and CEC. In 2021, total annual rainfall and mean air temperature registered were 816 mm and 15.6 °C, respectively.

FOR1 was sampled in a beech forest located in Cansiglio, a vast plateau between Veneto and Friuli Venezia Giulia regions (North-Eastern Italy, 46°04'N, 12°24'E; 1224 m a.s.l.). It is classified as Haplic Luvisols (WRB), characterized by an acid pH, high amount of organic carbon and a quite high content in total nitrogen. In 2021, total annual rainfall and mean air temperature registered were 1811 mm and 8.9 °C, respectively.

FOR2 was collected in a chestnut forest in Zocca, an area located between Bologna and Modena, in the Emilia-Romagna region (Northern Italy, 44°20'N, 10°59'E; 782 m a.s.l.). It is classified as Eutric Cambisols (WRB), characterized by a sub-acid pH. Compared to FOR1, it was depleted in terms of organic carbon and total nitrogen and had lower CEC. In 2021, total annual rainfall and mean air temperature registered were 606 mm and 10.7 °C, respectively.

Soils main characteristics are summarized in Table 3.2.

Table 3.2 - Soils main characteristics.

(EC = Electrical conductivity; OC= Organic carbon; TN= Total nitrogen; CEC = Cation exchange capacity)

Sample	pH	EC μS/cm	Sand %	Silt %	Clay %	OC %	TN %	CaCO ₃ %	CEC cmol ⁺ /kg
AGR1	7.78	174	60	26	14	2.16	0.86	6.5	23.4
AGR2	7.72	118	60	31	9	0.21	0.08	2.9	14.0
FOR1	4.74	55	34	54	12	4.21	0.35	6.9	37.9
FOR2	6.04	35	83	11	6	0.34	0.02	0	5.9



Figure 3.1 - Map of sampling sites.

Red dot: AGR1; Blue dot: AGR2; Green dot: FOR1; Black dot: FOR2

3.2.3 Adsorption and desorption study

3.2.3.1 HPLC-UV analysis

The quantitative determination of OXB was carried out by means of HPLC (1525 Binary HPLC Pump, Waters, Milford, USA) equipped with an UV detector (2487 Dual wavelength Absorbance Detector, Waters, Milford, USA) and a C₁₈ column (TSKgel ODS-100V, Tosoh Bioscience GmbH, Griesheim, Germany). During the analysis, the column was placed in a column oven (Temperature Controller Module and Heater, Waters, Milford, USA) set at 30°C, while the UV detector operated at 287 nm. The mobile phase was acetonitrile 100%, flowing at a rate of 1 mL min⁻¹. Run time was set to 5 minutes, the sample volume injected was 25 µL.

3.2.3.2 Adsorption kinetics

Evaluating the adsorption rates of OXB onto soils to establish the equilibrium time that will be next used in the adsorption isotherms experiment is fundamental. A 50 mg L⁻¹ OXB solution in 20 % (v/v) of acetonitrile was prepared and the soil-solution ratio chosen was 1:5 (w/v). Aliquots of 5 g of soil were placed in 50 mL glass flasks and suspended in 25 mL of OXB solution. The pH of the solutions was the same as that obtained in the soil analysis (Table 3.2). Glass flasks were preferred to plastic containers to avoid possible adsorption of OXB onto the internal surfaces. Samples were subjected to magnetic agitation (Multistirrer 15, Velp Scientific Inc., New York, USA) for each of the following five time intervals: 0.5, 3, 6, 24 and 48 hours. At the end of each time interval, the mixtures were centrifuged (10.000 rpm, 15 minutes, 20°C) and the supernatants were analysed by HPLC-UV. Solutions consisting of 25 mL of OXB solution (without soil) were included as blank samples and analysed at each time interval to ascertain the stability of OXB in the solution during the stirring time. The experiment was conducted in triplicate.

A first order kinetic fit was applied according to the following equation:

$$q = q_{\max} * (1 - e^{-kt}) \quad (1)$$

where q is the amount of OXB adsorbed expressed in mg kg^{-1} , t is the time expressed in minutes, q_{max} is the maximum amount that can be adsorbed expressed in mg kg^{-1} and k the first order kinetic constant expressed in minutes^{-1} .

3.2.3.3 Adsorption isotherms

Aliquots of 5 g of soil were placed in 50 mL glass flasks and suspended in 25 mL of 20% (v/v) acetonitrile solution of OXB at the following concentrations: 1, 5, 10, 25 and 50 mg L^{-1} (this range was selected to have a complete overview of the pollution intensity, from low to extremely high, based on the results of Ramos et al., 2015). Samples were subjected to magnetic agitation for 24 h, the time needed to reach the equilibrium. Then, the mixtures were centrifuged (10.000 rpm, 15 minutes, 20°C) and the supernatants were analysed by HPLC-UV. As in the previous experiment, solutions consisting of 25 mL of OXB solution (without soil) were included as blank samples and three replicates for each treatment were prepared.

Data obtained were fitted according to the non-linear Freundlich equation:

$$q = K * C_{\text{eq}}^{1/n} \quad (2)$$

where q is the amount of OXB adsorbed expressed in mg kg^{-1} , K is the Freundlich constant expressed in L kg^{-1} , C_{eq} is the equilibrium concentration of OXB remained in solution expressed as mg L^{-1} and $1/n$ (dimensionless) represents the degree of nonlinearity between solution concentration and amount adsorbed.

To extrapolate the Freundlich parameters K and $1/n$, the linear Freundlich equation was used:

$$\log q = \log K + (1/n * \log C_{\text{eq}}) \quad (3)$$

Furthermore, the organic carbon partition coefficient (K_{OC}) was calculated according to the following equation to relate the adsorption capacity of the soil to the organic carbon content. It is expressed as L kg^{-1} .

$$K_{\text{OC}} = (K/\text{OC}\%) \cdot 100 \quad (4)$$

3.2.3.4 Desorption isotherms

A desorption test was performed to study the release capacity of OXB from soils. The remaining soil from the previous separation of the supernatant (paragraph 3.2.3.3) was re-dissolved in a 20% acetonitrile (v/v) blank solution. The mixtures were subjected to magnetic agitation for 24 h to reach the equilibrium state. At the end of the stirring phase, samples were centrifuged (10.000 rpm, 15 minutes, 20°C) and the supernatants were analysed by HPLC-UV. The same conditions of the adsorption experiment were maintained for the blank samples and the number of replicates.

Data were fitted according to the nonlinear Freundlich equation:

$$C_s = K_{des} * C_{eq}^{1/n_{des}} \quad (5)$$

where C_s is the amount of OXB retained by the soil in mg kg^{-1} , K_{des} is the desorption Freundlich constant in L kg^{-1} , C_{eq} is the remained equilibrium concentration of OXB in the aqueous solution in mg L^{-1} and $1/n_{des}$ (dimensionless) the degree of nonlinearity between solution concentration and the amount of OXB retained by the soil.

To extrapolate the Freundlich parameters K_{des} and $1/n_{des}$, the linear equation was used:

$$\log C_s = \log K_{des} + (1/n_{des} * \log C_{eq}) \quad (6)$$

3.2.4 Humic acids

3.2.4.1 Extraction from soil

Humic acids (HA) extraction was conducted according to the method suggested by the International Humic Substances Society (IHSS) (Swift, 1996).

Briefly, an aliquot of 20 g of soil was placed in 250 mL centrifuge tube (Nalgene®) with 100 mL of 1 M HCl until $\text{pH} < 2$, then 0.1 M HCl until reaching 200 mL as total volume. The mixture was stirred for 1 hour on a horizontal shaker (SKO-D XL Digital Linear Shaker, Argolab, Carpi, Italy), then it was centrifuged (3000 rpm, 10 min, 20 °C). The supernatant containing the first fraction of fulvic acids (FA) was discarded.

The precipitated soil was neutralized by adding 100 mL of 1 M NaOH until $\text{pH} > 12$, followed by 100 mL of 0.1 M NaOH to obtain the same extraction ratio as the previous step. The mixture was stirred overnight and then centrifuged (3000 rpm, 10 min, 20 °C).

The precipitated soil (containing humin, the insoluble component of soil organic matter) was discarded, while the supernatant was acidified to $\text{pH} = 1$ by adding 6 M HCl (approximately 20 mL) under stirring. This operation allowed the precipitation of HA, which are insoluble at acidic pH. The mixture was stirred overnight, then it was centrifuged (6000 rpm, 10 min, 20°C). The supernatant, consisting of the second aliquot of FA, was discarded, while the HA fraction was purified as described below.

3.2.4.2 Purification

The purification step was carried out as described in Swift (1996).

An amount equal to 100 mL of 0.1 M KOH was added to the HA previously extracted and, once dissolved, 12.5 g of KCl were added to the solution. The solution was mixed by hand and then it was centrifuged (6000 rpm, 10 min, 20°C). This first operation allowed to remove the suspended solids, precipitated after the centrifugation step.

Humic acids were precipitated by adding 6 M HCl (approximately 20 mL) until $\text{pH} = 1$, then the solution was let stand overnight. A centrifugation step (6000 rpm, 10 min, 20°C) allowed us to isolate again the HA fraction, discarding the supernatant. To remove the ash content, the HA were re-suspended in 100 mL of 0.1 M HCl and 0.3 M HF, leaving the solution stirred overnight. A centrifugation step (6000 rpm, 10 min, 20°C) allowed us to separate the HA-ash free fraction from the supernatant.

HA were then dissolved in 100 mL of Milli-Q® water and placed into dialysis tubes (Visking dialysis tubing MWCO 12000 – 14000, Serva Electrophoresis GmbH, Heidelberg, Germany) against distilled water for 48 h. After that, they were freeze dried (Freeze Dry System Lyph-lock 6, Labconco Corporation, Kansas City, USA) and stored in dark vials to avoid light absorption.

Each sample was named as follows depending on the soil from which they were extracted: HA-AGR1, HA-AGR2, HA-FOR1, HA-FOR2.

The extraction and purification processes described above are graphically resumed in Figure 3.2.

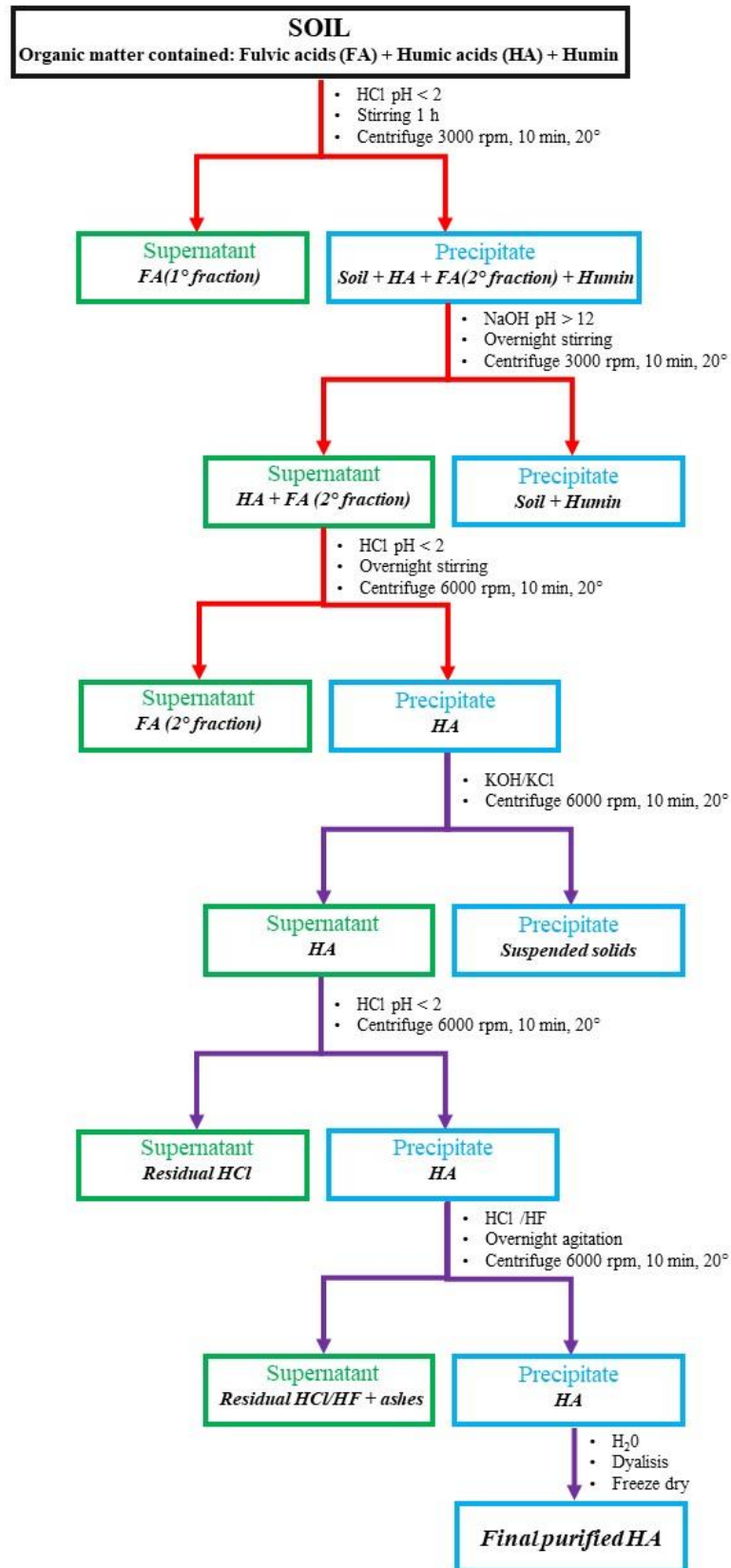


Figure 3.2 – Schematic diagram of the extraction (red arrows) and purification (violet arrows) of humic acids.

3.2.5 ATR-FTIR analysis of humic acids

A small aliquot of HA was deposited on the diamond Attenuated Total Reflection (ATR) device (Quest Single Reflection ATR Accessory, Specac Ltd., Orpington, England) connected to an infrared spectrophotometer (Tensor 27, Bruker Corporation, Billerica, USA). Background spectra of air were acquired before sample analysis. Once the sample had been analysed, the diamond surface was cleaned with a dampened ethanol cloth. Spectra were recorded from 4000 to 400 cm^{-1} , setting a spectral acquisition of 4 cm^{-1} and 64 scans.

Spectra were processed by means of Origin 2022b software (OriginLab Corporation, 2022). The intensity normalization was preliminarily performed. Seven peaks at the following wavenumbers were considered: 2920, 2850, 1620, 1540, 1420, 1220 and 1030 cm^{-1} . The relative absorbances (rA) were calculated by dividing the corrected peak height by the sum of the heights of all the peaks and multiplying it by 100. The Aromaticity Index (ArI) was calculated by dividing the intensity of absorption at 1620 cm^{-1} by the intensity of absorption at 2920 cm^{-1} , as suggested by Chefetz et al. (1996).

3.2.6 Raman analysis of oxybenzone

A small aliquot of solid OXB was placed on a microscope slide in the sample placement area.

Spectra were recorded by means of a Renishaw Raman inVia Spectrometer (Renishaw plc, Wotton-under-Edge, UK) equipped with a CCD camera and a Nd:YAG laser (excitation line: 532 nm). Laser power was tuned on 0.2 mW. The acquisition was collected by a single scan with an integration time of 10 seconds and a spectral resolution of 2 cm^{-1} .

3.2.7 SERS analysis

3.2.7.1 Preparation of silver nanoparticles

Two different types of silver nanoparticles (silver citrate and silver hydroxylamine) were prepared as substrates for the SERS analysis.

Silver citrate nanoparticles (AgCIT NPs) were synthesized according to the method suggested by Lee & Meisel (1982). Briefly, 8.5 mg of AgNO₃ were dissolved in 50 mL of Milli-Q® water and heated. At the boiling point, 1 mL of a 1% sodium citrate tribasic solution was added. The mixture was refluxed and heated for 1 h.

Silver hydroxylamine nanoparticles (AgHX NPs) were prepared according to the method described by Leopold & Lendl (2003). Briefly, 4.5 mL of 0.1 M NaOH were added to 5 mL of 6·10⁻³ M hydroxylamine chloride solution. The mixture was quickly added to 90 mL of 10⁻³ M AgNO₃ solution and mixed vigorously by hand.

For both nanoparticle types, the colloid was used the next day to ensure a better stabilization of the NPs. An aluminium foil was applied to the outer surfaces of the flask containing the colloid to avoid degradation by light.

3.2.7.2 Instrumentation and technical setting

The same operating conditions of the Raman analysis on OXB (paragraph 3.2.6) were maintained, except for the laser power which was tuned to 2 mW. Spectra normalization and subtraction were performed by means of Origin 2022b software (OriginLab Corporation, 2022).

3.2.7.3 Analysis of oxybenzone

A 0.1 M ethanolic solution of OXB was previously prepared.

AgCIT NPs: the sample for analysis was prepared by adding 10 µL of OXB solution and 20 µL of 0.5 M KNO₃ (required to activate the NPs) to 970 µL of colloid. The OXB final concentration was of 10⁻³ M.

AD8-AgHX NPs: an additional NPs functionalization with 1,8 diamino octane (AD8) was required to enhance OXB signals. Thus, a 0.2 M AD8 solution was previously prepared using a 0.5 M KCl solution as solvent. The sample for analysis was prepared by adding 10 µL of OXB solution and 10 µL of AD8 solution to 980 µL of colloid. The OXB and the AD8 final concentrations were 10⁻³ and 2·10⁻³ M, respectively. No KNO₃ was added as the KCl present in the AD8 solution activated the NPs.

In both cases, blank samples (all reagents except OXB) were tested to obtain OXB signals by subtraction.

3.2.7.4 Analysis of humic acids

Humic acids were tested using both types of NPs. Furthermore, spectra were acquired in both acidic (pH 4) and alkaline (pH 8) conditions.

An aliquot equal to 1 mg of HA was previously dissolved in 1 mL of 1 M NaOH.

AgCIT NPs: samples were prepared by adding 10 μL of HA solution and 20 μL of 0.5 M KNO_3 to 970 μL of colloid for the analysis at pH 8. Further 5 μL of 1 M HCl were added for the analysis at pH 4.

AD8-AgHX NPs: samples were prepared by adding 10 μL of HA solution and 10 μL of 0.2 M AD8 solution to 980 μL of colloid for the analysis at pH 8. Further 5 μL of 1 M HCl were added for the analysis at pH 4.

Blank samples were not performed as no relevant interference was present.

3.2.7.5 Analysis of the complex oxybenzone – humic acids

This analysis was conducted using the AD8-AgHX NPs as they provided the best performance, recording spectra in both acidic (pH 4) and alkaline (pH 8) conditions.

Samples were prepared by adding 10 μL of OXB solution, 10 μL of HA solution and 10 μL of AD8 solution to 970 μL of colloid for the analysis at pH 8. Further 5 μL of 1 M HCl were added for the analysis at pH 4.

Blank samples were not performed as no relevant interference was present.

3.3 RESULTS

3.3.1 Adsorption and desorption study

3.3.1.1 Adsorption kinetics

Adsorption kinetics curves are shown in Figure 3.3. Despite the absolute amount of OXB adsorbed was very different, all four soils showed kinetics with a similar shape. In particular, within the first six hours, a rapid phase occurs, in which more than 90% of the OXB is adsorbed; a slow second phase lasts up to 48 hours, in which the adsorption equilibrium can be considered stable. Soil FOR1 had the fastest adsorption, as demonstrated by the angled shape of the first order kinetic fit curve, while soil FOR2 showed the slowest adsorption, given the rounded angle that characterized its fitting.

Agricultural soils exhibited intermediate speeds, with AGR2 adsorbing OXB faster than AGR1.

An equilibration time of 24 h was considered sufficient to carry out the adsorption and desorption experiments.

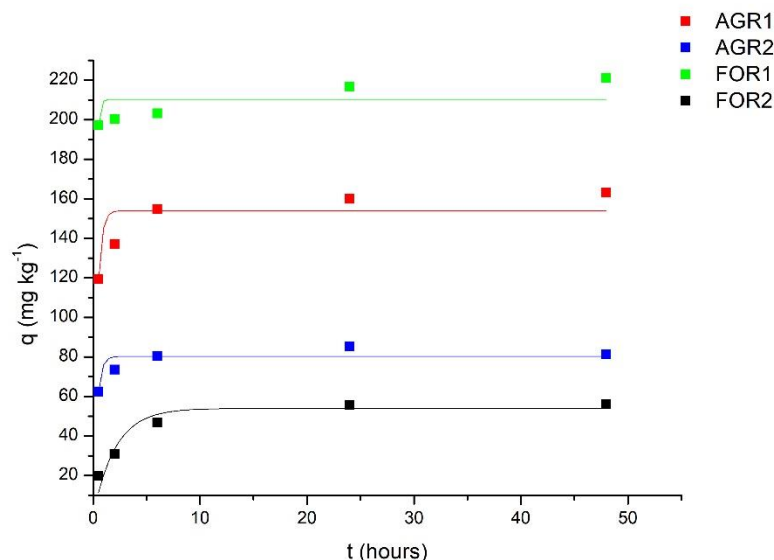


Figure 3.3 – First order kinetic fit of the adsorption kinetics test.

3.3.1.2 Adsorption isotherms

Non-linear Freundlich isotherm was chosen (compared to the Langmuir model, data not shown) to fit the experimental adsorption data (Figure 3.4). In particular, for soils AGR2 and FOR2 the Langmuir fit failed, while for soils AGR1 and FOR1 the Freundlich model was the best according to the Bayesian Information Criterion Test (BIC). It is an estimator of the relative quality of statistical models for a given set of data, according to which models with a lower BIC value explain a better goodness of fit. For soil AGR1, 10.8 was obtained for Freundlich model and 19.7 for Langmuir model, while for soil FOR1, 19.3 and 28.5 were obtained for Freundlich and Langmuir models, respectively (Table 3.3, results for Langmuir model not shown in the table). In Table 3.3 are also reported the Freundlich parameters (K and $1/n$) and the organic carbon partition coefficients (K_{OC}).

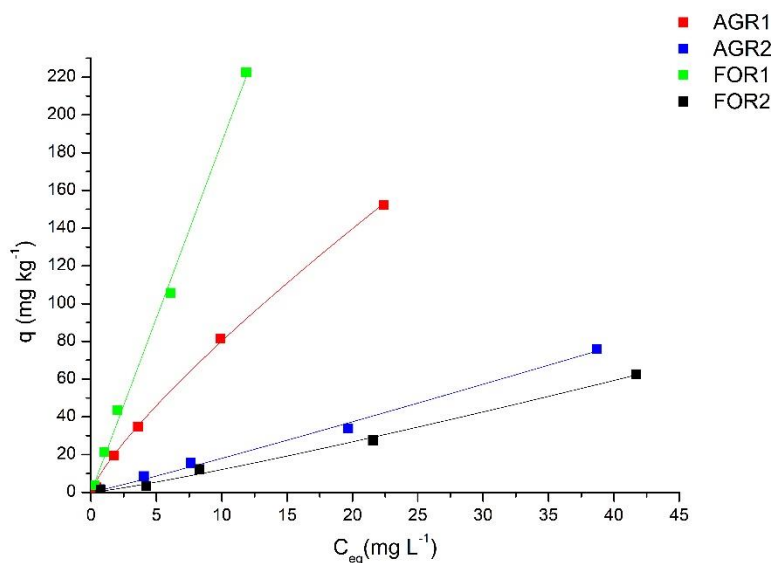


Figure 3.4 - Freundlich isotherms related to the adsorption experiment.

The four soils were characterized by a wide difference in the adsorption capacity, as demonstrated by the K ranging from 18.02 to 1.45 L kg⁻¹. These values also reflected the graph of the isotherms, since the higher is the K value the higher is the slope. Soil FOR1 is the one that showed the highest adsorption ($K = 18.02$ L kg⁻¹), followed by AGR1 ($K = 8.3$ L kg⁻¹), AGR2 ($K = 2.29$ L kg⁻¹) and FOR2 ($K = 1.45$ L kg⁻¹). Isotherms manifested a high level of linearity, as confirmed by the $1/n$ parameter, which ranged from 0.937 to 1.015.

Conversely, a remarkable difference was found in K_{OC} , which presented the lowest value for AGR1 ($K_{OC} = 384$ L kg⁻¹) and the highest one for AGR2 ($K_{OC} = 1090$ L kg⁻¹); intermediate and similar values were measured in the case of FOR1 ($K_{OC} = 428$ L kg⁻¹) and FOR2 ($K_{OC} = 426$ L kg⁻¹).

The Pearson correlation coefficient between K and soil OC was equal to 0.9937 (p-value = 0.006).

Table 3.3 – Freundlich adsorption parameters (K and $1/n$), Bayesian Information Criterion Test (BIC) values and organic carbon partition coefficient (K_{oc}) in the different soils.

Sample	K L kg ⁻¹	$1/n$	BIC	K_{oc} L kg ⁻¹
AGR1	8.3	0.937	10.8	384
AGR2	2.29	0.997	-	1090
FOR1	18.0	1.015	19.3	428
FOR2	1.45	0.964	-	426

3.3.1.3 Desorption isotherms

As in the previous case, the non-linear Freundlich model guaranteed the best fit with the experimental desorption data (Figure 3.5). In fact, the BIC test gave lower values (Table 3.4) for this model with respect to the Langmuir one (16.2, 3.74, 15.5 and 14.7 were estimated for soils AGR1, AGR2, FOR1 and FOR2, respectively. Results not shown in the table).

K_{des} showed a wide range of values (Table 3.4), indicating a different capacity of the soils to retain OXB. Soil FOR1 retained the most ($K_{des} = 26.74$ L kg⁻¹), followed by AGR1 ($K_{des} = 9.15$ L kg⁻¹), AGR2 ($K_{des} = 2.73$ L kg⁻¹) and FOR2 ($K_{des} = 1.17$ L kg⁻¹). Desorption isotherms (Figure 3.5) confirmed these results, since the slopes presented the same trend of K_{des} . Values of $1/n$ were found approximately near to the unit (1.033 – 1.067), as reflected by the linearity of the isotherms models.

The Pearson correlation coefficient between K_{des} and soil OC was equal to 0.9769 (p-value = 0.023).

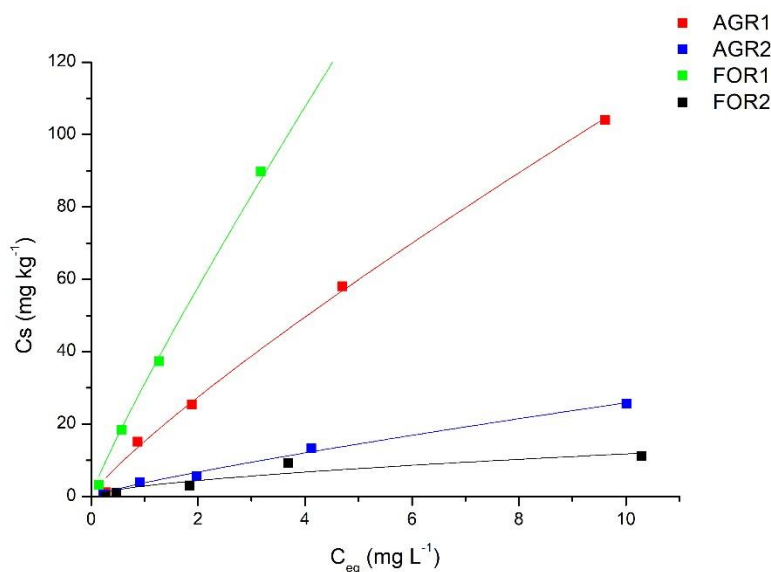


Figure 3.5 – Freundlich isotherms related to the desorption experiment.

Table 3.4 – Freundlich desorption parameters (K_{des} and $1/n_{des}$) and Bayesian Information Criterion (BIC) values.

Sample	K_{des} $L\ kg^{-1}$	$1/n_{des}$	BIC
AGR1	9.15	1.067	12
AGR2	2.73	1.028	1.96
FOR1	26.7	1.033	10
FOR2	1.17	1.015	9.04

3.3.2 Raman and SERS analysis of oxybenzone

Raman and SERS analysis of OXB were performed to study the detectability of the molecule needed for subsequent experiments.

The Raman spectrum of OXB is shown in Figure 3.6 and is characterized by a low fluorescence interference; the assignment of the main peaks is reported in Table 3.5 and is based on the work of Joseph et al. (2014).

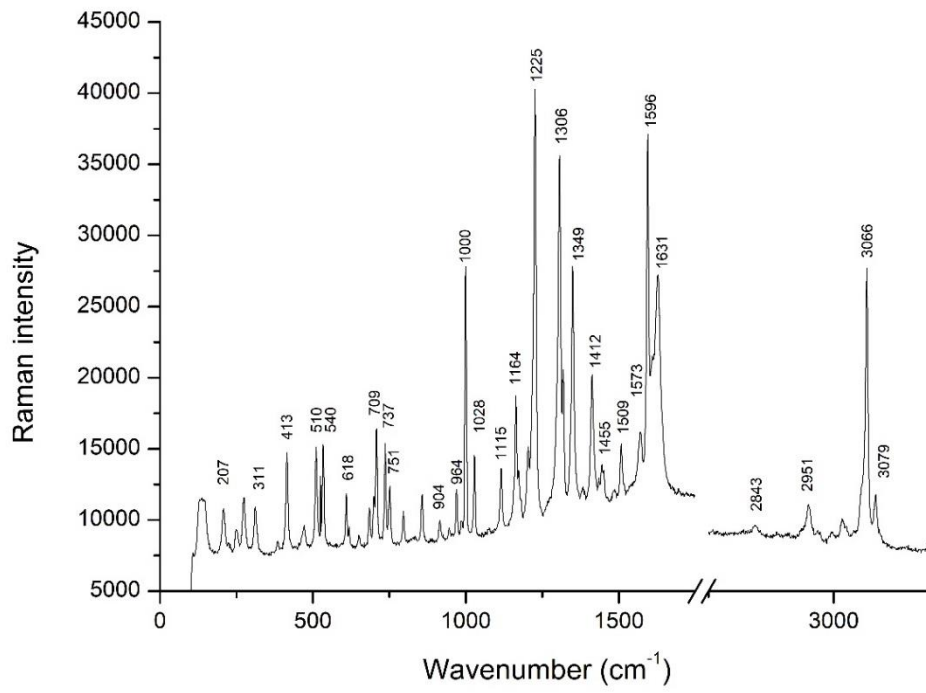


Figure 3.6 - Raman spectrum of OXB

Table 3.5 - Vibrational assignment of the main bands of OXB

Wavenumber (cm ⁻¹)	Vibrational assignment
3079	20a vCH
3065	2 vCH, 20b vCH, 20a vCH, 7a vCH
2951	CH ₃ _{ips}
2843	CH ₃ _{ss} , CH ₃ _{ips}
1631	vC=O, vCC, βCOH, 8b vCC, βCH
1596	8a vCC, βCH
1573	8b vCC, βCOH, βCH 19a βCH, vCC 19b βCH
1509	19a βCH, vCC
1455	CH ₃ _{sb}
1412	vCC, βCOH, βCH, βCCO
1349	14 vCC, 3 βCH, βCC
1306	14 vCC, βCH
1225	9a βCH, vCC
1164	vC-O, βCH, vCC, CH ₃ _{ipr} , CH ₃ _{opr}
1115	15 vCC, vCC _{sym} , vC-O, βCH
1028	12 γCH, τR1 _{tri} , vCC, γCH, vC-O
1000	1 vCC, vC-O, γCH
964	βR1 _{tri} , vCC, γCH
904	τR2 _{sym} , τR2 _{tri}
751	τCCOH, γCH
737	4 τR2 _{sym} , τR2 _{tri} , vCC, vC-O, βR2 _{sym} , βR2 _{asy}
709	6b τR2 _{tri} , τR2 _{sym}
618	6a βR1 _{sym} , 16b βCCO, βR2 _{asy} , τR1 _{tri}
540	βCCO, βR2 _{sym} , βCOC
510	βR2 _{sym} , βCCC, τR1 _{asy}
413	τR1 _{asy} , γCC, 16a τR2 _{tri}
311	τR2 _{tri} , τR2 _{sym} , γCC
207	βCC, βCCO, τCH ₃ , γCC, τCCCO, τR1 _{asy}

Legend - R1: phenyl ring 1; R2: phenyl ring 2; β: in-plane bending; τ: torsion; γ: out of plane bending; ss: symmetric stretching; asy: asymmetric deformation; sym: symmetric deformation; ips: in plane stretching; sb: symmetric bending; ipr: in plane rocking; opr: out of plane rocking; tri: trigonal deformation

Figure 3.7 showed the SERS spectrum of OXB (in red) using the AgCIT NPs as substrate, the spectrum of the only substrate (in black) and the subtracted spectrum (in blue) to highlight the OXB signals. Comparing the SERS and Raman spectra, it is easily seen that there is a close match in the 311-1315 and 2843-3066 cm^{-1} regions, while the SERS peaks recorded at 1492, 1548 and 1583 cm^{-1} are shifted downward.

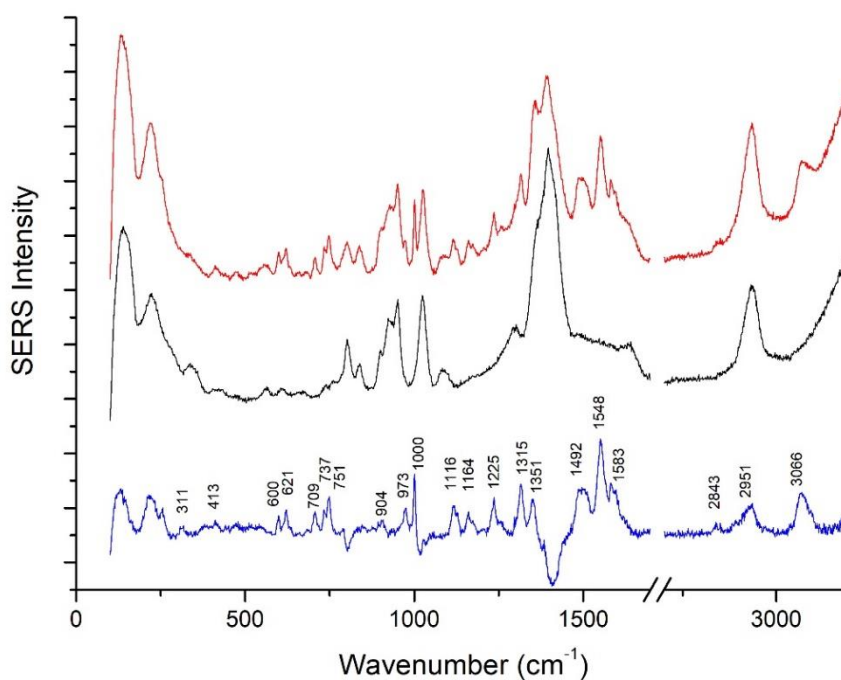


Figure 3.7 - SERS spectrum of OXB using AgCIT NPs. (Red line: OXB; Black line: substrate; Blue line: subtracted spectrum)

Regarding the AD8-AgHX NPs, the same experiments were conducted. Figure 3.8 illustrated the spectrum of OXB (in red), the spectrum of the only AD8-functionalised AgHX NPs (in black) and the subtracted spectrum (in blue). In this case, there was a stronger fit between the SERS and Raman OXB peaks.

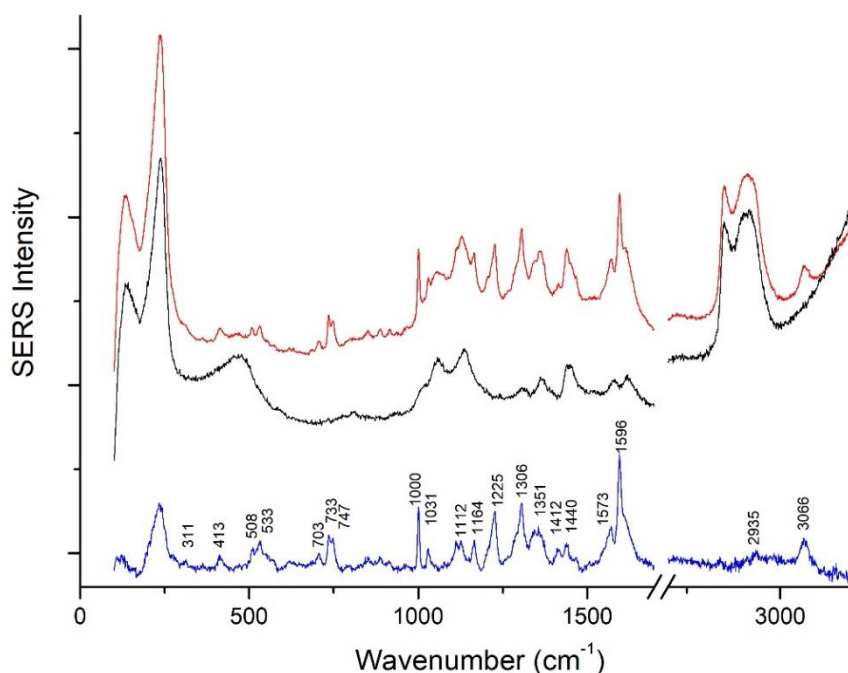


Figure 3.8 - SERS spectrum of OXB using AD8-AgHX NPs. (Red line: OXB; Black line: substrate; Blue line: subtracted spectrum)

3.3.3 Analysis of humic acids

3.3.3.1 ATR-FTIR analysis

The ATR-FTIR spectra of HA exhibited similar patterns (Figure 3.9). Relative absorbances (rA) and the Aromaticity Index (ArI) are shown in Table 3.6.

Peaks at 2920 and 2850 cm^{-1} showed higher intensities for HA-AGR1 and HA-AGR2 samples than for HA-FOR1 and HA-FOR2. Slight differences in terms of peaks shape and wavenumber were observed in the spectral zone between 1620 and 1530 cm^{-1} ; indeed, HA-AGR2 presented two distinct peaks at 1620 and 1539 cm^{-1} , while all the other samples showed a defined peak and a subsequent shoulder. In particular, HA-AGR1 exhibited these at 1605 and 1530 cm^{-1} , HA-FOR1 at 1617 and 1538 cm^{-1} , HA-FOR2 at 1615 and 1538 cm^{-1} . In general, rA associated to these peaks were higher for the HA extracted from forest soils. A remarkable difference in intensity was displayed for the peak at 1420 cm^{-1} , in fact HA-AGR1 showed an order of magnitude higher value than the

other samples. HA-AGR2 and HA-FOR2 exhibited similar and higher values for the peak at 1220 cm^{-1} , while no differences were detected at 1030 cm^{-1} .

The aromaticity index (rA_{1620}/rA_{2920}) ranged from 4.64 to 10.93, with the HA extracted from forest soils were characterized by higher values than the HA from agricultural soils.

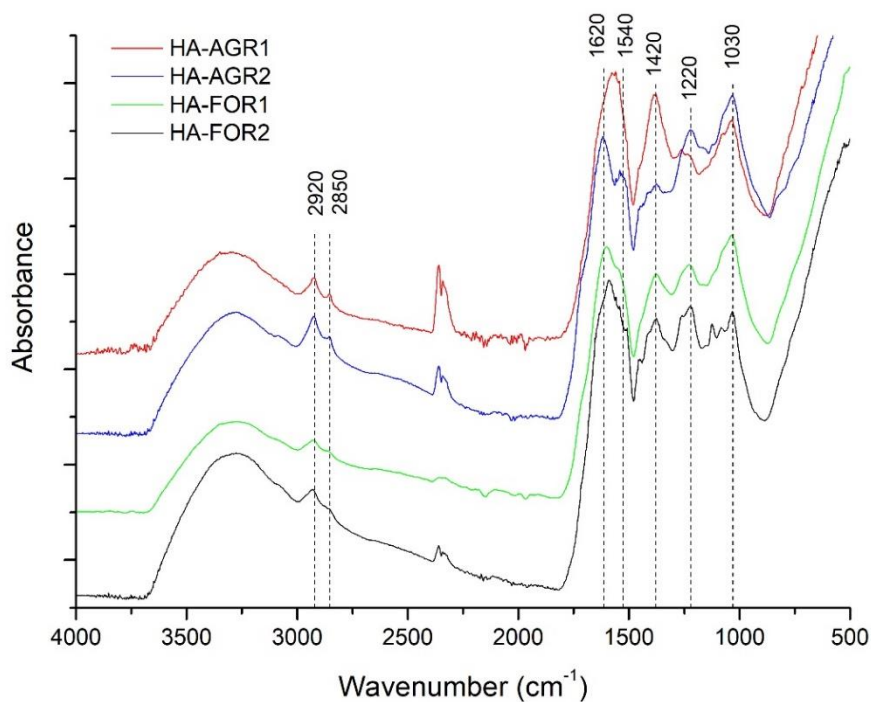


Figure 3.9 - ATR-FTIR spectra of HA samples

Table 3.6 - Relative absorbance of the related peaks and the calculated aromatic index

Sample	1030 cm^{-1}	1220 cm^{-1}	1420 cm^{-1}	1540 cm^{-1}	1620 cm^{-1}	2850 cm^{-1}	2920 cm^{-1}	ArI
AGR1	16.28	4.98	20.82	16.85	31.84	3.08	5.76	5.52
AGR2	16.71	10.81	9.59	19.34	32.26	4.32	6.95	4.64
FOR1	15.79	5.82	10.38	28.67	34.44	1.78	3.15	10.93
FOR2	15.35	8.94	10.74	19.56	39.25	2.15	4.3	9.12

3.3.3.2 SERS analysis

Figures 3.10 showed the SERS spectra of HA using the AgCIT NPs at pH 4 and pH 8. Slightly different patterns discriminated agricultural HA from forestry HA under both pH conditions. On average, under alkaline conditions, higher intensities characterized HA-FOR1 and HA-FOR2 in comparison with HA-AGR1 and HA-AGR2.

In acidic conditions, all four spectra showed broad bands at 1610 and 1375 cm^{-1} , but only the forestry HA spectra exhibited two additional shoulder bands at 1132 cm^{-1} and 1240 cm^{-1} .

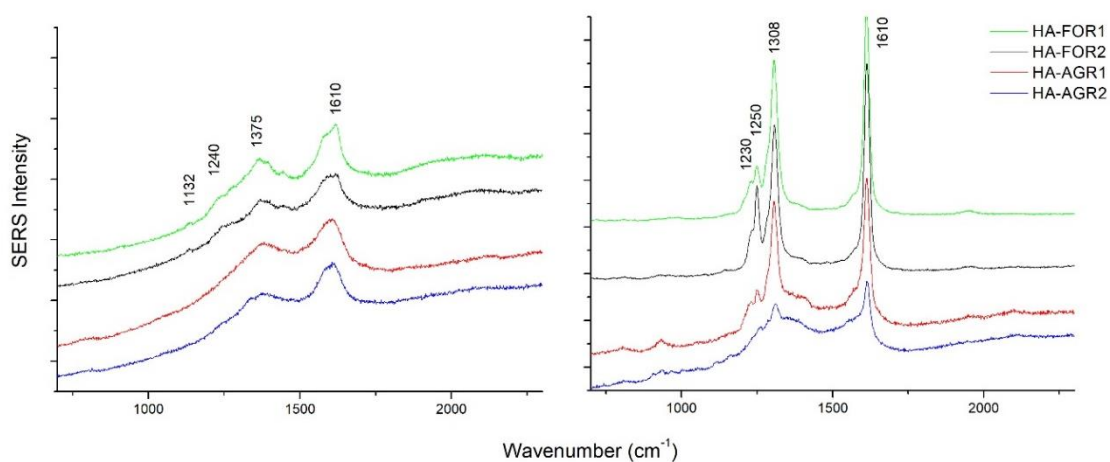


Figure 3.10 - SERS spectra of HA using AgCIT NPs at pH 4 (on the left) and at pH 8 (on the right)

SERS spectra of HA using the AD8-AgHX NPs are shown in Figure 3.11. In this case, marked differences emerged between the agricultural and forestry samples. In alkaline conditions, five peaks were observed at 1132, 1246, 1311, 1446 and 1615 cm^{-1} for the forestry samples, while the first three peaks were negligible in the agricultural HA. A similar situation was observed in the spectra recorded at pH 4; in fact, HA-AGR1 and HA-AGR2 presented two broad bands at 1368 and 1600 cm^{-1} , whereas HA-FOR1 and HA-FOR2 exhibited five peaks at 1136, 1244, 1368, 1444 and 1613 cm^{-1} .

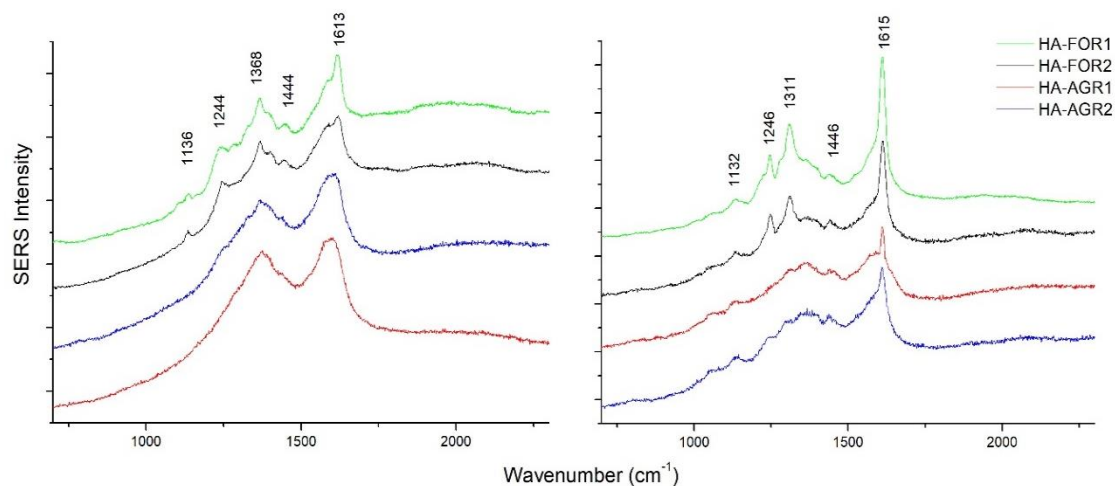


Figure 3.11 - SERS spectra of HA using AD8-AgHX NPs at pH 4 (on the left) and at pH 8 (on the right)

3.3.4 SERS analysis of the complex oxybenzone-humic acid

The complex OXB-HA was tested using AD8-AgHX NPs as substrate and performing the analysis both at pH 4 and pH 8. Figures 3.12 and 3.13 showed the spectra obtained for the agricultural and forest HA, respectively. Spectra of the complex OXB-HA (in red) were subtracted from the HA spectra (in black) to obtain the resulting OXB signals (in blue). Regarding the forestry HA, few OXB signals emerged and of low intensity under both pH conditions. Conversely, no OXB peaks were observed under acidic conditions for the agricultural HA, while a conspicuous number of signals characterized by a remarkable intensity were occurred under alkaline condition.

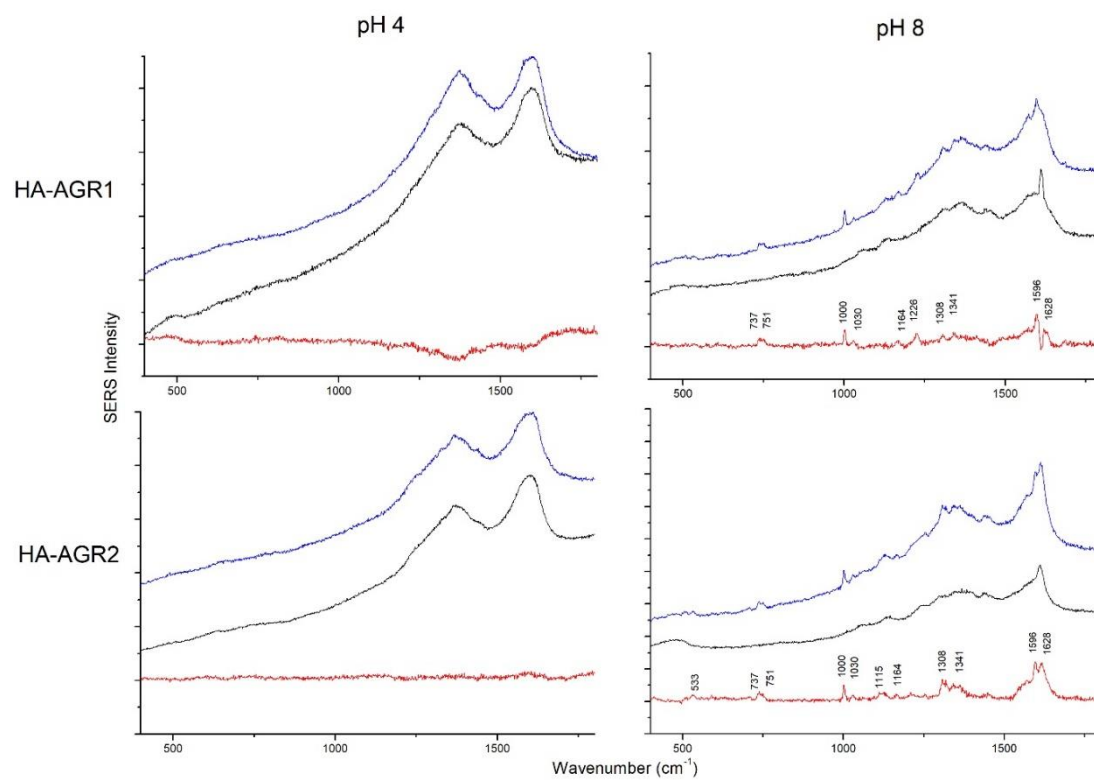


Figure 3.12 - SERS spectra of the complex HA-OXB for the HA extracted from agricultural soils. (Blue line: OXB+HA; Black line: HA; Red line: subtracted spectrum)

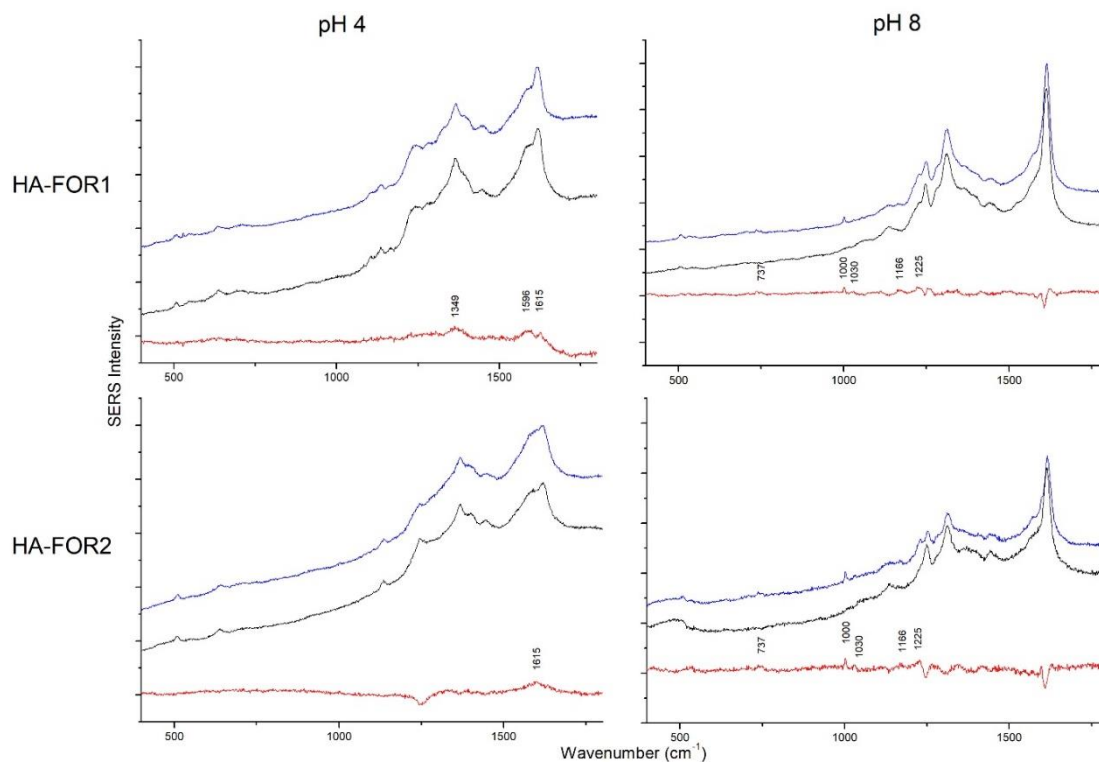


Figure 3.13 - SERS spectra of the complex HA-OXB for the HA extracted from forest soils. (Blue line: OXB+HA; Black line: HA; Red line: subtracted spectrum).

3.4 DISCUSSION

3.4.1 Adsorption and desorption study

These experiments were carried out to evaluate soil ability to adsorb and retain the organic contaminant. Kinetic study showed that the substantial part of adsorption occurred at the beginning phase, and it was faster in the soils richer in organic carbon content. This is probably due to the most available hydrophobic surfaces onto which OXB could adsorb, as suggested by Piwowarczyk & Holden (2012).

In order to study the adsorption and desorption phenomena, data were fitted according to the Freundlich model, since it presented a better fit in comparison with the Langmuir one (data not shown). C-type isotherms were obtained, thus indicating a steady partition of the OXB between the solution and the adsorbent in the concentration range considered. In addition, the $1/n$ Freundlich parameter, as expected, was approximately equal to unit, confirming the linearity of the curves. These findings agreed with the work of Calvet

(1989), according to whom this condition frequently occurs when soil adsorption (or desorption) involves hydrophobic compounds.

Regarding the adsorption phase, the Pearson correlation coefficient between K and soil OC was equal to 0.9937, suggesting as the soil OC is a dominating parameter able to affect the soil adsorption capacity against OXB. This trend is often recurring, as reported by several authors (Laabs & Amelung, 2005; Loffredo & Senesi, 2006; Vulava et al., 2016), who tested different hydrophobic organic molecules belonging to the classes of pesticides, endocrine disruptor compounds and pharmaceutically active compounds, respectively.

The K_{OC} coefficient was calculated with the aim to quantify the impact of the organic matter content on the adsorption phenomena. Indeed, the higher the K_{OC} value, the lower the contribution of the organic matter (Szabó et al., 2020). The fact that K_{OC} and K did not correlate implied that adsorption could be influenced by the quality of organic matter as well as by other soil components. As a result, comparable K_{OC} values were found for soils FOR1 and FOR2, suggesting that organic matter played a similar role in the adsorption despite the different total content. Conversely, the markedly higher value shown by soil AGR2 indicated that OXB may have substantially interacted with clay minerals or silt, as referred by Kumar & Philip (2006). In addition, in the AGR2 soil solution (with a pH of 7.72), OXB is predominantly in the anionic form ($pK_a = 7.1$), thus having the possibility to generate ionic bonds with the positive charges of aluminium and/or iron oxides (Brusseau & Chorover, 2019). These statements could explain the reason for which soil AGR2 have shown a higher adsorption capacity than FOR2, despite AGR2 was the poorest in OC content.

Soil AGR1 was characterized by a similar pH soil solution (7.78), however, OXB may have probably interacted mostly with the organic matter, as demonstrated by the lowest value of K_{OC} .

The desorption phase was also strictly dependent on the OC content, as proved by the Pearson correlation coefficient between K_{des} and soil OC equal to 0.977. Soils AGR1, AGR2 and FOR2 showed a K_{des} of the same magnitude of K , suggesting that the process of adsorption of OXB is reversible (Thorstensen et al., 2001). Conversely, for soil FOR1 the relation $K_{des} > K$ was found, indicating that OXB could lead to hysteresis in this type of soil. This phenomenon is commonly observed in adsorption studies, in particular when soils with a high OC content are chosen as substrates (Thorstensen et al., 2001;

Patakioutas & Albanis, 2002; Piwowarczyk & Holden, 2012; Sørensen et al., 2006). Hysteresis phenomena are not completely explained; indeed, they could be linked to irreversibility processes, but also to the need for a longer time for desorption to occur (Ainsworth et al., 1994; Bangash et al., 1992; Limousin et al., 2007). However, it is reasonable to assume that soil FOR1 could better retain the OXB, allowing less potential ground water contamination than the other soils considered.

3.4.2 Investigation of humic acids quality

In order to understand the mechanisms of interaction between organic matter and oxybenzone, we chose to preliminarily investigate the quality of humic acid. In particular, HA were extracted and analysed, since they are commonly considered as the most abundant and chemically active fraction of soil organic matter (Stevenson, 1994; Loffredo & Senesi, 2006). Fourier transform-infrared spectroscopy (FT-IR) and surface-enhanced raman spectroscopy (SERS) represent reliable and widely used tools in the field of HA characterization, as they permit a clear determination of the functional groups. (Corrado et al., 2008; Fookan & Liebezeit, 2003; Francioso et al., 1998; Francioso et al., 2019; Senesi et al., 2003).

The pattern of FT-IR spectra appeared very similar for all four HA sample analysed. Aliphatic asymmetric and symmetric C-H stretching associated to the presence of methyl and methylene groups were found at 2920 and 2850 cm^{-1} , respectively (Giovanela et al., 2004); higher intensities showed by HA-AGR1 and HA-AGR2 agree with the results obtained in the study of Allard (2006), in which several spectra of HA extracted from different sources were compared. In addition, these findings could be justified by the use of organic amendment from animal origin soils AGR1 and AGR2, which allowed the humification of residual fatty acid (Francioso et al., 2005).

The absence of peak at 1720 cm^{-1} , commonly associated to the C=O stretching of carboxylic groups (Niemeyer et al., 1992), could be related to the purification method, as referred by Tatzber et al. (2007). Furthermore, in the same article it was stated that the NaOH extraction ensured the acquisition of well-resolved spectra in the fingerprint area, as obtained in this work. The spectral zone between 1620 and 1600 cm^{-1} could be attributed to the aromatic C=C stretching and to the C=O stretching of carboxylic groups (Haberhauer et al., 1998; Pizzeghello et al., 2015; Tinti et al., 2015; Tivet et al., 2013).

The rA data agreed with the work of Senesi et al. (2003), in which the HA derived from a coniferous forest soil have shown the strongest intensity. The peak at 1540 cm^{-1} is commonly assigned to the carboxylate groups and to the C=C aromatic stretching (Francioso et al., 2005; Senesi et al., 2003). The higher rA found in this region and at 1620 cm^{-1} in the forestry samples suggested that HA-FOR1 and HA-FOR2 are characterized by the highest aromaticity. Moreover, these findings are corroborated by the ArI, which was calculated with the aim to quantify the aromatic component (Szabó et al., 2020; Traversa et al., 2011). The peak at 1420 cm^{-1} is attributed to the C-H bending (Francioso et al., 2005), while the band at 1220 cm^{-1} is commonly associated to the C-O stretching and the O-H deformation of carboxylic groups, phenols and unsaturated ethers (Conselvan et al., 2018; Niemeyer et al., 1992). No specific trend was observed for the latter peak, since HA-AGR2 and HA-FOR2 manifested the highest values. Regarding the rA associated to the peak at 1030 cm^{-1} , values of the same magnitude for all samples were found; this spectral area is usually assigned to the C-O stretching of polysaccharides (Conselvan et al., 2018) or to the Si-O vibrations of silicate impurities (Madejova & Komadel, 2001).

The SERS technique was a powerful tool that allows obtaining information, with the possibility to vary pH and substrate conditions. Experiments conducted in alkaline conditions (pH 8) using the AgCIT NPs as SERS substrate revealed the presence of two groups of peaks, defined as G band (1610 cm^{-1}) and D bands (1230 , 1250 and 1308 cm^{-1}) (Castiglioni et al., 2011; Castiglioni et al., 2004). These bands are due to the polycyclic aromatic hydrocarbon (PAH) structures belonging to the HA, as observed by previous studies (Carletti et al., 2010; Corrado et al., 2008; Francioso et al., 2005). In particular, the spectral area between 1230 and 1308 cm^{-1} appeared to be the one of major interest, since it could be attributable to the PAH structures with larger extent and characterized by different substituents (Francioso et al., 2019). Significant changes in peaks shape and position were observed by decreasing pH under acidic condition (pH 4). The reason is related to a morphological rearrangement of HA, from an uncoiled structure to a coiled one; this fact is induced by the decrease of electric repulsions and the parallel formation of H-bonds. The lowering of the intensity and broadening of the peaks are closely related to the location of the aromatic fractions, which are assumed to be positioned in the internal part of the HA in the coiled structure and, consequently, at a greater distance from the NPs surface (Sanchez-Cortes et al., 2006). The two peaks observed at 1136 and 1244 cm^{-1}

¹ in the spectra of HA-FOR1 and HA-FOR2 at pH 4 could be due to presence of polar functional groups (carboxylic and phenolic groups) of aromatic moieties also in the external part of the coiled HA structure, endorsing the hypothesis according to which the HA extracted from forest soils were richer in aromatic compounds. Additionally, these results were more evident in the experiments conducted using the AD8-AgHX NPs, since defined spectral profiles were observed only for the forestry HA samples under both pH conditions. The reason is certainly attributable to the surface functionalization with AD8, that allows the establishment of different bonds with respect to the citrate moieties. In the latter case, it is assumed that H-bonds represent the predominant linkage between the NPs and the HA, while the positive charges and the aliphatic chain of the AD8-AgHX NPs could also enable ionic and hydrophobic interactions. Regarding the spectra at pH 4, also in this case the D bands (1136, 1244 and 1368 cm^{-1}) showed by the forestry samples could be justified by the presence of oxygenated groups of aromatic structures in the external part of the coiled HA. Same considerations are valid for the spectra acquired under pH 8; in addition, the lowering of the peaks compared with the AgCIT-NPs experiment is probably due to the greater distance between the NPs and HA, since SERS is a distance-dependent technique.

FT-IR and SERS analysis showed results in mutual agreement, allowing to establish that forestry HA are characterized by a rich aromatic component, while the aliphatic component dominates in agricultural HA.

3.4.3 Study of oxybenzone-humic acids interactions

AD8-AgHX NPs were chosen as the best substrate to study the interactions of HA with OXB. Indeed, a less interfered spectrum was obtained in the case of OXB analysis compared to AgCIT NPs experiment; more defined spectra profiles were achieved in the HA analysis.

As readily observable in the acquired spectra, the behavior of OXB is affected both from pH and type of HA. Concerning the pH variations, it is reasonable to think that the coiled structure of HA in acidic pH entrapped the OXB in their inner part, promoting H-bonds with carboxylic or phenolic groups or interacting via π - π stacking with the aromatic moieties (Simpson, 2002). This condition favoured the lowering or total absence of the signal, since OXB molecules were located far from the metal surface to undergo the effect of the electromagnetic field (Roldán et al., 2011) (Figure 3.14 and 3.15). However, weak

signals were obtained for the forestry HA, thus confirming the presence of oxygenated groups in the external part of the coiled HA that were able to interact with OXB, as observed in the HA SERS analysis. Furthermore, the subtracted spectra showed the peak at 1615 cm^{-1} , which is assigned to the OXB carbonyl group, suggesting that the latter acts as H-bonds acceptor in the interaction with HA.

Conversely, the unrolling of HA, favoured by alkaline conditions, allowed more interactions with OXB due to external exposure of reactive functional groups. Notable differences distinguished the spectra of forestry and agricultural samples, supporting the results of the HA investigation, according to which the two types of HA are characterized by different chemical properties. At pH 8, OXB is mainly in the anionic form, being able to bind with the AD8 NH_3^+ groups via electrostatic attraction and, consequently, acting as a linker between the NPs and the HA. The larger number of peaks and the higher intensity showed by the agricultural samples could be related to the presence of aliphatic and aromatic alcohol and aldehydes groups able to interact via H-bonds with the carbonyl and/or the hydroxyl groups of OXB or π - π stacking (Figure 3.14). The H-bond interaction is supported by the peaks found at 1596 and 1628 cm^{-1} , whereas those found in the range $737 - 1341\text{ cm}^{-1}$ sustain the hypothesis of the π - π stacking, being related to the aromatic rings modal vibrations. Furthermore, literature reports that aliphatic HA exhibit high sorption capacities (Sierra et al., 2005; Simpson et al., 2003); this assertion is corroborated by FT-IR analysis, in which higher amount of aliphatic compounds were found in agricultural samples.

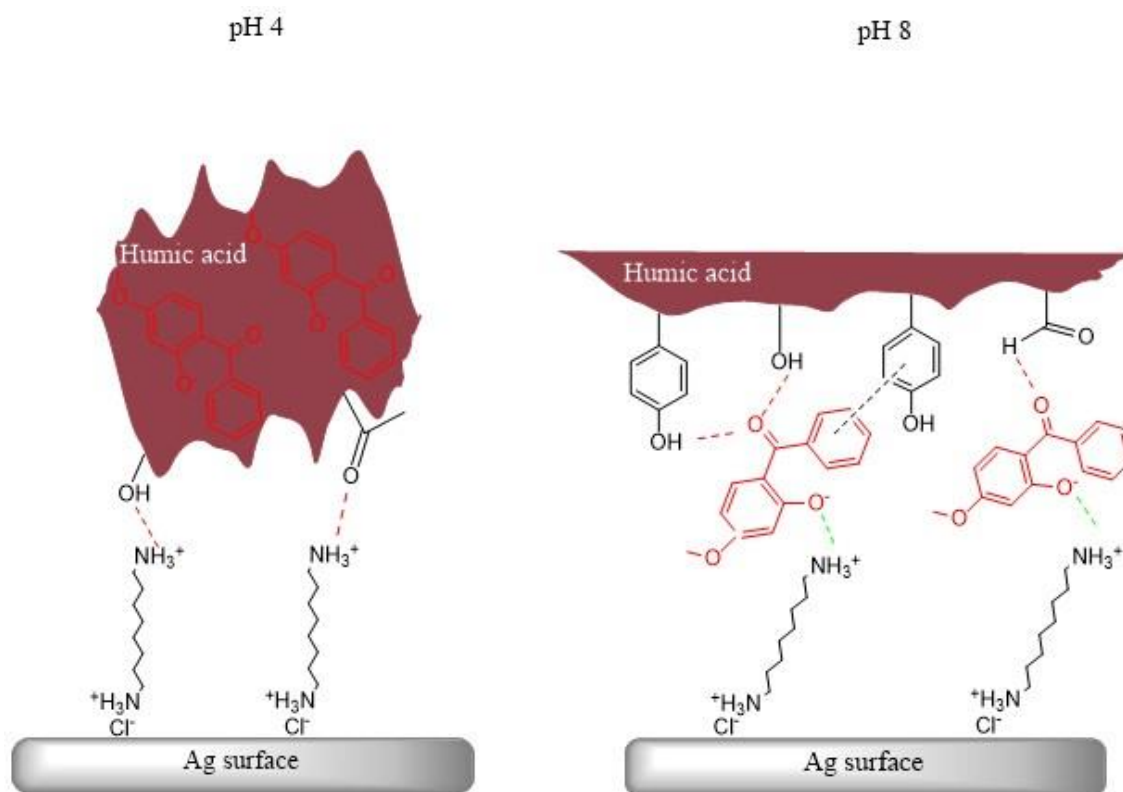


Figure 3.14 - Graphical representation of the proposed interactions concerning the agricultural HA. (Red molecules: OXB; Green hyphens: ionic attractions; Black hyphens: π - π stacking; Red hyphens: H-bonds)

Regarding the interaction with the forestry HA, OXB could be hindered by the high presence of ionized carboxylic groups (as supposed in the previous paragraph), developing ionic repulsions and/or competition for the positive charges of NH_3^+ (Figure 3.15). Another interpretation is provided by Roldán et al. (2011), according to whom HA rich in aromatic moieties lead to a greater aggregation and, consequently, to a lower adsorption potential. These facts could contribute to the removal of OXB from the metal surfaces, thus explaining the smaller number of peaks and the lowering of the intensity in the subtracted spectra. In this case, it is reasonable to assume that the π - π interaction is the dominant one, since the observed peaks were found in the range 737 - 1226 cm^{-1} .

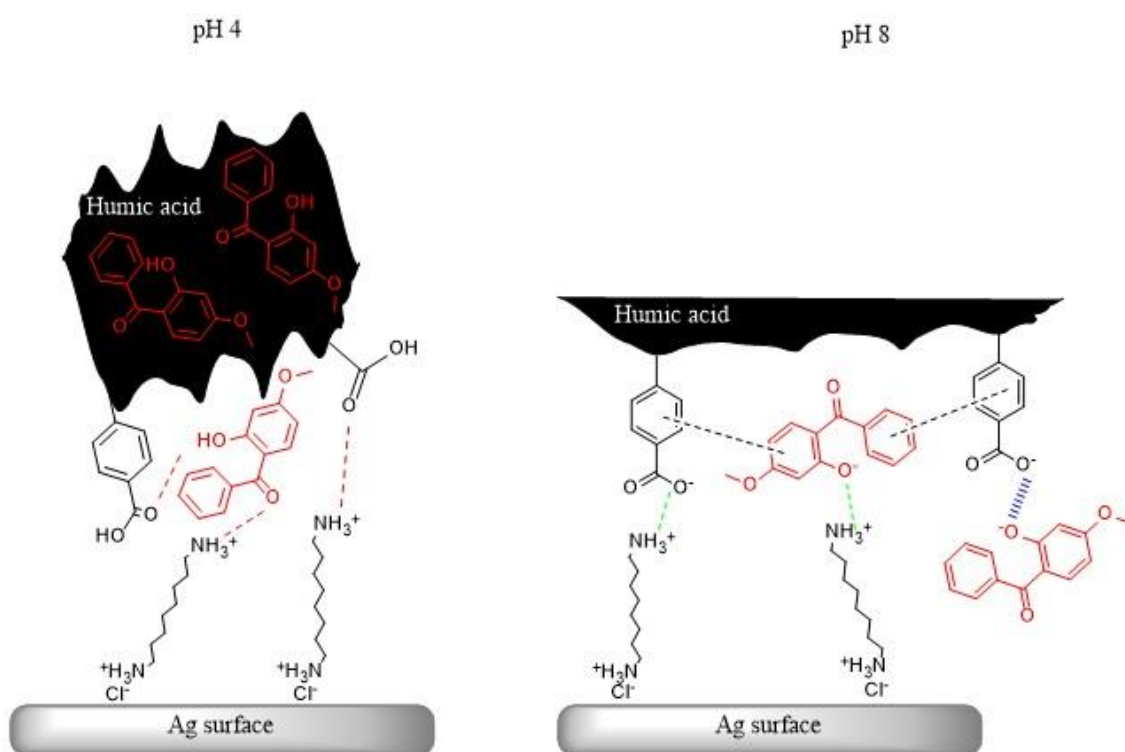


Figure 3.15 - Graphical representation of the proposed interactions concerning the forestry HA. (Red molecules: OXB; Green hyphens: ionic attractions; Black hyphens: π - π stacking; Red hyphens: H-bonds; Blue hyphens: ionic repulsions)

3.4.4 Relations between SERS results and adsorption/desorption study

SERS analysis has proven to be a useful tool for investigating the types of interactions involving OXB and HA. The assessment of these data, together with those obtained from the adsorption-desorption experiments, makes it possible to estimate the behavior of this contaminant in different soils. Soils FOR1 and FOR2 are characterized by an acid and a sub-acid pH, respectively. This condition should favour the development of circumstances like those observed in the SERS analysis at pH 4, in which OXB is preferably entrapped in the inner side of the HA by formation of H-bonds and π - π stacking, and interacting also with the carboxylic groups in the external side mainly by H-bonds. These strong interactions, along with the high amount of organic carbon content, represent the causes of the hysteresis phenomena observed in the adsorption-desorption test for the soil FOR1 (Chefetz et al., 2008).

Conversely, the sub-alkaline pH of soils AGR1 and AGR2 should promote an environment like that of the SERS analysis at pH 8. The prevalent bonds are assumed to

be the H-bonds and π - π stacking, in which the oxygenated aliphatic groups and aromatic phenols should play a dominant role.

3.5 CONCLUSIONS

Results suggested that the interaction of OXB with soil is strongly influenced by the OC content. Adsorption and desorption isotherms provided a useful indication of the potential mobility of the contaminant, suggesting retention in soils richer in organic matter. In order to better understand the mechanisms involved, HA were extracted from soils and analysed. FT-IR and SERS analysis showed different spectra profiles depending on the origin of HA. This finding is clearly related to their chemical structure, as the forestry samples were assumed to be richer in carboxylic groups and aromatic moieties, while the agricultural HA were richer in aliphatic compounds. The possibility to properly functionalize the Ag NPs in SERS allowed to deepen the knowledge on the mechanisms of interaction between OXB and HA. The obtained spectra led to assume that H-bonds and π - π stacking were the main interactions in both the types of HA, despite the involved functional groups of HA were different. It was demonstrated that the interaction OXB-HA is affected by both pH and HA type. Changes in pH induced changes in HA structures, leading to different areas of interactions. Regarding the type of HA, the agricultural HA showed a stronger interaction with respect to the forestry HA; however, this evidence did not affect the ability of soil to retain the contaminant, since its mobility is strongly influenced by organic matter content.

The need for sewage sludge use in agriculture calls for the development of new studies and methods to monitor the fate and behaviour of contaminants potentially present in sludge and thus entering the soil, with a focus on emerging organic contaminants. This research can be considered a reference in that direction.

GENERAL CONCLUSIONS

The results of this study highlighted the importance of evaluating several aspects in the application of sewage sludge in agriculture. Specifically, traceability, agronomic efficiency and potential environmental impact are three key factors investigated in this PhD thesis work.

Elemental and isotopic analysis of C and N, FT-IR and TG-DTA analysis demonstrated to be targeted techniques useful in discriminating municipal and tannery sludge. In particular, the analyses of C and N suggested that tannery sludge undergoes treatment processes that result in lower concentration of these two elements. Moreover, cattle feeding is supposed to affect the isotopic signatures of sewage sludge processed in the tannery wastewater treatment plant. The spectra resulting from the FT-IR and the thermal profiles of TG-DTA were clearly dissimilar, due to the different chemical compositions conditioned by both the influents reaching the treatment plants and the chemical used during the treatment phase. These potentialities can be exploited in the analysis of the organic fertilizers with the aim to trace the origin of sludge used. Furthermore, the performed analyses provided valuable information on treatment processes and chemicals used during its production, which could be important factors affecting nutrients release in soil.

Regarding this specific aspect, N release has a remarkable impact in the context of the agronomic efficiency. Since the main disadvantage in measuring this parameter is the long time required for the incubation essay, the hot-water extractable N was proposed as rapid and inexpensive alternative method to predict N release from sludge-based organic fertilizers.

Results were promising, as a good linear fit was found between the N_{bav} (i.e., nitrogen released during the parallel incubation essay) and the hot-water extractable N. In particular, the latter was slightly overestimated with respect to the N_{bav} in the case of the sludge-based organic fertilizers; however, it could provide immediate information for the purpose of proper application of these products in soil.

Finally, the environmental aspect was considered, evaluating the behavior of oxybenzone in soils with different physico-chemical properties. Oxybenzone is classified as an emerging contaminant and, among other environmental compartment, has also been found in sludge. Results showed that the organic carbon content is the factor that most contributes to the adsorption of oxybenzone in the soil. This outcome suggested that its

potential mobility is reduced in soil rich in organic matter. Analyses of organic matter revealed that humic acids from agricultural soils were richer in aliphatic compounds, while those extracted from forest soils were characterized by a greater amount of aromatic moieties. Interactions with oxybenzone occurred mainly through H-bonds and π - π stacking, but they were stronger and/or more abundant with the humic acids extracted from agricultural soils.

Technological development may lead, in some cases, to the introduction of new molecules that could prove to be contaminants to the environment. The search for innovative methods to study these emerging contaminants appears to be of relevant importance. In this context, SERS was satisfactory for analysing the behaviour of oxybenzone in soil and could potentially be applied to many other organic contaminants.

REFERENCES

- A.O.A.C. *Official Methods of Analysis* (15th ed.). (1990). Association of Official Analytical Chemist.
- Ainsworth, C. C., Gassman, P. L., Pilon, J. L., & Van Der Sluys, W. G. (1994). Cobalt, Cadmium, and Lead Sorption to Hydrous Iron Oxide: Residence Time Effect. *Soil Science Society of America Journal*, 58(6), 1615. <https://doi.org/10.2136/sssaj1994.03615995005800060005x>
- Albuquerque, J. A., de la Fuente, C., & Bernal, M. P. (2012). Chemical properties of anaerobic digestates affecting C and N dynamics in amended soils. *Agriculture, Ecosystems and Environment*, 160, 15–22. <https://doi.org/10.1016/j.agee.2011.03.007>
- Alcock, R. E., Bacon, J., Bardget, R. D., Beck, A. J., Haygarth, P. M., Lee, R. G. M., Parker, C. A., & Jones, K. C. (1996). Persistence and fate of polychlorinated biphenyls (PCBs) in sewage sludge-amended agricultural soils. *Environmental Pollution*, 93(1), 83–92. [https://doi.org/10.1016/0269-7491\(96\)00002-4](https://doi.org/10.1016/0269-7491(96)00002-4)
- Alibardi, L., & Cossu, R. (2016). Pre-treatment of tannery sludge for sustainable landfilling. *Waste Management*, 52, 202–211. <https://doi.org/10.1016/j.wasman.2016.04.008>
- Allard, B. (2006). A comparative study on the chemical composition of humic acids from forest soil, agricultural soil and lignite deposit: Bound lipid, carbohydrate and amino acid distributions. *Geoderma*, 130(1–2), 77–96. <https://doi.org/10.1016/j.geoderma.2005.01.010>
- Anjum, M., Al-Makishah, N. H., & Barakat, M. A. (2016). Wastewater sludge stabilization using pre-treatment methods. *Process Safety and Environmental Protection*, 102, 615–632. <https://doi.org/10.1016/j.psep.2016.05.022>
- Antil, R. S., Bar-Tal, A., Fine, P., & Hadas, A. (2011). Predicting Nitrogen and Carbon Mineralization of Composted Manure and Sewage Sludge in Soil. *Compost Science and Utilization*, 19(1), 33–43. <https://doi.org/10.1080/1065657X.2011.10736974>
- Antolín, M. C., Pascual, I., García, C., Polo, A., & Sánchez-Díaz, M. (2005). Growth, yield and solute content of barley in soils treated with sewage sludge under semiarid Mediterranean

- conditions. *Field Crops Research*, 94(2–3), 224–237. <https://doi.org/10.1016/j.fcr.2005.01.009>
- Aparicio, I., Santos, J. L., & Alonso, E. (2009). Limitation of the concentration of organic pollutants in sewage sludge for agricultural purposes: A case study in South Spain. *Waste Management*, 29(5), 1747–1753. <https://doi.org/10.1016/j.wasman.2008.11.003>
- Araujo, A. S. F., de Melo, W. J., Araujo, F. F., & Van den Brink, P. J. (2020). Long-term effect of composted tannery sludge on soil chemical and biological parameters. *Environmental Science and Pollution Research*, 27(33), 41885–41892. <https://doi.org/10.1007/s11356-020-10173-9>
- Banerjee, M. R., Burton, D. L., & Depoe, S. (1997). Impact of sewage sludge application, on soil biological characteristics. *Agriculture, Ecosystems and Environment*, 66(3), 241–249. [https://doi.org/10.1016/S0167-8809\(97\)00129-1](https://doi.org/10.1016/S0167-8809(97)00129-1)
- Bangash, M. A., Hanif, J., & Khan, M. A. (1992). Sorption behavior of cobalt on illitic soil. *Waste Management*, 12(1), 29–38. [https://doi.org/10.1016/0956-053X\(92\)90006-5](https://doi.org/10.1016/0956-053X(92)90006-5)
- Barberio, G., Cutaia, L., & Librici, V. (2013). Treatment and disposal of sewage sludge: comparative life cycle assessment on Italian case study. *Environmental Engineering and Management Journal*, 12(11), 7–10.
- Basegio, T., Berutti, F., Bernardes, A., & Bergmann, C. P. (2002). Environmental and technical aspects of the utilisation of tannery sludge as a raw material for clay products. *Journal of the European Ceramic Society*, 22(13), 2251–2259. [https://doi.org/10.1016/S0955-2219\(02\)00024-9](https://doi.org/10.1016/S0955-2219(02)00024-9)
- Behkami, S., Zain, S. M., Gholami, M., & Bakirdere, S. (2017). Isotopic ratio analysis of cattle tail hair: A potential tool in building the database for cow milk geographical traceability. *Food Chemistry*, 217, 438–444. <https://doi.org/10.1016/j.foodchem.2016.08.130>
- Benbi, D. K., & Richter, J. (2002). A critical review of some approaches to modelling nitrogen mineralization. *Biology and Fertility of Soils*, 35(3), 168–183. <https://doi.org/10.1007/s00374-002-0456-6>
- Bettiol, W., & Ghini, R. (2011). Impacts of Sewage Sludge in Tropical Soil: A Case Study in Brazil. *Applied and Environmental Soil Science*, 2011, 1–11. <https://doi.org/10.1155/2011/212807>
- Bhunias, S., Bhowmik, A., & Mukherjee, J. (2019). Use of rural slaughterhouse wastes (SHWs) as

fertilizer in agriculture: A review. *UEMGREEN 2019 - 1st International Conference on Ubiquitous Energy Management for Green Environment, July 2021*.

<https://doi.org/10.1109/UEMGREEN46813.2019.9221556>

Billen, G., Garnier, J., & Lassaletta, L. (2013). The nitrogen cascade from agricultural soils to the sea: Modelling nitrogen transfers at regional watershed and global scales. *Philosophical Transactions of the Royal Society B: Biological Sciences*, 368(1621).

<https://doi.org/10.1098/rstb.2013.0123>

Boecklen, W. J. (2011). Use of stable isotopes in foraging ecology and food web analysis. *Annual Review of Ecology, Evolution, and Systematics*, 42. <https://doi.org/10.1146/annurev-ecolsys-102209-144726>

Bontempo, L., Lombardi, G., Paoletti, R., Ziller, L., & Camin, F. (2012). H, C, N and O stable isotope characteristics of alpine forage, milk and cheese. *International Dairy Journal*, 23(2), 99–104. <https://doi.org/10.1016/j.idairyj.2011.10.005>

Brausch, J. M., & Rand, G. M. (2011). A review of personal care products in the aquatic environment: Environmental concentrations and toxicity. *Chemosphere*, 82(11), 1518–1532. <https://doi.org/10.1016/j.chemosphere.2010.11.018>

Bremner, J. M., & Keeney, D. R. (1965). Steam Distillation Methods for Determination of Ammonium, Nitrate and Nitrite. *Analytica Chimica Acta*, 32, 485–495.

Brooke, D. N., Burns, J. S., & Crookes, M. J. (2008). UV-filters in cosmetics – prioritisation for environmental assessment. In *Environment Agency*.

Brusseau, M. L., & Chorover, J. (2019). Chemical Processes Affecting Contaminant Transport and Fate. In *Environmental and Pollution Science* (3rd ed.). Elsevier Inc. <https://doi.org/10.1016/b978-0-12-814719-1.00008-2>

BS ISO 19698 : 2020 — Sludge recovery, recycling, treatment and disposal — Beneficial use of biosolids — Land application. (2020).

Bustillo-Lecompte, C. F., & Mehrvar, M. (2015). Slaughterhouse wastewater characteristics, treatment, and management in the meat processing industry: A review on trends and advances. *Journal of Environmental Management*, 161, 287–302. <https://doi.org/10.1016/j.jenvman.2015.07.008>

- Calderón, F. J., McCarty, G. W., & Reeves, J. B. (2005). Analysis of manure and soil nitrogen mineralization during incubation. *Biology and Fertility of Soils*, *41*(5), 328–336. <https://doi.org/10.1007/s00374-005-0843-x>
- Calvet, R. (1989). Adsorption of Organic Chemicals in Soils. *Environmental Health Perspectives*, *83*, 145. <https://doi.org/10.2307/3430653>
- Camino-Sánchez, F. J., Zafra-Gómez, A., Dorival-García, N., Juárez-Jiménez, B., & Vílchez, J. L. (2016). Determination of selected parabens, benzophenones, triclosan and triclocarban in agricultural soils after and before treatment with compost from sewage sludge: A lixiviation study. *Talanta*, *150*, 415–424. <https://doi.org/10.1016/j.talanta.2015.12.031>
- Campos, D., Gravato, C., Fedorova, G., Burkina, V., Soares, A. M. V. M., & Pestana, J. L. T. (2017). Ecotoxicity of two organic UV-filters to the freshwater caddisfly *Sericostoma vittatum*. *Environmental Pollution*, *228*, 370–377. <https://doi.org/10.1016/j.envpol.2017.05.021>
- Capodaglio, A., Hlavinek, P., & Raboni, M. (2016). Advances in wastewater nitrogen removal by biological processes: state of the art review. *Revista Ambiente e Agua*, *9*(3), 445–458. <https://doi.org/10.4136/1980-993X>
- Carbonell, G., Imperial, R. M. de, Torrijos, M., Delgado, M., & Rodriguez, J. A. (2011). Effects of municipal solid waste compost and mineral fertilizer amendments on soil properties and heavy metals distribution in maize plants (*Zea mays* L.). *Chemosphere*, *85*(10), 1614–1623. <https://doi.org/10.1016/j.chemosphere.2011.08.025>
- Carletti, P., Roldán, M. L., Francioso, O., Nardi, S., & Sanchez-Cortes, S. (2010). Structural characterization of humic-like substances with conventional and surface-enhanced spectroscopic techniques. *Journal of Molecular Structure*, *982*(1–3), 169–175. <https://doi.org/10.1016/j.molstruc.2010.08.028>
- Cassity-Duffey, K., Cabrera, M., Gaskin, J., Franklin, D., Kissel, D., & Saha, U. (2020). Nitrogen mineralization from organic materials and fertilizers: Predicting N release. *Soil Science Society of America Journal*, *84*(2), 522–533. <https://doi.org/10.1002/saj2.20037>
- Castiglioni, C., Milani, A., Fazzi, D., & Negri, F. (2011). Modulation of the electronic structure of polyconjugated organic molecules by geometry relaxation: A discussion based on local Raman parameters. *Journal of Molecular Structure*, *993*(1–3), 26–37. <https://doi.org/10.1016/j.molstruc.2010.12.021>

- Castiglioni, C., Tommasini, M., & Zerbi, G. (2004). Raman spectroscopy of polyconjugated molecules and materials: confinement effect in one and two dimensions. *Philosophical Transactions of the Royal Society A: Mathematical, Physical and Engineering Sciences*, 362, 2425–2459. <https://doi.org/10.1098/rsta.2004.1448>
- Cayuela, M. L., Velthof, G. L., Mondini, C., Sinicco, T., & van Groenigen, J. W. (2010). Nitrous oxide and carbon dioxide emissions during initial decomposition of animal by-products applied as fertilisers to soils. *Geoderma*, 157(3–4), 235–242. <https://doi.org/10.1016/j.geoderma.2010.04.026>
- Chefetz, B., Hatcher, P. G., Hadar, Y., & Chen, Y. (1996). Chemical and Biological Characterization of Organic Matter during Composting of Municipal Solid Waste. *Journal of Environmental Quality*, 25(4), 776–785. <https://doi.org/10.2134/jeq1996.00472425002500040018x>
- Chefetz, B., Mualem, T., & Ben-Ari, J. (2008). Sorption and mobility of pharmaceutical compounds in soil irrigated with reclaimed wastewater. *Chemosphere*, 73(8), 1335–1343. <https://doi.org/10.1016/j.chemosphere.2008.06.070>
- Ciavatta, C., Manoli, C., Cavani, L., Franceschi, C., & Sequi, P. (2012). Chromium-Containing Organic Fertilizers from Tanned Hides and Skins: A Review on Chemical, Environmental, Agronomical and Legislative Aspects. *Journal of Environmental Protection*, 03(11), 1532–1541. <https://doi.org/10.4236/jep.2012.311169>
- Ciešlik, B. M., Namieśnik, J., & Konieczka, P. (2015). Review of sewage sludge management: Standards, regulations and analytical methods. *Journal of Cleaner Production*, 90, 1–15. <https://doi.org/10.1016/j.jclepro.2014.11.031>
- Clarke, B. O., Porter, N. A., Marriott, P. J., & Blackbeard, J. R. (2010). Investigating the levels and trends of organochlorine pesticides and polychlorinated biphenyl in sewage sludge. *Environment International*, 36(4), 323–329. <https://doi.org/10.1016/j.envint.2010.01.004>
- Clarke, B. O., & Smith, S. R. (2011). Review of “emerging” organic contaminants in biosolids and assessment of international research priorities for the agricultural use of biosolids. *Environment International*, 37(1), 226–247. <https://doi.org/10.1016/j.envint.2010.06.004>
- Clarke, R. M., & Cummins, E. (2015). Evaluation of “Classic” and Emerging Contaminants Resulting from the Application of Biosolids to Agricultural Lands: A Review. *Human and*

- Ecological Risk Assessment*, 21(2), 492–513. <https://doi.org/10.1080/10807039.2014.930295>
- Conselvan, G. B., Fuentes, D., Merchant, A., Peggion, C., Francioso, O., & Carletti, P. (2018). Effects of humic substances and indole-3-acetic acid on Arabidopsis sugar and amino acid metabolic profile. *Plant and Soil*, 426(1–2), 17–32. <https://doi.org/10.1007/s11104-018-3608-7>
- Corrado, G., Sanchez-Cortes, S., Francioso, O., & Garcia-Ramos, J. V. (2008). Surface-enhanced Raman and fluorescence joint analysis of soil humic acids. *Analytica Chimica Acta*, 616(1), 69–77. <https://doi.org/10.1016/j.aca.2008.04.019>
- Corte, L., Dell'Abate, M. T., Magini, A., Migliore, M., Felici, B., Roscini, L., Sardella, R., Tancini, B., Emiliani, C., Cardinali, G., & Benedetti, A. (2014). Assessment of safety and efficiency of nitrogen organic fertilizers from animal-based protein hydrolysates—a laboratory multidisciplinary approach. *Journal of the Science of Food and Agriculture*, 94(2), 235–245. <https://doi.org/10.1002/jsfa.6239>
- Cuetos, M. J., Gómez, X., Otero, M., & Morán, A. (2010). Anaerobic digestion of solid slaughterhouse waste: Study of biological stabilization by Fourier Transform infrared spectroscopy and thermogravimetry combined with mass spectrometry. *Biodegradation*, 21(4), 543–556. <https://doi.org/10.1007/s10532-009-9322-7>
- Curtin, D., Wright, C. E., Beare, M. H., & McCallum, F. M. (2006). Hot Water-Extractable Nitrogen as an Indicator of Soil Nitrogen Availability. *Soil Science Society of America Journal*, 70(5), 1512–1521. <https://doi.org/10.2136/sssaj2005.0338>
- De Oliveira Silva, J., Filho, G. R., Da Silva Meireles, C., Ribeiro, S. D., Vieira, J. G., Da Silva, C. V., & Cerqueira, D. A. (2012). Thermal analysis and FTIR studies of sewage sludge produced in treatment plants. the case of sludge in the city of Uberlândia-MG, Brazil. *Thermochimica Acta*, 528, 72–75. <https://doi.org/10.1016/j.tca.2011.11.010>
- Deeks, L. K., Chaney, K., Murray, C., Sakrabani, R., Gedara, S., Le, M. S., Tyrrel, S., Pawlett, M., Read, R., & Smith, G. H. (2013). A new sludge-derived organo-mineral fertilizer gives similar crop yields as conventional fertilizers. *Agronomy for Sustainable Development*, 33(3), 539–549. <https://doi.org/10.1007/s13593-013-0135-z>
- Delin, S., Stenberg, B., Nyberg, A., & Brohede, L. (2012). Potential methods for estimating nitrogen fertilizer value of organic residues. *Soil Use and Management*, 28(3), 283–291. <https://doi.org/10.1111/j.1475-2743.2012.00417.x>

- Dell'Abate, M. T., Benedetti, A., Trinchera, A., & Galluzzo, D. (2003). Nitrogen and carbon mineralisation of leather meal in soil as affected by particle size of fertiliser and microbiological activity of soil. *Biology and Fertility of Soils*, *37*(2), 124–129. <https://doi.org/10.1007/s00374-002-0568-z>
- Devi, P., & Saroha, A. K. (2017). Utilization of sludge based adsorbents for the removal of various pollutants: A review. *Science of the Total Environment*, *578*, 16–33. <https://doi.org/10.1016/j.scitotenv.2016.10.220>
- Di Giacomo, G., & Romano, P. (2022). Evolution and Prospects in Managing Sewage Sludge Resulting from Municipal Wastewater Purification. *Energies*, *15*(15). <https://doi.org/10.3390/en15155633>
- Diacono, M., & Montemurro, F. (2010). Long-term effects of organic amendments on soil fertility. A review. *Agronomy for Sustainable Development*, *30*(2), 401–422. <https://doi.org/10.1051/agro/2009040>
- Díaz-Cruz, M. S., García-Galán, M. J., Guerra, P., Jelic, A., Postigo, C., Eljarrat, E., Farré, M., López de Alda, M. J., Petrovic, M., Barceló, D., & Petrovic, M. (2009). Analysis of selected emerging contaminants in sewage sludge. *TrAC - Trends in Analytical Chemistry*, *28*(11), 1263–1275. <https://doi.org/10.1016/j.trac.2009.09.003>
- Drechsel, P., Qadir, M., & Wichelns, D. (2015). Wastewater: Economic asset in an urbanizing world. *Wastewater: Economic Asset in an Urbanizing World, December*, 1–282. <https://doi.org/10.1007/978-94-017-9545-6>
- Duan, B., Liu, F., Zhang, W., Zheng, H., Zhang, Q., Li, X., & Bu, Y. (2015). Evaluation and source apportionment of heavy metals (HMs) in sewage sludge of municipal wastewater treatment plants (WWTPs) in Shanxi, China. *International Journal of Environmental Research and Public Health*, *12*(12), 15807–15818. <https://doi.org/10.3390/ijerph121215022>
- Durdevic, D., Zikovic, S., & Blecich, P. (2022). Sustainable Sewage Sludge Management Technologies Selection Based on Techno-Economic-Environmental Criteria: Case Study of Croatia. *Energies*, *15*(3941).
- EC. (1986). *COUNCIL DIRECTIVE of 12 June 1986 on the protection of the environment, and in particular of the soil, when sewage sludge is used in agriculture.*

- EC. (2009). *REGULATION (EC) No 1223/2009 OF THE EUROPEAN PARLIAMENT AND OF THE COUNCIL of 30 November 2009 on cosmetic products.*
- EC. (2020). *COMMUNICATION FROM THE COMMISSION TO THE EUROPEAN PARLIAMENT, THE COUNCIL, THE EUROPEAN ECONOMIC AND SOCIAL COMMITTEE AND THE COMMITTEE OF THE REGIONS A new Circular Economy Action Plan For a cleaner and more competitive Europe.*
- EPA. (2021). *Basic Information about Biosolids.* <https://www.epa.gov/biosolids/basic-information-about-biosolids>
- Eskicioglu, C., Kennedy, K. J., & Droste, R. L. (2006). Characterization of soluble organic matter of waste activated sludge before and after thermal pretreatment. *Water Research, 40*(20), 3725–3736. <https://doi.org/10.1016/j.watres.2006.08.017>
- Fernández, J. M., Plaza, C., García-Gil, J. C., & Polo, A. (2009). Biochemical properties and barley yield in a semiarid Mediterranean soil amended with two kinds of sewage sludge. *Applied Soil Ecology, 42*(1), 18–24. <https://doi.org/10.1016/j.apsoil.2009.01.006>
- Folgueras, M. B., Díaz, R. M., Xiberta, J., & Prieto, I. (2003). Volatilisation of trace elements for coal-sewage sludge blends during their combustion. *Fuel, 82*(15–17), 1939–1948. [https://doi.org/10.1016/S0016-2361\(03\)00152-2](https://doi.org/10.1016/S0016-2361(03)00152-2)
- Fooker, U., & Liebezeit, G. (2003). An IR study of humic acids isolated from sediments and soils. *Senckenbergiana Maritima, 32*(1–2), 183–189. <https://doi.org/10.1007/BF03043094>
- Francioso, O., Sánchez-Cortés, S., Corrado, G., Gioacchini, P., & Ciavatta, C. (2005). Characterization of soil organic carbon in long-term amendment trials. *Spectroscopy Letters, 38*(3), 283–291. <https://doi.org/10.1081/SL-200058704>
- Francioso, O., Sánchez-Cortés, S., Tugnoli, V., Ciavatta, C., & Gessa, C. (1998). Characterization of peat fulvic acid fractions by means of FT-IR, SERS, and ¹H, ¹³C NMR spectroscopy. *Applied Spectroscopy, 52*(2), 270–277. <https://doi.org/10.1366/0003702981943347>
- Francioso, Ornella, López-Tobar, E., Torreggiani, A., Iriarte, M., & Sanchez-Cortes, S. (2019). Stimulated Adsorption of Humic Acids on Capped Plasmonic Ag Nanoparticles Investigated by Surface-Enhanced Optical Techniques. *Langmuir, 35*(13), 4518–4526. <https://doi.org/10.1021/acs.langmuir.9b00190>

- Francioso, Ornella, Rodriguez-Estrada, M. T., Montecchio, D., Salomoni, C., Caputo, A., & Palenzona, D. (2010). Chemical characterization of municipal wastewater sludges produced by two-phase anaerobic digestion for biogas production. *Journal of Hazardous Materials*, 175(1–3), 740–746. <https://doi.org/10.1016/j.jhazmat.2009.10.071>
- Fuentes, A., Lloréns, M., Sáez, J., Aguilar, M. I., Ortuño, J. F., & Meseguer, V. F. (2004). Phytotoxicity and heavy metals speciation of stabilised sewage sludges. *Journal of Hazardous Materials*, 108(3), 161–169. <https://doi.org/10.1016/j.jhazmat.2004.02.014>
- Gago-ferrero, P., Díaz-cruz, M. S., & Barceló, D. (2011). Occurrence of multiclass UV filters in treated sewage sludge from wastewater treatment plants. *Chemosphere*, 84(8), 1158–1165. <https://doi.org/10.1016/j.chemosphere.2011.04.003>
- Gale, E. S., Sullivan, D. M., Cogger, C. G., Bary, A. I., Hemphill, D. D., & Myhre, E. A. (2006). Estimating Plant-Available Nitrogen Release from Manures, Composts, and Specialty Products. *Journal of Environmental Quality*, 35(6), 2321–2332. <https://doi.org/10.2134/jeq2006.0062>
- Galloway, J. N., Aber, J. D., Erisman, J. W., Seitzinger, S. P., Howarth, R. W., Cowling, E. B., & Cosby, B. J. (2003). The nitrogen cascade. *BioScience*, 53(4), 341–356. [https://doi.org/10.1641/0006-3568\(2003\)053\[0341:TNC\]2.0.CO;2](https://doi.org/10.1641/0006-3568(2003)053[0341:TNC]2.0.CO;2)
- Gee, G. W. ; Bauder, J. W. (1986). Particle size analysis. *Methods of Soil Analysis, Part 1. Physical and Mineralogical Methods-Agronomy Monograph No. 9 (2nd Edition)*, 54(4), 17–26.
- Gherghel, A., Teodosiu, C., & De Gisi, S. (2019). A review on wastewater sludge valorisation and its challenges in the context of circular economy. *Journal of Cleaner Production*, 228, 244–263. <https://doi.org/10.1016/j.jclepro.2019.04.240>
- Giacometti, C., Cavani, L., Gioacchini, P., Ciavatta, C., & Marzadori, C. (2012). Soil application of tannery land plaster: Effects on nitrogen mineralization and soil biochemical properties. *Applied and Environmental Soil Science*, 2012(Iii). <https://doi.org/10.1155/2012/395453>
- Gil, A., Siles, J. A., Martín, M. A., Chica, A. F., Estévez-Pastor, F. S., & Toro-Baptista, E. (2018). Effect of microwave pretreatment on semi-continuous anaerobic digestion of sewage sludge. *Renewable Energy*, 115, 917–925. <https://doi.org/10.1016/j.renene.2017.07.112>
- Giovanela, M., Parlanti, E., Soriano-Sierra, E. J., Soldi, M. S., & Sierra, M. M. D. (2004).

- Elemental compositions, FT-IR spectral and thermal behavior of sedimentary fulvic and humic acids from aquatic and terrestrial environments. *Geochemical Journal*, 38(3), 255–264. <https://doi.org/10.2343/geochemj.38.255>
- Głodniok, M., Deska, M., & Kaszycki, P. (2022). *Impact of the Stabilized Sewage Sludge-Based Granulated Fertilizer on Sinapis alba Growth and Biomass Chemical Characteristics*. 35. <https://doi.org/10.3390/ieag2021-09736>
- Gomes, R. L., Scrimshaw, M. D., & Lester, J. N. (2009). Fate of conjugated natural and synthetic steroid estrogens in crude sewage and activated sludge batch studies. *Environmental Science and Technology*, 43(10), 3612–3618. <https://doi.org/10.1021/es801952h>
- Grigatti, M., Cavani, L., di Biase, G., & Ciavatta, C. (2019). Current and residual phosphorous availability from compost in a ryegrass pot test. *Science of the Total Environment*, 677, 250–262. <https://doi.org/10.1016/j.scitotenv.2019.04.349>
- Guo-Tao, F., Zhi-Hua, S., Shuqing, L., & Hui, C. (2013). The Production of Organic Fertilizer Using Tannery Sludge. *J. Am. Leather Chem. Assoc.*, 108, 189–196.
- Haberhauer, G., Rafferty, B., Strebl, F., & Gerzabek, M. H. (1998). Comparison of the composition of forest soil litter derived from three different sites at various decompositional stages using FTIR spectroscopy. *Geoderma*, 83, 331–342.
- Haroun, M., Idris, A., & Syed Omar, & S. R. (2007). Characterisation and Composting of Tannery Sludge. *Malaysian Society of Soil Science Malaysian Journal of Soil Science*, 11(January 2007), 71–80.
- Harper, E. (1980). Collagenases. *Ann. Rev. Biochem.*, 49, 1063–1078.
- Hei, L., Jin, P., Zhu, X., Ye, W., & Yang, Y. (2016). Characteristics of Speciation of Heavy Metals in Municipal Sewage Sludge of Guangzhou as Fertilizer. *Procedia Environmental Sciences*, 31, 232–240. <https://doi.org/10.1016/j.proenv.2016.02.031>
- Hoeinghaus, D. J., & Zeug, S. C. (2008). Can stable isotope ratios provide for community-wide measures of trophic structure? reply. *Ecology*, 89(8), 2358–2359. <https://doi.org/10.1890/08-0167.1>
- Honeycutt, C. W., Zibilske, L. M., & Clapham, W. M. (1988). Heat Units for Describing Carbon Mineralization and Predicting Net Nitrogen Mineralization. *Soil Science Society of America*

- Journal*, 52(5), 1346–1350. <https://doi.org/10.2136/sssaj1988.03615995005200050026x>
- Huo, Y. X., Wernick, D. G., & Liao, J. C. (2012). Toward nitrogen neutral biofuel production. *Current Opinion in Biotechnology*, 23(3), 406–413. <https://doi.org/10.1016/j.copbio.2011.10.005>
- Hussain, F., Malik, K. A., & Azam, F. (1984). Evaluation of acid permanganate extraction as an index of soil nitrogen availability. *Plant and Soil*, 79(2), 249–254. <https://doi.org/10.1007/BF02182347>
- ISO 10390:2005 Soil quality — Determination of pH. (2005).
- ISO 11265:1994 Soil quality — Determination of the specific electrical conductivity. (1994).
- ISO 14256-2:2005 Soil quality — Determination of nitrate, nitrite and ammonium in field-moist soils by extraction with potassium chloride solution — Part 2: Automated method with segmented flow analysis. (2005).
- Jastrzębska, M., Kostrzevska, M. K., & Saeid, A. (2022). Phosphorus Fertilizers from Sewage Sludge Ash and Animal Blood as an Example of Biobased Environment-Friendly Agrochemicals: Findings from Field Experiments. *Molecules*, 27(9). <https://doi.org/10.3390/molecules27092769>
- Jeon, H. K., Chung, Y., & Ryu, J. C. (2006a). Simultaneous determination of benzophenone-type UV filters in water and soil by gas chromatography-mass spectrometry. *Journal of Chromatography A*, 1131(1–2), 192–202. <https://doi.org/10.1016/j.chroma.2006.07.036>
- Jeon, H. K., Chung, Y., & Ryu, J. C. (2006b). Simultaneous determination of benzophenone-type UV filters in water and soil by gas chromatography-mass spectrometry. *Journal of Chromatography A*, 1131(1–2), 192–202. <https://doi.org/10.1016/j.chroma.2006.07.036>
- Joseph, L., Sajan, D., Chaitanya, K., Suthan, T., Rajesh, N. P., & Isac, J. (2014). Molecular structure, NBO analysis, electronic absorption and vibrational spectral analysis of 2-Hydroxy-4-Methoxybenzophenone: Reassignment of fundamental modes. *Spectrochimica Acta - Part A: Molecular and Biomolecular Spectroscopy*, 120, 216–227. <https://doi.org/10.1016/j.saa.2013.09.128>
- Juel, M. A. I., Chowdhury, Z. U. M., & Ahmed, T. (2016). Heavy metal speciation and toxicity characteristics of tannery sludge. *AIP Conference Proceedings*, 1754.

<https://doi.org/10.1063/1.4958450>

Kacprzak, M., Neczaj, E., Fijałkowski, K., Grobelak, A., Grosser, A., Worwag, M., Rorat, A., Brattebo, H., Almås, Å., & Singh, B. R. (2017). Sewage sludge disposal strategies for sustainable development. *Environmental Research*, 156(January), 39–46.

<https://doi.org/10.1016/j.envres.2017.03.010>

Kandeler, E., Tscherko, D., Bruce, K. D., Stemmer, M., Hobbs, P. J., Bardgett, R. D., & Amelung, W. (2000). Structure and function of the soil microbial community in microhabitats of a heavy metal polluted soil. *Biology and Fertility of Soils*, 32(5), 390–400.

<https://doi.org/10.1007/s003740000268>

Kataki, S., Hazarika, S., & Baruah, D. C. (2017). Assessment of by-products of bioenergy systems (anaerobic digestion and gasification) as potential crop nutrient. *Waste Management*, 59, 102–117. <https://doi.org/10.1016/j.wasman.2016.10.018>

Kavouras, P., Pantazopoulou, E., Varitis, S., Vourlias, G., Chrissafis, K., Dimitrakopoulos, G. P., Mitrakas, M., Zouboulis, A. I., Karakostas, T., & Xenidis, A. (2015). Incineration of tannery sludge under oxic and anoxic conditions: Study of chromium speciation. *Journal of Hazardous Materials*, 283, 672–679. <https://doi.org/10.1016/j.jhazmat.2014.09.066>

Kim, S., & Choi, K. (2014). Occurrences, toxicities, and ecological risks of benzophenone-3, a common component of organic sunscreen products: A mini-review. *Environment International*, 70, 143–157. <https://doi.org/10.1016/j.envint.2014.05.015>

Kizilkaya, R., & Bayrakli, B. (2005). Effects of N-enriched sewage sludge on soil enzyme activities. *Applied Soil Ecology*, 30(3), 192–202. <https://doi.org/10.1016/j.apsoil.2005.02.009>

Kołodziej, B., Antonkiewicz, J., Stachyra, M., Bielińska, E. J., Wiśniewski, J., Luchowska, K., & Kwiatkowski, C. (2015). Use of sewage sludge in bioenergy production-A case study on the effects on sorghum biomass production. *European Journal of Agronomy*, 69(2015), 63–74. <https://doi.org/10.1016/j.eja.2015.06.004>

Kominko, H., Gorazda, K., & Wzorek, Z. (2019). Potentiality of sewage sludge-based organo-mineral fertilizer production in Poland considering nutrient value, heavy metal content and phytotoxicity for rapeseed crops. *Journal of Environmental Management*, 248(February), 109283. <https://doi.org/10.1016/j.jenvman.2019.109283>

- Kominko, H., Gorazda, K., Wzorek, Z., & Wojtas, K. (2018). Sustainable Management of Sewage Sludge for the Production of Organo-Mineral Fertilizers. *Waste and Biomass Valorization*, 9(10), 1817–1826. <https://doi.org/10.1007/s12649-017-9942-9>
- Köninger, J., Lugato, E., Panagos, P., Kochupillai, M., Orgiazzi, A., & Briones, M. J. I. (2021). Manure management and soil biodiversity: Towards more sustainable food systems in the EU. *Agricultural Systems*, 194(July). <https://doi.org/10.1016/j.agsy.2021.103251>
- Koutroubas, S. D., Antoniadis, V., Fotiadis, S., & Damalas, C. A. (2014). Growth, grain yield and nitrogen use efficiency of Mediterranean wheat in soils amended with municipal sewage sludge. *Nutrient Cycling in Agroecosystems*, 100(2), 227–243. <https://doi.org/10.1007/s10705-014-9641-x>
- Kowalski, M., Kowalska, K., Wiszniowski, J., & Turek-Szytow, J. (2018). Qualitative analysis of activated sludge using FT-IR technique. *Chemical Papers*, 72(11), 2699–2706. <https://doi.org/10.1007/s11696-018-0514-7>
- Kumar, M., & Philip, L. (2006). Adsorption and desorption characteristics of hydrophobic pesticide endosulfan in four Indian soils. *Chemosphere*, 62(7), 1064–1077. <https://doi.org/10.1016/j.chemosphere.2005.05.009>
- Kumpiene, J., Lagerkvist, A., & Maurice, C. (2008). Stabilization of As, Cr, Cu, Pb and Zn in soil using amendments - A review. *Waste Management*, 28(1), 215–225. <https://doi.org/10.1016/j.wasman.2006.12.012>
- Laabs, V., & Amelung, W. (2005). Sorption and aging of corn and soybean pesticides in tropical soils of Brazil. *Journal of Agricultural and Food Chemistry*, 53(18), 7184–7192. <https://doi.org/10.1021/jf050969c>
- Lal, R. (2004). Soil carbon sequestration to mitigate climate change. *Geoderma*, 123(1–2), 1–22. <https://doi.org/10.1016/j.geoderma.2004.01.032>
- Lamastra, L., Suci, N. A., & Trevisan, M. (2018). Sewage sludge for sustainable agriculture: Contaminants' contents and potential use as fertilizer. *Chemical and Biological Technologies in Agriculture*, 5(1), 1–6. <https://doi.org/10.1186/s40538-018-0122-3>
- Langford, K. H., Reid, M. J., Fjeld, E., Øxnevad, S., & Thomas, K. V. (2015). Environmental occurrence and risk of organic UV filters and stabilizers in multiple matrices in Norway.

Environment International, 80, 1–7. <https://doi.org/10.1016/j.envint.2015.03.012>

Lassaletta, L., Billen, G., Grizzetti, B., Anglade, J., & Garnier, J. (2014). 50 year trends in nitrogen use efficiency of world cropping systems: The relationship between yield and nitrogen input to cropland. *Environmental Research Letters*, 9(10). <https://doi.org/10.1088/1748-9326/9/10/105011>

Lazicki, P., Geisseler, D., & Lloyd, M. (2020). Nitrogen mineralization from organic amendments is variable but predictable. *Journal of Environmental Quality*, 49(2), 483–495. <https://doi.org/10.1002/jeq2.20030>

Lee, P. C., & Meisel, D. (1982). Adsorption and surface-enhanced Raman of dyes on silver and gold sols. *Journal of Physical Chemistry*, 86(17), 3391–3395. <https://doi.org/10.1021/j100214a025>

Leopold, N., & Lendl, B. (2003). A new method for fast preparation of highly surface-enhanced raman scattering (SERS) active silver colloids at room temperature by reduction of silver nitrate with hydroxylamine hydrochloride. *Journal of Physical Chemistry B*, 107(24), 5723–5727. <https://doi.org/10.1021/jp027460u>

Liao, C., & Kannan, K. (2014). Widespread occurrence of benzophenone-type uv light filters in personal care products from China and the United States: An assessment of human exposure. *Environmental Science and Technology*, 48(7), 4103–4109. <https://doi.org/10.1021/es405450n>

Liknaw, G., Tekalign, T., & Guya, K. (2017). Impacts of Tannery Effluent on Environments and Human Health. *Journal of Environmental and Earth Science*, 7(3), 88–97. www.iiste.org

Limeneh, D. Y., Tesfaye, T., Ayele, M., Husien, N. M., Ferede, E., Haile, A., Mengie, W., Abuhay, A., Gelebo, G. G., Gibril, M., & Kong, F. (2022). A Comprehensive Review on Utilization of Slaughterhouse By-Product: Current Status and Prospect. *Sustainability (Switzerland)*, 14(11). <https://doi.org/10.3390/su14116469>

Limousin, G., Gaudet, J. P., Charlet, L., Szenknect, S., Barthès, V., & Krimissa, M. (2007). Sorption isotherms: A review on physical bases, modeling and measurement. *Applied Geochemistry*, 22(2), 249–275. <https://doi.org/10.1016/j.apgeochem.2006.09.010>

Lloret, E., Pascual, J. A., Brodie, E. L., Bouskill, N. J., Insam, H., Juárez, M. F. D., & Goberna, M. (2016). Sewage sludge addition modifies soil microbial communities and plant performance

- depending on the sludge stabilization process. *Applied Soil Ecology*, *101*, 37–46.
<https://doi.org/10.1016/j.apsoil.2016.01.002>
- Loffredo, E., & Senesi, N. (2006a). Fate of anthropogenic organic pollutants in soils with emphasis on adsorption/desorption processes of endocrine disruptor compounds. *Pure and Applied Chemistry*, *78*(5), 947–961. <https://doi.org/10.1351/pac200678050947>
- Loffredo, E., & Senesi, N. (2006b). The role of humic substances in the fate of anthropogenic organic pollutants in soil with emphasis on endocrine disruptor compounds. *Soil and Water Pollution Monitoring, Protection and Remediation*, 3–23.
<https://doi.org/10.1351/pac200678050947>
- Luo, G., Li, L., Friman, V. P., Guo, J., Guo, S., Shen, Q., & Ling, N. (2018). Organic amendments increase crop yields by improving microbe-mediated soil functioning of agroecosystems: A meta-analysis. *Soil Biology and Biochemistry*, *124*(May), 105–115.
<https://doi.org/10.1016/j.soilbio.2018.06.002>
- Madejova & Komadel. (2001). Baseline studies of the clay minerals society source Clays: Infrared methods. *Clays and Clay Minerals*, *49*(5), 410–432.
<https://doi.org/10.1346/CCMN.2001.0490502>
- Malara, A., & Oleszczuk, P. (2013). Application of a battery of biotests for the determination of leachate toxicity to bacteria and invertebrates from sewage sludge-amended soil. *Environmental Science and Pollution Research*, *20*(5), 3435–3446.
<https://doi.org/10.1007/s11356-012-1268-3>
- Manara, P., & Zabaniotou, A. (2012). Towards sewage sludge based biofuels via thermochemical conversion - A review. *Renewable and Sustainable Energy Reviews*, *16*(5), 2566–2582.
<https://doi.org/10.1016/j.rser.2012.01.074>
- Mao, F., He, Y., & Gin, K. Y. H. (2019). Occurrence and fate of benzophenone-type UV filters in aquatic environments: A review. *Environmental Science: Water Research and Technology*, *5*(2), 209–223. <https://doi.org/10.1039/c8ew00539g>
- Martín-Pozo, L., de Alarcón-Gómez, B., Rodríguez-Gómez, R., García-Córcoles, M. T., Çipa, M., & Zafra-Gómez, A. (2019). Analytical methods for the determination of emerging contaminants in sewage sludge samples. A review. *Talanta*, *192*(June 2018), 508–533.
<https://doi.org/10.1016/j.talanta.2018.09.056>

- Mattana, S., Petrovičová, B., Landi, L., Gelsomino, A., Cortés, P., Ortiz, O., & Renella, G. (2014). Sewage sludge processing determines its impact on soil microbial community structure and function. *Applied Soil Ecology*, *75*, 150–161. <https://doi.org/10.1016/j.apsoil.2013.11.007>
- McBride, M. B. (2003). Toxic metals in sewage sludge-amended soils: Has promotion of beneficial use discounted the risks? *Advances in Environmental Research*, *8*(1), 5–19. [https://doi.org/10.1016/S1093-0191\(02\)00141-7](https://doi.org/10.1016/S1093-0191(02)00141-7)
- McCarty, P. L. (2018). What is the Best Biological Process for Nitrogen Removal: When and Why? *Environmental Science and Technology*, *52*(7), 3835–3841. <https://doi.org/10.1021/acs.est.7b05832>
- Mininni, G., Mauro, E., Piccioli, B., Colarullo, G., Brandolini, F., & Giacomelli, P. (2019). Production and characteristics of sewage sludge in Italy. *Water Science and Technology*, *79*(4), 619–626. <https://doi.org/10.2166/wst.2019.064>
- Montecchio, D., Francioso, O., Carletti, P., Pizzeghello, D., Chersich, S., Previtali, F., & Nardi, S. (2006). Thermal analysis (TG-DTA) and drift spectroscopy applied to investigate the evolution of humic acids in forest soil at different vegetation stages. *Journal of Thermal Analysis and Calorimetry*, *83*(2), 393–399. <https://doi.org/10.1007/s10973-005-7292-5>
- Mooshammer, M., Wanek, W., Hämmerle, I., Fuchslueger, L., Hofhansl, F., Knoltsch, A., Schneckner, J., Takriti, M., Watzka, M., Wild, B., Keiblinger, K. M., Zechmeister-Boltenstern, S., & Richter, A. (2014). Adjustment of microbial nitrogen use efficiency to carbon:Nitrogen imbalances regulates soil nitrogen cycling. *Nature Communications*, *5*, 1–7. <https://doi.org/10.1038/ncomms4694>
- Moukakis, I., Pellerá, F. M., & Gidarakos, E. (2018). Slaughterhouse by-products treatment using anaerobic digestion. *Waste Management*, *71*, 652–662. <https://doi.org/10.1016/j.wasman.2017.07.009>
- Nazari, L., Yuan, Z., Santoro, D., Sarathy, S., Ho, D., Batstone, D., Xu, C. C., & Ray, M. B. (2017). Low-temperature thermal pre-treatment of municipal wastewater sludge: Process optimization and effects on solubilization and anaerobic degradation. *Water Research*, *113*, 111–123. <https://doi.org/10.1016/j.watres.2016.11.055>
- Niemeyer, J., Chen, Y., & Bollag, J.-M. (1992). Characterization of Humic Acids, Composts, and Peat by Diffuse Reflectance Fourier-Transform Infrared Spectroscopy. *Soil Science Society of*

- America Journal*, 56(1), 135–140. <https://doi.org/10.2136/sssaj1992.03615995005600010021x>
- Norme AFNOR NFX 31-130 Determination de la capacité d' échange cationique et des cations extractibles*. (1993).
- Ohkouchi, N., Ogawa, N. O., Chikaraishi, Y., Tanaka, H., & Wada, E. (2015). Biochemical and physiological bases for the use of carbon and nitrogen isotopes in environmental and ecological studies. *Progress in Earth and Planetary Science*, 2(1), 1–17. <https://doi.org/10.1186/s40645-015-0032-y>
- Onodera, T., Kanaya, G., Syutsubo, K., Miyaoka, Y., Hatamoto, M., & Yamaguchi, T. (2015). Spatial changes in carbon and nitrogen stable isotope ratios of sludge and associated organisms in a biological sewage treatment system. *Water Research*, 68, 387–393. <https://doi.org/10.1016/j.watres.2014.10.020>
- Onodera, T., Komatsu, K., Kohzu, A., Kanaya, G., Mizuochi, M., & Syutsubo, K. (2021). Differences in the isotopic signature of activated sludge in four types of advanced treatment processes at a municipal wastewater treatment plant. *Journal of Environmental Management*, 286(February). <https://doi.org/10.1016/j.jenvman.2021.112264>
- OriginLab Corporation. (2022). *Origin(Pro), Version 2022b*. <https://www.originlab.com/>
- Ott, C., & Rechberger, H. (2012). The European phosphorus balance. *Resources, Conservation and Recycling*, 60, 159–172. <https://doi.org/10.1016/j.resconrec.2011.12.007>
- Ouchene, L., Litvinov, I. V., & Netchiporouk, E. (2019). Hawaii and Other Jurisdictions Ban Oxybenzone or Octinoxate Sunscreens Based on the Confirmed Adverse Environmental Effects of Sunscreen Ingredients on Aquatic Environments. *Journal of Cutaneous Medicine and Surgery*, 23(6), 648–649. <https://doi.org/10.1177/1203475419871592>
- Paredes, E., Perez, S., Rodil, R., Quintana, J. B., & Beiras, R. (2014). Ecotoxicological evaluation of four UV filters using marine organisms from different trophic levels *Isochrysis galbana*, *Mytilus galloprovincialis*, *Paracentrotus lividus*, and *Siriella armata*. *Chemosphere*, 104, 44–50. <https://doi.org/10.1016/j.chemosphere.2013.10.053>
- Pascual, I., Azcona, I., Morales, F., Aguirreolea, J., & Sánchez-Díaz, M. (2009). Growth, yield and physiology of *Verticillium*-inoculated pepper plants treated with ATAD and composted sewage sludge. *Plant and Soil*, 319(1–2), 291–306. <https://doi.org/10.1007/s11104-008-9870-3>

- Patakioutas, G., & Albanis, T. A. (2002). Adsorption-desorption studies of alachlor, metolachlor, EPTC, chlorothalonil and pirimiphos-methyl in contrasting soils. *Pest Management Science*, 58(4), 352–362. <https://doi.org/10.1002/ps.464>
- Piwowarczyk, A. A., & Holden, N. M. (2012). Adsorption and desorption isotherms of the nonpolar fungicide chlorothalonil in a range of temperate maritime agricultural soils. *Water, Air, and Soil Pollution*, 223(7), 3975–3985. <https://doi.org/10.1007/s11270-012-1165-x>
- Pizzeghello, D., Cocco, S., Francioso, O., Ferrari, E., Cardinali, A., Nardi, S., Agnelli, A., & Corti, G. (2015). Snow vole (*Chionomys nivalis* Martins) affects the redistribution of soil organic matter and hormone-like activity in the alpine ecosystem: Ecological implications. *Ecology and Evolution*, 5(20), 4542–4554. <https://doi.org/10.1002/ece3.1727>
- Post, D. M. (2002). The long and short of food-chain length. *Molecular Cell*, 10(3), 435–437. [https://doi.org/10.1016/S1097-2765\(02\)00657-3](https://doi.org/10.1016/S1097-2765(02)00657-3)
- Prado, J., Ribeiro, H., Alvarenga, P., & Fangueiro, D. (2022). A step towards the production of manure-based fertilizers: Disclosing the effects of animal species and slurry treatment on their nutrients content and availability. *Journal of Cleaner Production*, 337(December 2021), 130369. <https://doi.org/10.1016/j.jclepro.2022.130369>
- R Core Team. (2022). *R: A language and environment for statistical computing*. R Foundation for statistical computing. <http://www.r-project.org/index.html>
- Ramos, S., Homem, V., Alves, A., & Santos, L. (2015). Advances in analytical methods and occurrence of organic UV-filters in the environment - A review. *Science of the Total Environment*, 526, 278–311. <https://doi.org/10.1016/j.scitotenv.2015.04.055>
- Ramos, S., Homem, V., Alves, A., & Santos, L. (2016). A review of organic UV-filters in wastewater treatment plants. *Environment International*, 86, 24–44. <https://doi.org/10.1016/j.envint.2015.10.004>
- Rapisarda, S., Di Biase, G., Mazzon, M., Ciavatta, C., & Cavani, L. (2022). Nitrogen Availability in Organic Fertilizers from Tannery and Slaughterhouse By-Products. *Sustainability*, 14(12921). <https://doi.org/https://doi.org/10.3390/su141912921>
- Riaz, U., Murtaza, G., Saifullah, & Farooq, M. (2018). Influence of different sewage sludges and composts on growth, yield, and trace elements accumulation in rice and wheat. *Land*

- Degradation and Development*, 29(5), 1343–1352. <https://doi.org/10.1002/ldr.2925>
- Roig, N., Sierra, J., Martí, E., Nadal, M., Schuhmacher, M., & Domingo, J. L. (2012). Long-term amendment of Spanish soils with sewage sludge: Effects on soil functioning. *Agriculture, Ecosystems and Environment*, 158, 41–48. <https://doi.org/10.1016/j.agee.2012.05.016>
- Roldán, M. L., Corrado, G., Francioso, O., & Sanchez-Cortes, S. (2011). Interaction of soil humic acids with herbicide paraquat analyzed by surface-enhanced Raman scattering and fluorescence spectroscopy on silver plasmonic nanoparticles. *Analytica Chimica Acta*, 699(1), 87–95. <https://doi.org/10.1016/j.aca.2011.05.001>
- Sáez, J. A., Flores, P., Bustamante, M. Á., Sanchez-Hernandez, J. C., Moral, R., & Pérez-Murcia, M. D. (2020). Nitrogen isotope fractionation during composting of sewage and agri-food sludge with pruning waste. *Agronomy*, 10(12), 1–13. <https://doi.org/10.3390/agronomy10121954>
- Salvati, L. (2014). Toward a “Sustainable” land degradation? Vulnerability degree and component balance in a rapidly changing environment. *Environment, Development and Sustainability*, 16(1), 239–254. <https://doi.org/10.1007/s10668-013-9463-z>
- Samolada, M. C., & Zabaniotou, A. A. (2014). Comparative assessment of municipal sewage sludge incineration, gasification and pyrolysis for a sustainable sludge-to-energy management in Greece. *Waste Management*, 34(2), 411–420. <https://doi.org/10.1016/j.wasman.2013.11.003>
- Sánchez-Brunete, C., Miguel, E., Albero, B., & Tadeo, J. L. (2011). Analysis of salicylate and benzophenone-type UV filters in soils and sediments by simultaneous extraction cleanup and gas chromatography-mass spectrometry. *Journal of Chromatography A*, 1218(28), 4291–4298. <https://doi.org/10.1016/j.chroma.2011.05.030>
- Sanchez-Cortes, S., Corrado, G., Trubetskaya, O. E., Trubetskoj, O. A., Hermosin, B., & Saiz-Jimenez, C. (2006). Surface-enhanced Raman spectroscopy of chernozem humic acid and their fractions obtained by coupled size exclusion chromatography-polyacrylamide gel electrophoresis (SEC-PAGE). *Applied Spectroscopy*, 60(1), 48–53. <https://doi.org/10.1366/000370206775382695>
- Sánchez Rodríguez, A., Rodrigo Sanz, M., & Betancort Rodríguez, J. R. (2015). Occurrence of eight UV filters in beaches of Gran Canaria (Canary Islands). An approach to environmental risk assessment. *Chemosphere*, 131, 85–90.

<https://doi.org/10.1016/j.chemosphere.2015.02.054>

- Sathish, M., Sreeram, K. J., Raghava Rao, J., & Unni Nair, B. (2016). Cyclic Carbonate: A Recyclable Medium for Zero Discharge Tanning. *ACS Sustainable Chemistry and Engineering*, 4(3), 1032–1040. <https://doi.org/10.1021/acssuschemeng.5b01121>
- Schabenberger, O., & Pierce, F. J. (2001). *Contemporary Statistical Models for the Plant and Soil Sciences* (1st ed.). CRC Press.
- Sciubba, L., Cavani, L., Negroni, A., Zanaroli, G., Fava, F., Ciavatta, C., & Marzadori, C. (2014). Changes in the functional properties of a sandy loam soil amended with biosolids at different application rates. *Geoderma*, 221–222, 40–49. <https://doi.org/10.1016/j.geoderma.2014.01.018>
- Senesi, N., D’Orazio, V., & Ricca, G. (2003). Humic acids in the first generation of EUROSOLS. *Geoderma*, 116(3–4), 325–344. [https://doi.org/10.1016/S0016-7061\(03\)00107-1](https://doi.org/10.1016/S0016-7061(03)00107-1)
- Sharma, B., Sarkar, A., Singh, P., & Singh, R. P. (2017). Agricultural utilization of biosolids: A review on potential effects on soil and plant growth. *Waste Management*, 64, 117–132. <https://doi.org/10.1016/j.wasman.2017.03.002>
- Sharma, B., Vaish, B., Monika, Singh, U. K., Singh, P., & Singh, R. P. (2019). Recycling of Organic Wastes in Agriculture: An Environmental Perspective. *International Journal of Environmental Research*, 13(2), 409–429. <https://doi.org/10.1007/s41742-019-00175-y>
- Sierra, M. M. D., Rauen, T. G., Tormen, L., Debacher, N. A., & Soriano-Sierra, E. J. (2005). Evidence from surface tension and fluorescence data of a pyrene-assisted micelle-like assemblage of humic substances. *Water Research*, 39(16), 3811–3818. <https://doi.org/10.1016/j.watres.2005.07.005>
- Sigurnjak, I., De Waele, J., Michels, E., Tack, F. M. G., Meers, E., & De Neve, S. (2017). Nitrogen release and mineralization potential of derivatives from nutrient recovery processes as substitutes for fossil fuel-based nitrogen fertilizers. *Soil Use and Management*, 33(3), 437–446. <https://doi.org/10.1111/sum.12366>
- Simpson, A. J. (2002). Determining the molecular weight, aggregation, structures and interactions of natural organic matter using diffusion ordered spectroscopy. *Magnetic Resonance in Chemistry*, 40(SPEC. ISS.). <https://doi.org/10.1002/mrc.1106>
- Simpson, M. J., Chefetz, B., & Hatcher, P. G. (2003). Phenanthrene Sorption to Structurally

- Modified Humic Acids. *Journal of Environmental Quality*, 32(5), 1750–1758.
<https://doi.org/10.2134/jeq2003.1750>
- Singh, R. P., & Agrawal, M. (2008). Potential benefits and risks of land application of sewage sludge. *Waste Management*, 28(2), 347–358. <https://doi.org/10.1016/j.wasman.2006.12.010>
- Singh, R. P., & Agrawal, M. (2010a). Effect of different sewage sludge applications on growth and yield of *Vigna radiata* L. field crop: Metal uptake by plant. *Ecological Engineering*, 36(7), 969–972. <https://doi.org/10.1016/j.ecoleng.2010.03.008>
- Singh, R. P., & Agrawal, M. (2010b). Variations in heavy metal accumulation, growth and yield of rice plants grown at different sewage sludge amendment rates. *Ecotoxicology and Environmental Safety*, 73(4), 632–641. <https://doi.org/10.1016/j.ecoenv.2010.01.020>
- Smidt, E., & Schwanninger, M. (2005). Characterization of waste materials using FTIR spectroscopy: Process monitoring and quality assessment. *Spectroscopy Letters*, 38(3), 247–270. <https://doi.org/10.1081/SL-200042310>
- Soil Survey Staff Soil Taxonomy: A Basic System of Soil Classification for Making and Interpreting Soil Surveys* (2nd ed.). (1999). U.S. Department of Agriculture Handbook.
- Song, K., Xue, Y., Zheng, X., Lv, W., Qiao, H., Qin, Q., & Yang, J. (2017). Effects of the continuous use of organic manure and chemical fertilizer on soil inorganic phosphorus fractions in calcareous soil. *Scientific Reports*, 7(1), 1–9. <https://doi.org/10.1038/s41598-017-01232-2>
- Sørensen, S. R., Schultz, A., Jacobsen, O. S., & Aamand, J. (2006). Sorption, desorption and mineralisation of the herbicides glyphosate and MCPA in samples from two Danish soil and subsurface profiles. *Environmental Pollution*, 141(1), 184–194.
<https://doi.org/10.1016/j.envpol.2005.07.023>
- Spångberg, J., Hansson, P. A., Tidåker, P., & Jönsson, H. (2011). Environmental impact of meat meal fertilizer vs. chemical fertilizer. *Resources, Conservation and Recycling*, 55(11), 1078–1086. <https://doi.org/10.1016/j.resconrec.2011.06.002>
- Sparks, D. L., Page, A. L., Helmke, P. A., Loeppert, R. H., Soltanpour, P. N., Tabatabai, M. A., Johnstone, C. T., & Summer, M. E. (1996). *Methods of Soil Analysis: Part 3 Chemical Methods*. SSSA Book Series, Soil Science Society of America.

- Stanford, G., & Smith, S. J. (1972). Nitrogen Mineralization Potentials of Soils. *Soil Science Society of America Journal*, 36, 465–472.
- Stevens, J., Green, N. J. L., & Jones, K. C. (2001). Survey of PCDD/Fs and non-ortho PCBs in UK sewage sludges. *Chemosphere*, 44(6), 1455–1462. [https://doi.org/10.1016/S0045-6535\(00\)00474-4](https://doi.org/10.1016/S0045-6535(00)00474-4)
- Stevenson, F. J. (1994). *Humus Chemistry: Genesis, Composition, Reactions* (Wiley (Ed.); 2nd ed.).
- Suciu, N. A., Lamastra, L., & Trevisan, M. (2015). PAHs content of sewage sludge in Europe and its use as soil fertilizer. *Waste Management*, 41, 119–127. <https://doi.org/10.1016/j.wasman.2015.03.018>
- Sundar, V. J., Gnanamani, A., Muralidharan, C., Chandrababu, N. K., & Mandal, A. B. (2011). Recovery and utilization of proteinous wastes of leather making: A review. *Reviews in Environmental Science and Biotechnology*, 10(2), 151–163. <https://doi.org/10.1007/s11157-010-9223-6>
- Sutton, M. A., & Bleeker, A. (2013). Environmental science: The shape of nitrogen to come. *Nature*, 494(7438), 435–437. <https://doi.org/10.1038/nature11954>
- Svanbäck, A., McCrackin, M. L., Swaney, D. P., Linefur, H., Gustafsson, B. G., Howarth, R. W., & Humborg, C. (2019). Reducing agricultural nutrient surpluses in a large catchment – Links to livestock density. *Science of the Total Environment*, 648, 1549–1559. <https://doi.org/10.1016/j.scitotenv.2018.08.194>
- Swift, R. S. (1996). Organic Matter Characterization. *Methods of Soil Analysis. Part 3. Chemical Methods-SSSA Book Series No. 5.*, 1011–1068. <https://doi.org/10.2134/agronmonogr9.2.2ed.c30>
- Szabó, L., Vancsik, A., Király, C., Ringer, M., Kondor, A., Jakab, G., Szalai, Z., & Filep, T. (2020). Investigation of the sorption of 17 α -ethynylestradiol (EE2) on soils formed under aerobic and anaerobic conditions. *Chemosphere*, 240. <https://doi.org/10.1016/j.chemosphere.2019.124817>
- Tahiri, S., & De la Guardia, M. (2009). Treatment and Valorization of Leather Industry Solid Wastes : A Review**. *J. Am. Leather Chem. Assoc.*, 104, 52–67.
- Tarazona, I., Chisvert, A., León, Z., & Salvador, A. (2010). Determination of hydroxylated benzophenone UV filters in sea water samples by dispersive liquid-liquid microextraction

- followed by gas chromatography-mass spectrometry. *Journal of Chromatography A*, 1217(29), 4771–4778. <https://doi.org/10.1016/j.chroma.2010.05.047>
- Tatzber, M., Stemmer, M., Spiegel, H., Katzlberger, C., Haberhauer, G., Mentler, A., & Gerzabek, M. H. (2007). FTIR-spectroscopic characterization of humic acids and humin fractions obtained by advanced NaOH, Na₄P₂O₇, and Na₂CO₃ extraction procedures. *Journal of Plant Nutrition and Soil Science*, 170(4), 522–529. <https://doi.org/10.1002/jpln.200622082>
- Tejada, M., Parrado, J., Hernández, T., & García, C. (2011). The biochemical response to different Cr and Cd concentrations in soils amended with organic wastes. *Journal of Hazardous Materials*, 185(1), 204–211. <https://doi.org/10.1016/j.jhazmat.2010.09.019>
- Thorstensen, C. W., Lode, O., Martin Eklo, O., & Christiansen, A. (2001). Sorption of Bentazone, Dichlorprop, MCPA, and Propiconazole in Reference Soils from Norway. *J. Environ. Qual.* 30:2046–2052 (2001), 30, 2046–2052.
- Tinti, A., Tugnoli, V., Bonora, S., & Francioso, O. (2015). Recent applications of vibrational mid-infrared (IR) spectroscopy for studying soil components: A review. *Journal of Central European Agriculture*, 16(1), 1–22. <https://doi.org/10.5513/JCEA01/16.1.1535>
- Tivet, F., de Moraes Sá, J. C., Lal, R., Milori, D. M. B. P., Briedis, C., Letourmy, P., Pinheiro, L. A., Borszowski, P. R., & da Cruz Hartman, D. (2013). Assessing humification and organic C compounds by laser-induced fluorescence and FTIR spectroscopies under conventional and no-till management in Brazilian Oxisols. *Geoderma*, 207–208(1), 71–81. <https://doi.org/10.1016/j.geoderma.2013.05.001>
- Traversa, A., Said-Pullicino, D., D’Orazio, V., Gigliotti, G., & Senesi, N. (2011). Properties of humic acids in Mediterranean forest soils (Southern Italy): Influence of different plant covering. *European Journal of Forest Research*, 130(6), 1045–1054. <https://doi.org/10.1007/s10342-011-0491-7>
- van Dijk, K. C., Lesschen, J. P., & Oenema, O. (2016). Phosphorus flows and balances of the European Union Member States. *Science of the Total Environment*, 542, 1078–1093. <https://doi.org/10.1016/j.scitotenv.2015.08.048>
- Vela-Soria, F., Jiménez-Díaz, I., Rodríguez-Gómez, R., Zafra-Gómez, A., Ballesteros, O., Navalón, A., Vílchez, J. L., Fernández, M. F., & Olea, N. (2011). Determination of benzophenones in human placental tissue samples by liquid chromatography-tandem mass spectrometry. *Talanta*,

- 85(4), 1848–1855. <https://doi.org/10.1016/j.talanta.2011.07.030>
- Vesper, I. (2020). Hawaii seeks to ban “reef-unfriendly” sunscreen. *Nature*, February, 2017–2019. <https://doi.org/10.1038/nature.2017.21332>
- Veyssi re, S., Laperche, B., & Blanquart, C. (2022). Territorial development process based on the circular economy: a systematic literature review. *European Planning Studies*, 30(7), 1192–1211. <https://doi.org/10.1080/09654313.2021.1873917>
- Vicent, T., Caminal, G., Eljarrat, E., & Barcel , D. (2013). *The Handbook of Environmental Chemistry: Emerging Organic Contaminants in Sludges* (Vol. 24).
- Vulava, V. M., Cory, W. C., Murphey, V. L., & Ulmer, C. Z. (2016). Sorption, photodegradation, and chemical transformation of naproxen and ibuprofen in soils and water. *Science of the Total Environment*, 565, 1063–1070. <https://doi.org/10.1016/j.scitotenv.2016.05.132>
- Wang, X., Chen, T., Ge, Y., & Jia, Y. (2008). Studies on land application of sewage sludge and its limiting factors. *Journal of Hazardous Materials*, 160(2–3), 554–558. <https://doi.org/10.1016/j.jhazmat.2008.03.046>
- Whalen, J. K., Thomas, B. W., & Sharifi, M. (2019). Novel Practices and Smart Technologies to Maximize the Nitrogen Fertilizer Value of Manure for Crop Production in Cold Humid Temperate Regions. *Advances in Agronomy*, 153, 1–85. <https://doi.org/10.1016/bs.agron.2018.09.002>
- Wild, S. R., Berrow, M. L., & Jones, K. C. (1991). The persistence of polynuclear aromatic hydrocarbons (PAHs) in sewage sludge amended agricultural soils. *Environmental Pollution*, 72(2), 141–157. [https://doi.org/10.1016/0269-7491\(91\)90064-4](https://doi.org/10.1016/0269-7491(91)90064-4)
- Wi niowska, E., & W odarczyk-Maku a, M. (2016). Effect of Silicates on Methane Digestion of Sewage Sludge. *Engineering and Protection of Environment*, 19(4), 493–502. <https://doi.org/10.17512/ios.2016.4.5>
- Xue, J., Liu, W., & Kannan, K. (2017). Bisphenols, Benzophenones, and Bisphenol A Diglycidyl Ethers in Textiles and Infant Clothing. *Environmental Science and Technology*, 51(9), 5279–5286. <https://doi.org/10.1021/acs.est.7b00701>
- Yang, G., Zhang, G., & Wang, H. (2015). Current state of sludge production, management, treatment and disposal in China. *Water Research*, 78, 60–73.

<https://doi.org/10.1016/j.watres.2015.04.002>

- Yuan, T., Tazaki, A., Hashimoto, K., Al Hossain, M. M. A., Kurniasari, F., Ohgami, N., Aoki, M., Ahsan, N., Akhand, A. A., & Kato, M. (2021). Development of an efficient remediation system with a low cost after identification of water pollutants including phenolic compounds in a tannery built-up area in Bangladesh. *Chemosphere*, 280(April).
<https://doi.org/10.1016/j.chemosphere.2021.130959>
- Zdruli, P. (2014). Land resources of the Mediterranean: Status, pressures, trends and impacts on future regional development. *Land Degradation and Development*, 25(4), 373–384.
<https://doi.org/10.1002/ldr.2150>
- Zdruli, Pandi, Jones, R. J. A., & Montanarella, L. (2004). *Organic matter in the soils of southern Europe, European Soil Bureau Research Report*.
- Zhai, S., Xiong, Y., Li, M., Wang, D., & Fu, S. (2020). Roles of hydrothermal-alkaline treatment in tannery sludge reduction: Rheological properties and sludge reduction mechanism analysis. *RSC Advances*, 10(24), 14291–14298. <https://doi.org/10.1039/c9ra11010k>
- Zhang, G., Sun, B., Zhao, H., Wang, X., Zheng, C., Xiong, K., Ouyang, Z., Lu, F., & Yuan, Y. (2019). Estimation of greenhouse gas mitigation potential through optimized application of synthetic N, P and K fertilizer to major cereal crops: A case study from China. *Journal of Cleaner Production*, 237. <https://doi.org/10.1016/j.jclepro.2019.117650>
- Zhang, Y., Buchanan, J. K., Holmes, G., Mansel, B. W., & Prabakar, S. (2019). Collagen structure changes during chrome tanning in propylene carbonate. *Journal of Leather Science and Engineering*, 1(1), 1–7. <https://doi.org/10.1186/s42825-019-0011-y>
- Zhang, Z., Ren, N., Li, Y. F., Kunisue, T., Gao, D., & Kannan, K. (2011). Determination of benzotriazole and benzophenone UV filters in sediment and sewage sludge. *Environmental Science and Technology*, 45(9), 3909–3916. <https://doi.org/10.1021/es2004057>
- Zhao, J., Wu, Q., Tang, Y., Zhou, J., & Guo, H. (2022). Tannery wastewater treatment: conventional and promising processes, an updated 20-year review. *Journal of Leather Science and Engineering*, 4(1). <https://doi.org/10.1186/s42825-022-00082-7>